2009

Merged electrospray ionization mass spectrometry

Jianan Dong
Louisiana State University and Agricultural and Mechanical College, jdong1@tigers.lsu.edu

MERGED ELECTROSPRAY IONIZATION MASS SPECTROMETRY

A Dissertation

Submitted to the Graduate Faculty of the
Louisiana State University
Agricultural and Mechanical College
In partial fulfillment of the
Requirements for the degree of
Doctor of Philosophy

In

The Department of Chemistry

By

Jianan Dong
B.S. Nanjing University of Technology, 1997
December 2009

ACKNOWLEDGEMENTS

Dr. Kermit K. Murray. I deeply appreciate the opportunity you give me to work in your research group. Thank you for your enthusiastic guidance, indispensable support and helpful criticism during this research and writing effort.

Doctoral Committee Members: Dr. Robin McCarley, Dr. Doug Gilman, Dr. Bin Chen and Dr. Craig Hart. Thank you for your time and helpful advices over the years. I appreciate all the comments and suggestions you gave me to enhance this dissertation.

Mass Sepctrometry Facility (MSF) of LSU. Thank you for allowing me to use the instruments and giving me opportunities to learn and troubleshoot a number of mass spectrometers. Thanks Dr. Azeem Hasan for your kindly help and suggestions during my study.

Dr. Yohanness Rezenom. Thank you for your generous help and friendship. It is always enjoyable to work with you.

Dr. Justin Birdwell. I deeply appreciate that you spent so much time to rigorously proofread my dissertation and give me helpful suggestions.

The Murray Research Group. Thank you for being my family away from home. I appreciate your friendship and support.

My Family and Friends. Thank you for always believing in me. Without your love and support, I could not have accomplished my study.

TABLE OF CONTENTS

LIST OF TABLES

LIST OF FIGURES

LIST OF ABBREVIATIONS

APS	aerodynamic particle sizer
APCI	atmospheric-pressure chemical ionization
AP-MALDI	atmospheric-pressure matrix assisted laser desorption ionization
CE	capillary electrophoresis
CI	chemical ionization
Cf^{252} PD	californium-252 plasma desorption
CRM	charge residue model
Da	dalton
DESI	desorption electrospray ionization
DART	direct-analysis in real time
EA	erythromycin A
EESI	extractive electrospray ionization
ELDI	electrospray-assisted laser desorption ionization
EI	electron ionization
ESI	electrospray ionization
Er:YAG	erbium-doped yttrium aluminium garnet
FAB	fast-atom bombardment
FD-ESI	fused-droplet electrospray ionization
FT-ICR	fourier transform ion cyclotron resonance
GC-MS	gas chromatography mass spectrometry
HPLC	high-performance liquid chromatography
IEM	ion evaporation model
IR	infrared
LAMMA	laser microprobe mass sectrometry
LDI	laser desorption ionization
LIF	laser induced fluorescence spectroscopy
LOD	limit of detection
MALDI	matrix-assisted laser desorption ionization
MALDESI	matrix-assisted laser desorption electrospray ionization
MS	mass spectrometry
m/z	mass to charge ratio
ND-EESI	neutral desorption extractive electrospray ionization
o-TOF	orthogonal time of flight
PAH	polycyclic aromatic hydrocarbon
PCD	photomultiplier conversion dynode
PDMS	plasma desorption mass spectrometry
RF	radio frequency
UV	ultraviolet

ABSTRACT

Ambient ionization allows the analysis of materials in their native environment without sample preparation by creating ions outside the mass spectrometer. The goal of this research was to develop new ambient ionization techniques for application to solids, liquids and particles under ambient conditions. Samples to be analyzed were directly merged with an electrospray of droplets, and then ionized and detected by a mass spectrometer. An ion trap mass spectrometer was modified with a nanoelectrospray source and configured for three experiments: merged electrospray ionization of dry particles, merged electrospray ionization of combustion products, and infrared laser desorption/ablation using electrospray for post-ionization.

In the first set of experiments, materials in powdered samples were ionized directly by interaction with an electrospray of charged solvent droplets. The powdered samples were dispersed as dry particles with an aerosol generator. The study included amino acids and antibiotics, as well as food and pharmaceutical samples. Singly-charged peaks, corresponding to major components in the powdered samples, were detected using this method. The second set of experiments directly analyzed combustion products generated from the burning of cigarettes, incense, candles, and organic fuels by merging these with electrospray for ionization. This approach allowed the detection of major components in the smoke of cigarettes, incense, and candles, and polycyclic aromatic hydrocarbons generated from combustion of organic fuels. In the third set of experiments, an infrared laser was used to desorb and ablate samples placed on a stainless steel sample target, and electropray droplets interacted with the ablated materials to generate ions. Protein standards, biological fluids, and pharmaceutical products were analyzed using this technique. The spectra of the materials analyzed were similar to conventional electrospray.

CHAPTER 1. INTRODUCTION

1.1 Mass Spectrometry

Mass spectrometry is a highly selective analytical technique with a low limit of detection that is used to separate ions according to their mass-to-charge ratio (*m/z*).[1] Since the first use of mass spectrometers in the early twentieth century, the technique has undergone extensive development and has been applied in a wide range of scientific disciplines such as analytical chemistry, environmental science, and biomedical research.

A mass spectrometer is composed of three fundamental units: the ionization source, mass analyzer, and detector. The ions are generated by inducing either the loss or gain of a charge in the ionization source, separated in the mass analyzer according to their *m/z*, and finally converted to a signal at the detector. The ion flux at the detector is amplified to produce an electrical signal, and the signal then is converted into a mass spectrum that can provide mass and structural information.

Mass spectrometry requires ions in the gas phase. Getting the sample of interest into the gas phase in the form of ions is the first and often the most important step of mass spectrometry. Various ionization techniques have been developed. Electron ionization (EI) is one of the earliest ionization techniques, and it a simple technique with a low detection limit.[2, 3] EI has been a popular mode of ionization for organic compounds and uses an energetic electron beam to bombard the sample in the gas phase. Ions are formed by electron displacement during this collision process. However, EI can only be used to analyze gases or high vapor pressure liquids. Furthermore, fragmentation can make identification of the molecular ion difficult. For these reasons, EI is limited to volatile molecules smaller than several hundred Da.

1.2 Soft Ionization

Soft ionization is defined as ionization with minimal fragmentation, which indicates that minimum internal energy is transmitted to the analytes during the ionization process.[4] Chemical ionization (CI) was one of the first soft ionization techniques developed.[5] In CI, a reagent gas such as methane, isobutene or ammonia is ionized with an electron beam or discharge to produce reagent ions. Then reagent ions react with the sample molecules to form ions. With methane as the reagent gas, the primary ions are formed through reaction

$$CH_4 + e^- \rightarrow CH_4^{+\cdot} + 2e^-.$$

The primary ions undergo further reactions with neutral methane through

$$CH_4 + CH_4^{+\cdot} \rightarrow CH_5^+ + CH_3^{\cdot}$$

or

$$CH_4 + CH_3^+ \rightarrow C_2H_5^+ + H_2$$

to produce secondary reagent ions. The ionization of the sample molecules (M) can take place, for example, through the proton transfer reaction

$$M + CH_5^+ \rightarrow [M+H]^+ + CH_4.$$

The collisions between reagent ions and analyte molecule occur at thermal energies. Thus, CI primarily generates the protonated molecule ion signal and can be used to determine the molecular mass of compounds. However, CI is also limited to volatile molecules smaller than several hundred Da.

The discovery of fast-atom bombardment (FAB)[6] and Californium-252 plasma desorption (^{252}Cf PD)[7] ionization methods extended the application of soft ionization to the analysis of nonvolatile biomolecules as well as other polar and involatile compounds. FAB uses a high energy beam of Xe atoms or Cs^+ ions to sputter the sample and matrix from the surface,

while PDMS uses a fission product generated from a thin 10-μCi ^{252}Cf film to desorb the condensed phase sample. Both methods have been used to obtain molecular mass information for a variety of compounds.[8-10] However, due to the limitations of the mass range, the popularity of these two methods has declined.

In the 1980s, the breakthrough development of two soft ionization techniques, electrospray ionization (ESI)[11] and matrix-assisted laser desorption ionization (MALDI),[12] made it possible to analyze higher molecular weight biomolecules than FAB or PDMS with limited to no covalent bond fragmentation. Since then, these two methods have become the major ionization techniques on the identification and structural determination of high molecular weight compounds, such as proteins and synthetic polymers.

1.2.1 Electrospray Ionization (ESI)

ESI coupled with mass spectrometry was first demonstrated for the analysis of large molecules in 1984.[11] ESI is a technique that allows the transfer of ions from a solution to the gas phase at atmospheric pressure. ESI is the dispersion of a liquid into electrically charged droplets, and combines two processes: droplet formation and droplet charging.[13] As illustrated in Figure 1-1, the application of a several thousand volt potential to a capillary induces a charge on the surface of the liquid that emerges from the tip of the capillary in a conical shape, known as a Taylor cone.[14] Charged droplets are formed at the tip of the Taylor cone and directed toward a mass spectrometer inlet. A nebulizing gas and heat can be applied before the droplets enter the vacuum of the mass spectrometer, causing the solvent to evaporate from the surface of the droplets. As the evaporation proceeds, the droplet radius decreases, and the charge of the droplet remains constant. This leads to an increase of the electrostatic repulsion of the charges at the surface. As a result, the highly charged droplets become unstable and produce gas-phase ions.

The creation of gas-phase ions from charged droplets can occur by one of the two mechanisms known as charge residue model (CRM) or ion evaporation model (IEM).[15, 16] In the IEM, analyte molecules carrying some of the droplet charge are ejected into the gas phase when the electric field on the charged droplet is large enough.[17] This happens because the potential energy of the ions near the surface becomes large and the Coulombic repulsion overcomes the surface tension. In the CRM, gas-phase ions are formed when successive fissions of charged droplets leads to the ejection of highly charged analyte ions; this theory is purported to be dominant in the case of ions with high *m/z*.[18]

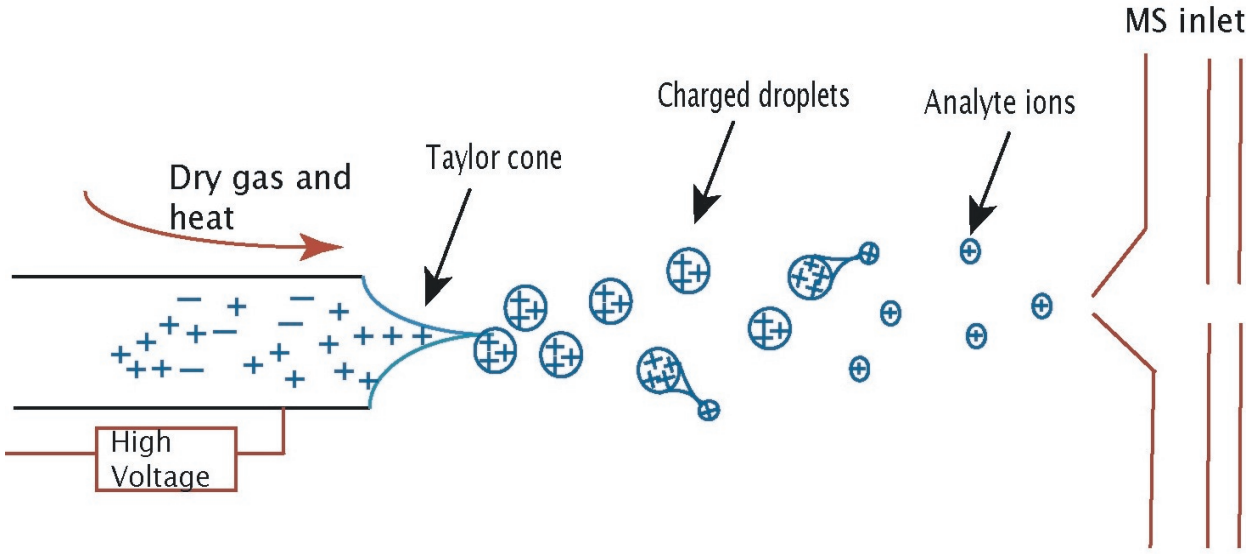

Figure 1-1. Electrospray ionization illustration.

ESI has been widely applied in the analysis of large biomolecules, such as peptides, proteins, oligonucleotides, and lipids.[19] An important feature of ESI is that it produces ions with multiple charges; thus it is possible to observe large molecules with a mass analyzer having a relatively low *m/z* range. With ESI-MS, the molecular masses of biomolecules in the mass range up to 100 kDa or more can be determined.[20] Electrospray samples are in a liquid solution; thus,

ESI can also be easily coupled with separations, such as high performance liquid chromatography (HPLC)[21] and capillary electrophoresis (CE).[22] However, ESI has low impurity tolerance. When using ESI, contaminants can compete with the analytes for charge and may influence the results.[23]

1.2.2 Matrix Assisted Laser Desorption Ionization (MALDI)

A second form of soft ionization is MALDI, which was developed simultaneously by Hillenkamp[12, 24] and Tanaka[25] in mid 1980s as a modification of laser desorption ionization (LDI).[26] MALDI is used to ionize samples in the condensed phase, typically under vacuum. In MALDI, a sample is first dissolved in a suitable solvent and mixed with a crystalline or liquid matrix. Subsequently, it is deposited on a stainless steel target and air-dried. Under these circumstances, the sample is co-crystallized with the matrix. Then, a pulsed ultraviolet (UV) or infrared (IR) laser is directed at the matrix and analyte deposit to generate gas phase ions. Figure 1-2 represents the process by which ions are formed during MALDI. The use of a chemical matrix in the form of small, laser-absorbing organic molecules in large excess over the analyte is at the core of the MALDI principle. The matrix plays a key role by absorbing the laser energy, preventing analyte aggregation, and providing protons for analyte ionization.[1] Typically, singly charged ions of analyte are generated; fragmentation is typically not observed by MALDI.

The mechanism of MALDI is still under investigation.[27, 28] Two major models have been proposed to explain experimental results: photochemical ionization and cluster ionization.[29] The photochemical ionization model considers the generation of neutral analyte species as the first step, which are then charged by proton-transfer reactions with photonionized matrix molecules in the expanding gaseous plume. The cluster ionization model assumes large clusters of matrix and of analyte-matrix are desorbed during the laser irradiation. The generation of charged species within a cluster is accomplished by charge separation.[29]

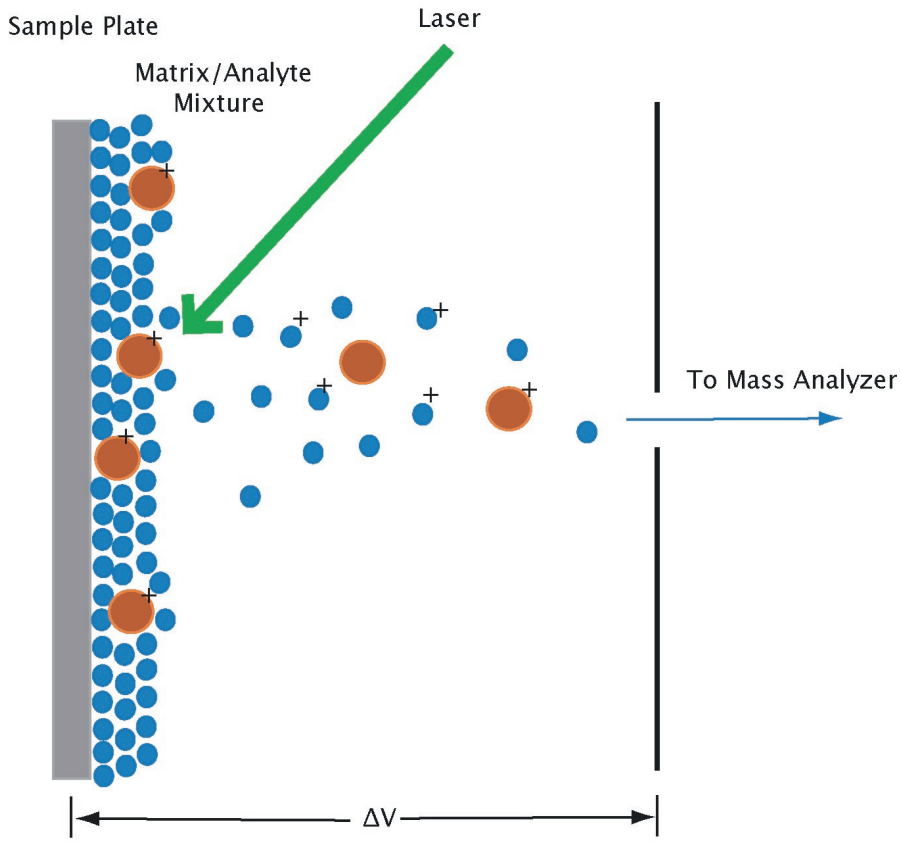

Figure 1-2. Schematic of matrix-assisted laser desorption/ionization.

MALDI is a simple and low-sample-consumption ionization method. The best analysis range of MALDI is in 1000 Da to 30 kDa. MALDI has been broadly used for most proteomic analysis without pre-separation,[30, 31] and has also been used for the analysis of oligonucleotides,[32] polysaccharides,[33] lipids[34] and synthetic polymers.[35, 36] Even though MALDI is tolerant of impurities when compared to ESI, separation is still necessary when dealing with complex samples. There are challenges when coupling MALDI with separation techniques, because MALDI samples are typically dried on a surface before MS analysis. An interface between MALDI ion source and the separation system is typically necessary in order to do on-line analysis.

1.3 Ambient Ionization

Ambient ionization is the creation of ions outside of the mass spectrometer at ambient pressure with minimum or in some cases no sample treatment.[37, 38] With ambient ionization, material is liberated from solid or liquid samples that are bombarded with charged droplets or ions, sometimes in conjunction with a laser. Ambient ionization can be used for direct analysis of samples in the open atmosphere of the laboratory or in their natural environment. It has been widely applied in many areas, such as forensics, environmental analysis, drug discovery, and medical diagnostics.[39]

1.3.1 Atmospheric Pressure Matrix Assisted Laser Desorption Ionization (AP MALDI)

Atmospheric pressure MALDI (AP MALDI) was one of the first developed ambient ionization techniques. It is a variant of MALDI,[40, 41] in which desorption and ionization take place at atmospheric pressure outside the mass spectrometer. The ionization process and mechanism of AP MALDI are similar to vacuum MALDI. However, an interface, similar to that used in ESI, is needed to transfer the ions into the mass analyzer.

AP MALDI has been applied to the analysis of peptides and proteins, and has been shown to eliminate some of the drawbacks of conventional MALDI, such as sample handling and mass resolution at high laser fluence.[42] Also, it allows the use of a wide range of liquid matrices. Thus AP MALDI can be interfaced with liquid chromatography.[42, 43] An AP MALDI system was used to analyze a mixture that was separated by a HPLC system.[42] In their study, the sample droplet formed at the end of a capillary that was extended from the HPLC column, and a pulsed laser was focused from below onto the surface of the droplet to ionize the analyte. However, the sampling efficiency of AP-MALDI is lower than vacuum MALDI, due to the transferring of ions from atmospheric pressure to the vacuum region of the mass spectrometer.

1.3.2 Desorption Electrospray Ionization (DESI)

Desorption electrospray ionization (DESI) was first introduced by Cooks and coworkers in 2004.[44] As illustrated in Figure 1-3, a fine spray of charged solvent droplets from an ESI source is used to desorb and ionize the analyte material. Nitrogen gas at high pressure (usually around 150 psi or 1000 kPa) is used to transport the charged solvent droplets to the analyte surface. The solvent on the surface is then lifted off as secondary charged droplets. The solvent picks up the analyte while it is in contact with the target surface, and the subsequently formed analyte ions are delivered to the mass spectrometer.

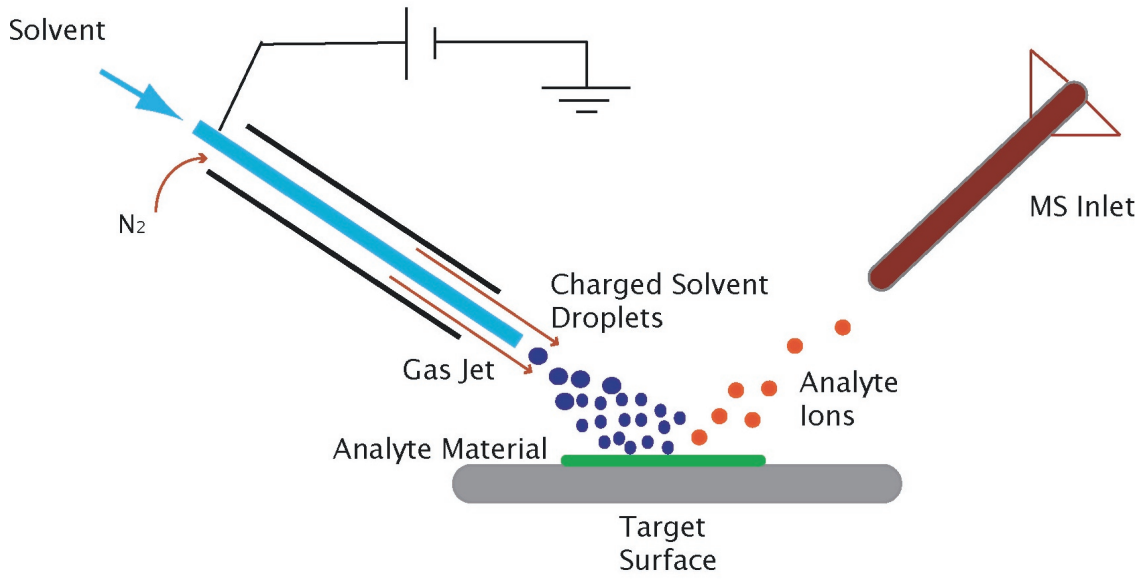

Figure 1-3. Desorption electrospray ionization illustration.

The mechanism of DESI involves the incorporation of the analyte molecules into the solution at the sample surface, which is followed by removal of the analyte-containing charged droplets in the secondary spray.[37] The ions are then formed through an ESI-like mechanism. Recent studies, including systematic measurements of the droplet size and velocity,[45] computer

simulations,[46] surface charging effects,[47] and evaluation of the mass spectra of various analytes in conjunction with variations in the experimental parameters,[48] suggest that the droplet pickup model is the primary ionization mechanism of DESI, especially for the ionization of peptides and proteins. The hypothesis states that the mechanism does not depend on quasi-elastic droplet-surface impact events or the survival of intact droplets after surface collision. Instead, the surface is wetted by initial droplets, and the analyte dissolves in this solvent layer. Later-arriving droplets hit this solvent-layer and break it up, creating numerous secondary droplets containing the dissolved analyte. For lower mass compounds, the ionization mechanism is dominated by the vapor phase process of chemical sputtering, droplet pick up, or a combination of these mechanisms. Chemical sputtering is the process of charge and momentum transfer during droplet reactive collision with the surface.[49] Lower mass compounds with a high vapor pressure may react with free ions above the surface of the sample, or can be incorporated into the liquid droplet with droplets approaching or leaving the surface. Shockwave formation does not contribute to the ionization during the DESI process because of the relatively low velocity of the projectiles.[45]

DESI has been used for the analysis of diverse categories of compounds, including pharmaceutical products,[50, 51] biological samples,[52-55] explosives,[56-59] bacteria,[60, 61] and polymers.[62] By employing solvent additives that bind to certain analytes, selective ionization is possible.[57] DESI can also be used in imaging of sections of biological tissue.[63] The limit of detection of DESI is between 1 and 10 fmol,[39] and varies depending on the analyte. Although DESI provides a useful method for ionizing analytes under ambient conditions, the spatial resolution of DESI imaging is limited to approximately 200 μm due to the spot size as well as diffusion of small molecules in the solvent.[64] The spot size depends on the inner diameter of the spray capillary and the tip-to-surface distance.

1.3.3 Direct Analysis in Real Time (DART)

Direct analysis in real time (DART) was introduced by Cody and coworkers in 2005.[65] In DART, ionization is brought about by exposing the sample to a stream of metastable atoms. In this method, an electrical discharge is created in nitrogen or helium gas to form a plasma of metastable atoms and ions. The plasma passes through perforated lenses or grids, which remove charged particles. After passing through the perforations, metastable atoms and molecules aimed directly at the sample surface desorb low-molecular weight molecules from the sample.

The ionization mechanism of DART depends on the polarity of ions and reagent gas, the proton affinity and ionization potential of the analyte, and the presence of additives or dopants.[65] It is postulated that thermal desorption plays a role when the gas stream is heated. The transfer of energy to the surface by metastable atoms and molecules also facilitates desorption and ionization when the analyte has a low vapor pressure.

Penning ionization[66] is a fundamental process of DART. In Penning ionization, energy is transferred from an excited state gas molecule M* to an analyte molecule A. If analyte A has a lower ionization potential than the energy of M*, a radical molecular cation, $A^{+\cdot}$ and an electron will be produced by Penning ionization, according to

$$M^* + A \rightarrow M + A^{+\cdot} + e^-.$$

When helium is used in the DART source,[65] which is common to most analysis, Penning ionization occurs, generating water cluster ions, according to

$$He^* + nH_2O \rightarrow He + (H_2O)_{n-1}H^+ + OH^-.$$

These cluster ions react with desorbed analytes to form protonated molecules, according to

$$(H_2O)_{n-1}H^+ + AB \rightarrow [AB+H]^+ + H_2O_{n-1}.$$

DART ionization has been widely applied to various analytes, including drugs in dose form, drugs in body fluids or tissues, foods, explosives, synthetic organic compounds, inks and dyes, flavors and fragrances.[65, 67, 68] Using a internal standard, a quantitative analysis of drugs in dilute solutions like urine can be achieved.[65, 69] Analytes on different surfaces, such as glass, concrete, paper, and thin layer chromatography (TLC) plates, can be directly analyzed without any pretreatment.[69] However, DART is mainly used for small molecule analysis.

1.3.4 Merged Electrospray Ionization

Merged electrospray ionization is a technique that combines an electrospray source with a neutral sample source. The sample source generates particles, gas molecules, or both from the bulk sample. An electrospray of solvent is used to directly ionize particles or gas molecules from the sample under ambient conditions. This two-stage ionization method permits the direct analysis of trace compounds in complex matrices. Extractive electrospray ionization (EESI),[70] laser desorption electrospray ionization (LDESI),[71] and matrix-assisted laser desorption electrospray ionization (MALDESI)[72] are examples of this approach. In EESI, a nebulizer is used to generate particles from liquid analyte. The particles are merged with the electrospray of charged droplets, and ionized. In LDESI and MALDESI, a laser is used to desorb the condensed phase sample, and the material is then merged with the electrospray charged droplets. The interaction of particles and gas molecules with the electrospray generates ions, which are sampled by the mass spectrometer.

1.3.4.1 Extractive Electrospray Ionization (EESI)

In extractive electrospray ionization (EESI), a neutral spray containing the sample and a solvent-only electrospray are allowed to interact.[70] Analyte molecules are extracted from the

neutral sample droplets into the charged droplets. Fused droplet-electrospray ionization (FD-ESI) is a method similar to EESI, but for simplicity, we will refer to both processes as EESI below.[73]

In contrast to traditional ESI, EESI separates the neubulization of the sample solution and the ionization processes. Thus, EESI avoids problems such as adduct formation, sample carry-over, and build-up of nonvolatile components, which can affect standard ESI. In EESI, entraining materials in the charged droplets of an electrospray is accomplished through the interaction of charged solvent droplets and a neutral analyte aerosol. Uncharged analyte aerosol particles are sprayed from a neubulizer. The stream of uncharged analyte droplets is then merged with the charged electrospray droplets from the ESI source, and analyte ions are formed through this interaction.

The ionization mechanism of EESI is not yet fully understood, but it depends on the extraction of material between the colliding charge droplets from the electrospray and neutral particles from the nebulizer. A hypothesis is that non-polar compounds are at the surface of neutral sample droplets, while salts and other polar molecules are stabilized by increased solvation at the droplet center.[70] The molecules at the surface of the neutral droplets are extracted into the charged droplets during droplet collision events. This explains why the removal of salts and impurities is unnecessary in EESI. After the molecules are extracted into the charged droplets, analyte ions with multiple charges are produced by an electrospray mechanism.[19]

EESI has been used to analyze small organic molecules,[74] peptides,[73] and proteins.[75] It has also been reported that, by altering the electrospray solvent, it is possible to suppress the signal from certain components within the mixture. This results in a high-salt tolerance in the detection of large biomolecules.[76] EESI has also been used for the analysis of trace compounds in complex mixtures. For example, it has been shown that urine, milk, and wastewater can be

directly and continuously monitored by this method, and the signal intensity can be maintained for several hours.[70]

A variation of EESI is called neutral desorption EESI (ND-EESI).[77] In ND-EESI, the analyte is desorbed from the sample surface with nitrogen gas, followed by merging with the desolvation gas line of an ESI source. ND-EESI shows that gas molecules are ionized directly by merging with electrospray. Similar work has been reported in which small molecules at the exit of a gas chromatograph are ionized by an electrospray source.[78] ND-EESI has been used to analyze skin *in vivo* and frozen meat.[77] Coupling ND-EESI to a quadrupole-time-of-flight MS allowed metabolic fingerprinting of various classes of biological samples with detection limits as low as 10 fg/cm^3.[79]

1.3.4.2 Laser Desorption Electrospray Ionization

Another example of merged electrospray ionization uses a pulsed laser to desorb and ablate material from a solid sample; the resulting material is then merged with an electrospray. This technique uses laser energy to remove material from a sample and deliver it to the electrospray for ionization. When a matrix is used, this technique is called matrix assisted laser desorption electrospray ionization (MALDESI),[72] and when a matrix is not used, it is called laser desorption electrospray ionization (LDESI).[71] LDESI has also been called electrospray assisted laser desorption ionization (ELDI),[71] but, for simplicity and consistency, we will use LDESI in this work.

In MALDESI and LDESI, a UV or IR laser is used to desorb the analyte that is deposited from a solution onto a sample target. An ESI source is used to spray the charged solvent droplets that interact with the desorbed analyte to form ions. Differing from MALDI and AP MALDI, these techniques generate spectra similar to ESI and DESI. The role of the matrix for LDESI and

MALDESI is still under debate. Although the mechanism of ionization is still not clear, recent studies of particle formation under MALDI conditions suggest that ablated particles may play a role.[80-84]

Both LDESI and MALDESI have many applications. LDESI has been used to ionize peptides, proteins and other biomolecules in biological fluids such as tears, saliva, serum and blood.[85] A recent report shows that this method can be used to characterize the major chemical compounds in solid samples such as synthetic polymers, dried milk and porcine brain tissue.[86] MALDESI can also be applied to the quantitative analysis of peptides and proteins.[87]

MALDESI separates the desorption and ionization into two steps, which has many advantages. For example, better resolution for imaging can be achieved because of the smaller size of a laser beam compared to an electrospray stream. An electrospray is limited to approximately 200 μm spatial resolution due to the spot size as well as diffusion of small molecules in the solvent.[88] A laser can be focused onto a sample spot that is nearly an order of magnitude smaller than a spray. In addition, the application of AP-MALDI has been limited due to its low ionization efficiency at ambient condition. In MALDESI, the laser desorption/ablation with electrospray post-ionization can aid in solving this problem.

1.3.5 Comparison of Ambient Ionization Techniques

A comparison of the different ambient ionization methods is presented in Table 1. DESI, LDESI, MALDESI, and EESI are derived from ESI and generate multiply charged analyte peaks in their mass spectra. These ionization techniques are applicable to various mass analyzers. DART is more suitable for small molecule analysis. The limit of detection (LOD) and mass range of these methods are summarized in Table 1.[38, 39, 89] As the instrumentation used in these analyses continues to improve, and the ionization mechanisms behind these ionization techniques

are better understood, analytical figures of merit for these ambient ionization methods are also expected to improve.

Table 1-1. Comparison of various ambient ionization techniques

Technique	Sample type	Mass range	LOD	Imaging capability	References
DESI	Condensed phase	~ 66 kDa	1-10 fmol	Yes	37, 38
DART	Condensed phase and gas phase	~ 1 kDa	7 fmol	N/A	38, 39, 65
AP-MALDI	Condensed phase and liquid sample	~ 16 kDa	~ 8 fmol	Yes	40, 41
LDESI	Condensed phase	~ 66 kDa	~ 20 fmol	Yes	38, 71
MALDESI	Condensed phase	~ 2.1 kDa	630 amol	Yes	38, 72
EESI/ND-EESI	Liquid sample and condensed phase	~ 18 kDa	1 pmol/L	Yes	39, 70

1.4 Research Objectives

The goal of this research was to develop new methods for merged electrospray ionization for the direct analysis of solids, liquids and particulate materials. When using these methods, the sample in complex matrices can be analyzed with no pretreatment.

This work is divided into three parts. The first study focused on direct ionization of laboratory generated dry particles by merging with an electrospray. Second, combustion products were analyzed with merged electrospray ionization. Third, this ionization method was extended with the ionization of IR laser desorbed and ablated materials by electrospray.

In Chapter 2, the mass spectrometer and other instrumentation used for the research is described along with the experimental configurations for the different experiments. In Chapter 3, the use of electrospray ionization to directly ionize laboratory generated dry particles is presented. In Chapter 4, the direct ionization of combustion products generated from fuel-rich flames as well as different types of smoke is introduced and discussed. In Chapter 5, details of IR laser ablation of various analytes, including peptides, biological fluids and pharmaceutical

products with electrospray is presented. Chapter 6 contains a summary of the conclusions obtained from the studies in Chapter 3-5, along with a discussion of the future applications of merged electrospray ionization in the analysis of biomoleucles.

CHAPTER 2. EXPERIMENTAL

Three experimental setups were used in this research: merged electrospray of dry aerosol particle, merged electrospray of combustion products, and infrared laser desorption electrospray ionization. All three setups were configured with a commercial quadrupole ion trap mass spectrometer. The descriptions of the fundamentals of quadrupole ion trap mass spectrometer operation along with detailed information of three experimental setups are provided in the subsequent sections.

2.1 Mass Spectrometer

The mass spectrometer used in this research is a Hitachi M-8000 3DQ ion trap mass spectrometer. For the experiments conducted in this research, the stock electrospray assembly was removed. A nanoelectrospray emitter was used to spray the solvent directly toward the skimmer cone of the mass spectrometer.

2.1.1 Three-Dimensional Quadrupole Ion Trap

A three-dimensional quadrupole ion trap[90, 91] consists two hyperbolic end-cap electrodes and a ring electrode that is positioned symmetrically between the end-cap electrodes, as shown in Figure 2-1. The radius of the ring electrode in the central horizontal plane (r_0) determines the size of the ion trap. The distance from the center of the ring electrode to the end-cap electrode is defined as z_0. For an ideal quadrupole ion trap, the ratio of r_0^2 to z_0^2 is generally 2, but this relation is not necessarily restricted to this value.[90]

A quadrupole ion trap can store ions and can also function as a mass spectrometer. For most commercial quadrupole ion traps, the end-cap electrodes are held at ground potential and a radio frequency (RF) voltage in the megahertz range is applied to the ring electrode.

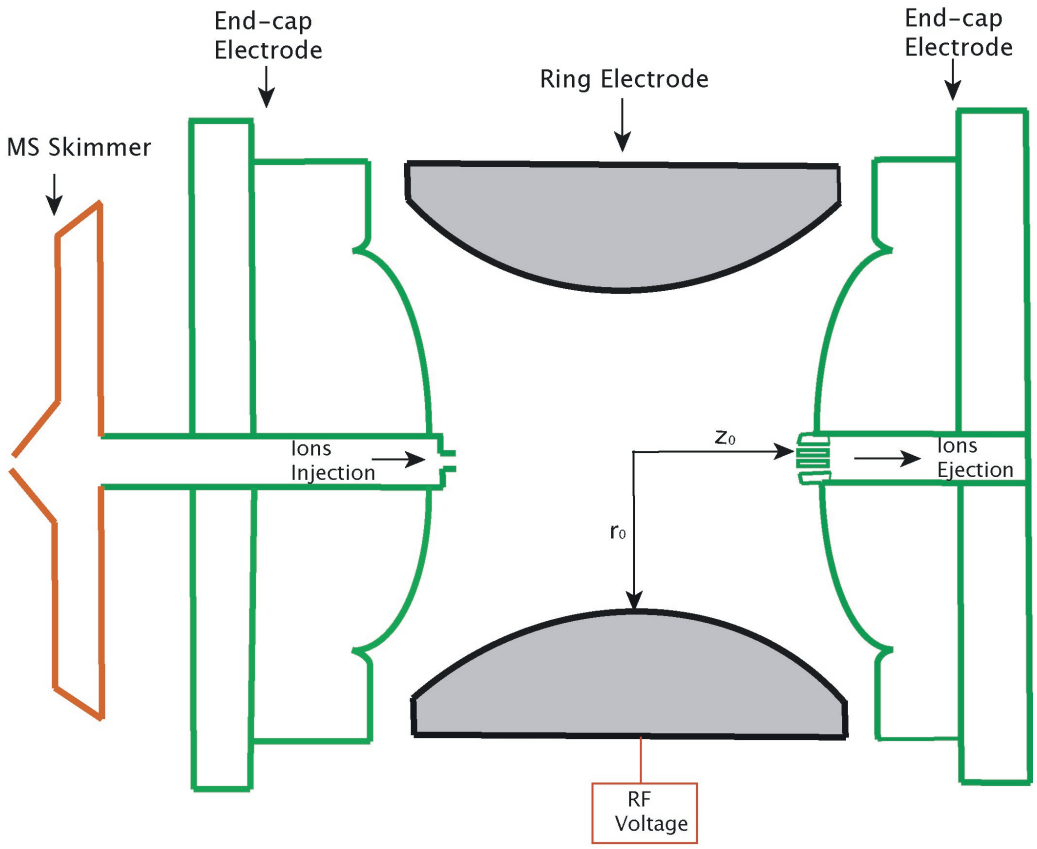

Figure 2-1. Cross-sectional view of an ion trap mass analyzer.

The motion of ions in a quadrupole field can be described by solutions of Mathieu equation[92]

$$\frac{\partial^2 u}{\partial^2 \xi} + \left(a_u - 2q_u \cos 2\xi\right)u = 0 \quad (1),$$

where *u* represents the coordinate axes x, y and z, ξ is a dimensionless parameter, and a_u and q_u are additional dimensionless quantities known as trapping parameters. The quadrupole potential at any point in the trap can be expressed in cylindrical coordinates using

$$\Phi_{r,z} = \Phi_0 \left\{ \frac{\left(r^2 - 2z^2\right)}{r_0^{\,2}} \right\} + \frac{\Phi_0}{2} \quad (2),$$

where *r* and *z* are the radial and axial dimensions, respectively. This equation shows that an ion at the center ($r = 0$) experiences a potential of $\Phi_0 /2$, where

$$\Phi_0 = U + V\cos\omega t \quad (3),$$

U is the dc potential, *V* is the amplitude of the RF applied to the ring electrode, and ω is the angular frequency.

The mass-selective instability mode is used for measuring the *m/z* of ions confined in the trap.[93] Ejection of ions from the ion trap is accomplished by changing the amplitude of the RF potential applied to the ring electrode. Each *m/z* is ejected from the trap at a specific RF amplitude. The motion of ions in the trap is expressed in terms of trapping parameters: a_z and q_z as given by

$$a_z = \frac{-8zU}{mr_0^2\omega^2} \quad (4)$$

and

$$q_z = \frac{4zV}{mr_0^2\omega^2} \quad (5).$$

Most commercial ion trap instruments do not offer the flexibility of applying a DC potential to the electrodes, thus a_z is typically equal to zero. The trap is operated along the q_z axis of the stability diagram as shown in Figure 2-2. The basis of mass analysis of the trap is the relation given by

$$\frac{m}{z} = \frac{4V}{q_{\max}r_0^2\omega^2} \quad (6),$$

where q_{max} is the maximum value of q_z at which ions exit the stability region ($q_{max} = 0.908$ under normal operating conditions). As shown in the equation, an ion with a high *m/z* becomes unstable at a higher RF amplitude compared to one with a low *m/z*.

In Figure 2-2, the trajectory is stable within the shaded region. Outside the shaded area indicated, the trajectory is unstable. Ions move in a manner that is described by the mass-selective instability scan line as raising the RF voltage until they become unstable at the boundary and then exit the trap and are detected. Ions leave the trap in the order of ascending *m/z*.

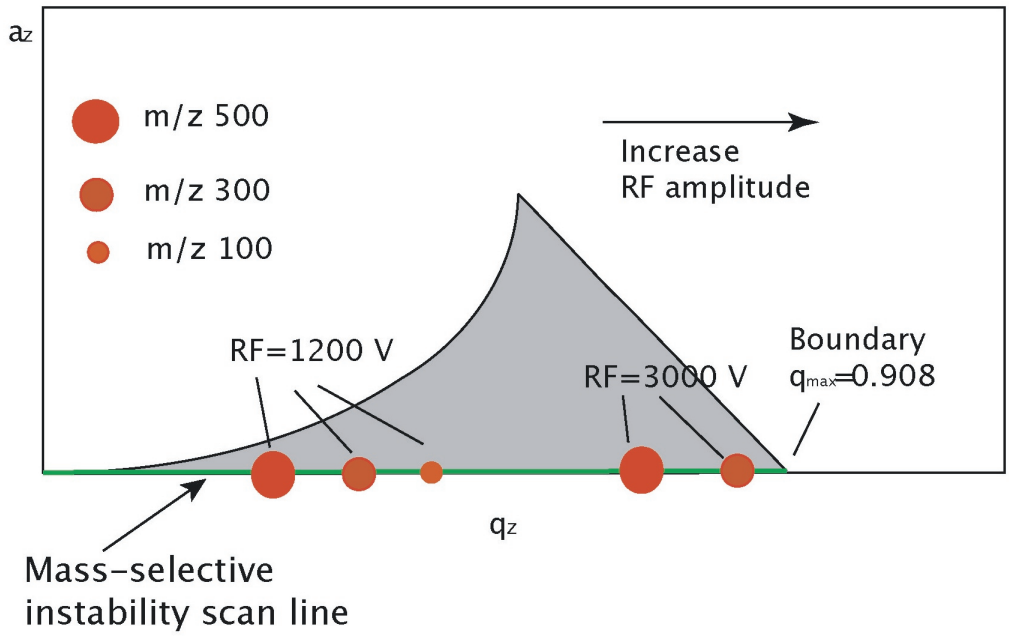

Figure 2-2. Mathieu stability diagram for a mass-selective instability scan of a quadrupole ion trap. Ions move as described by the mass-selective instability scan line (green line) with the changing of the voltage on the ring electrode, and eventually escape from the trap at the boundary.

2.1.2 Hitachi Ion Trap Mass Spectrometer

All mass spectrometry experiments described below were performed with a Hitachi M-8000 3DQ quadrupole ion trap mass spectrometer (Hitachi America, San Francisco, CA) equipped with an electrospray ionization source and a conversion dynode detector. The instrument is shown in cross-section in Figure 2-3. An ESI source was used to create ions that

pass through drift region (Aperture 1 and Aperture 2) and enter the quadrupole ion trap. Ions are trapped inside the mass analyzer and sequentially ejected into the conversion dynode detector. The inner radius of the ring electrode, r_0, is 0.707 cm. Helium gas at a pressure of 10^{-3} Torr in the trap is used as the buffer gas. The mass spectrometer is capable of measurements in a *m/z* range up to 2000. The resolution is 5000. The instrument was calibrated with two standards caffeine and bradykinin. After calibration, the mass accuracy was measured and calculated as 36 ppm for the caffeine, and 124 ppm for the bradykinin.

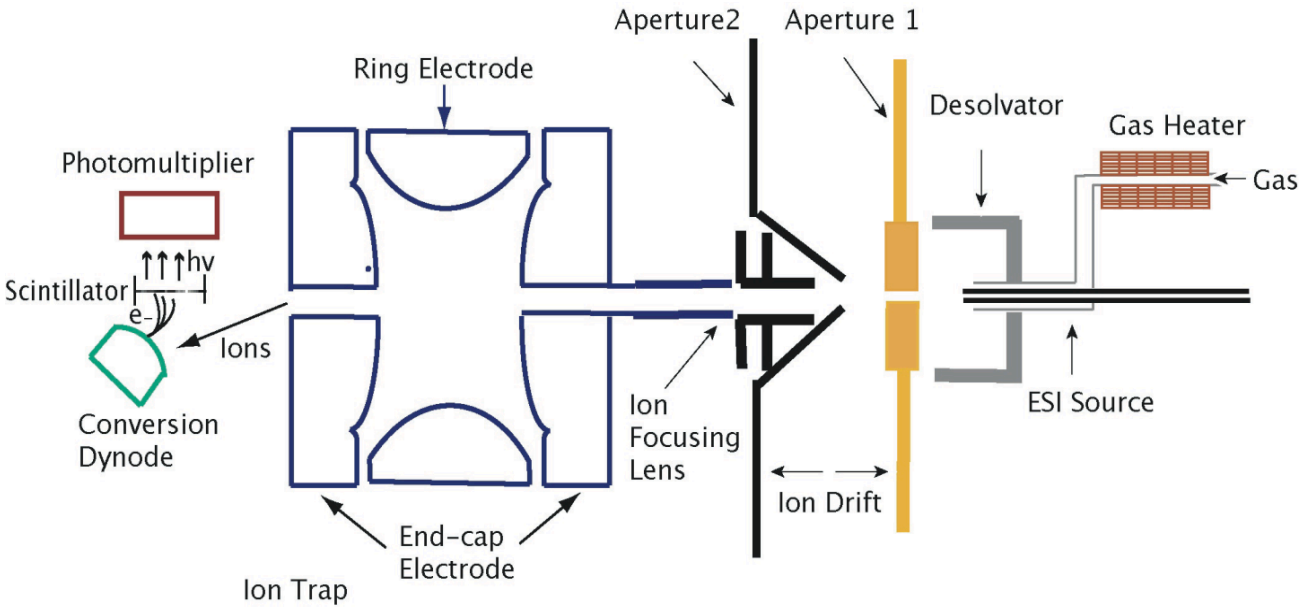

Figure 2-3. Hitachi M-8000 3DQ ion trap mass spectrometer is composed of an ESI probe, ion trap mass analyzer and a photomultiplier conversion dynode detector.

As each ion species leaves the trap in turn, the ions impinge upon an external detector. A photomultiplier conversion dynode (PCD) detector is used for this mass spectrometer. The PCD is one of the most commonly used detectors in mass spectrometry.[26] The working principle of the PCD is that the ions initially strike a dynode resulting in the emission of electrons. The electrons then strike a phosphor screen, which produces photons, which are then detected by a

photomultiplier. Ions impinging on the PCD create a series of ion signals dispersed in time, which is converted into the mass spectrum.

For the standard electrospray analysis shown below, the analyte was dissolved in 80% methanol and 0.1% acetic acid and injected into the ESI source through a syringe pump at flow rate 0.2 μL/min. The electric field applied to the ESI probe was 4 kV. The temperatures on the gas heater, desolvator, Aperture 1, and Aperture 2 were at 180 ºC, 180 ºC, 150 ºC and 120 ºC, respectively. The ion drift voltage and ion focus voltage were set to 100 V and 30 V. Figure 2-4 is the ESI mass spectrum of caffeine generated under the above described conditions. The singly charged caffeine peak is observed at *m/z* 195, and is used for calibration. The low intensity peak at *m/z* 211 may have come from solvent contamination.

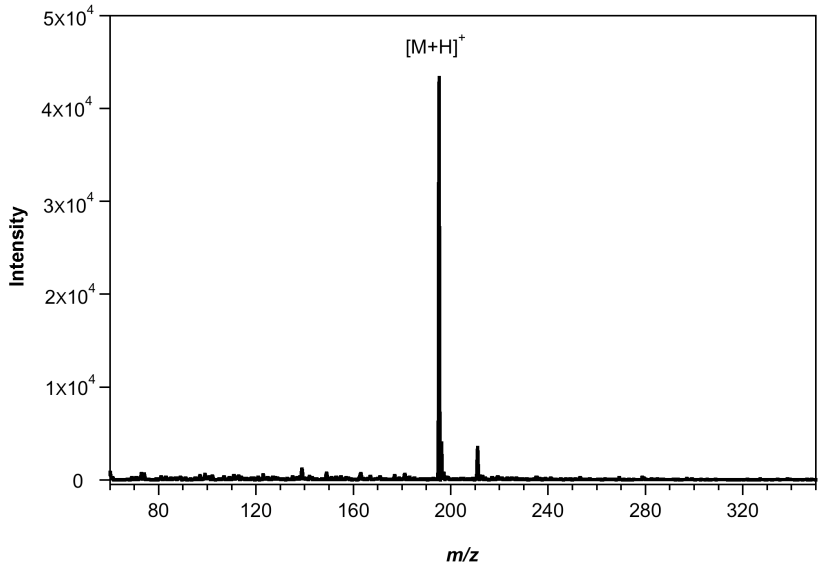

Figure 2-4. Caffeine ESI mass spectrum.

The Hitachi M8000 mass spectrometer is controlled by the 3DQ software package running on a Microsoft Windows NT computer. All mass spectra were acquired in positive ion mode for this research. The spectrum acquisition time was varied for different experiments: dry

particle ionization acquisition spectra were averaged for two minutes; combustion and IR laser desorption acquisition spectra were averaged for one minute.

2.2 Nanoelectrospray Ion Source

The original ESI source on the Hitachi ion trap was replaced with a nanoelectrospray emitter (PV 300, New Objective, Woburn, WA) as shown in Figure 2-5. This nanoelectrospray emitter had a 50 μm ID fused-silica capillary that was tapered at the tip to a 30 μm ID and a stainless steel sleeve. The emitter faced the MS skimmer cone and the tip directed at the MS skimmer orifice at distance that varied between 4 mm and 8 mm. The other side of the emitter was connected through a 50 cm long fused-silica capillary tube to a syringe pump (Harvard Apparatus, Holliston, MA). The nanoelectrospray emitter was placed on a 3-axis translating stage for easy adjustment.

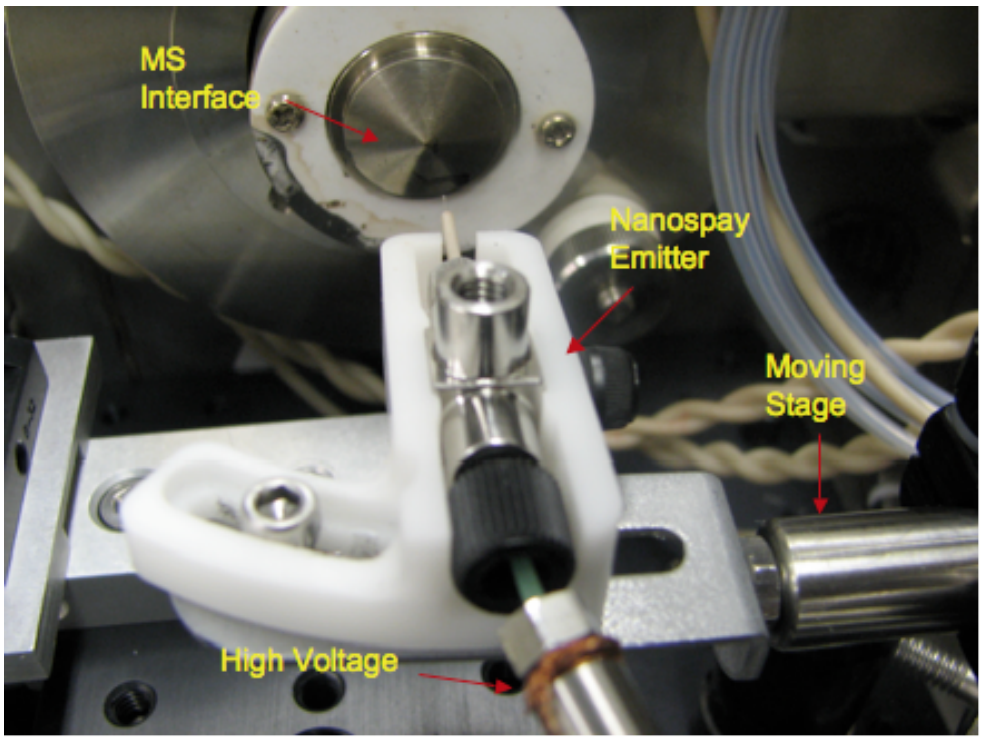

Figure 2-5. Photograph of the nanoelectrospray emitter coupled with the Hitachi ion trap MS.

Unlike conventional ESI, which requires 3 to 4 kV, a stable spray can be achieved for nanoelectrospray at 1 kV. Another advantage of nanoelectrospray is that no pneumatic gas or additional heat is required.[94] For conventional ESI, a relatively large volume of liquid exits the emitter, and pneumatic neubulization and heating is necessary to obtain a stable spray. For nanoelectrospray, only the applied voltage is required to generate a spray. However, for merged electrospray of dry particles, low-pressure nitrogen gas was used to assist the desorption and ionization process. For different experiments, the voltage on the nanoelectrospray emitter was adjusted from 1.0 kV to 2.5 kV, and the flow rate was varied from 500 to 800 nL/min. The size of the charged droplets generated by nanoelectrospray are approximately 100 times smaller than the droplets generated by conventional ESI.[95] The ionization efficiency of nanoelectrospray is higher in comparison to conventional electrospray.

Figure 2-6 is the mass spectrum of a 200 μM caffeine sample using nanoelectrospray. The singly charged protonated caffeine peak $[M + H]^+$ is observed as it is in the mass spectrum of a 200 μM caffeine sample by conventional electrospray in Figure 2-4. However, the peak obtained by nanoelectrospray is 3.5 times more intense than the peak obtained by electrospray.

2.3 Material Generation

Three types of sample sources were used: dry particle, combustion, and IR laser desoption. The sample generation and experimental configurations of each are described in the subsequent sections.

2.3.1 Merging of Dry Particles

Powder samples were dispersed using a fluidized bed aerosol generator. The particles were merged with charged droplets from the nanoelectrospray source.

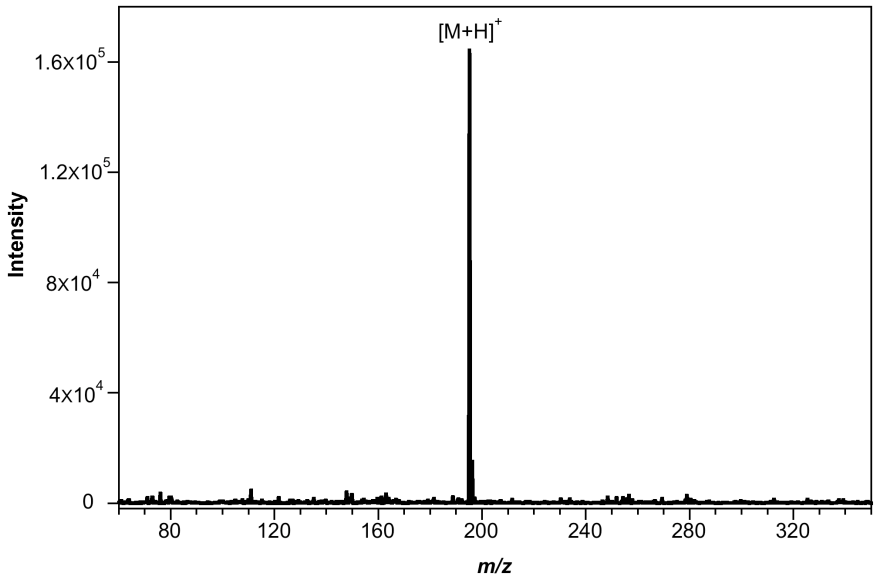

Figure 2-6. Caffeine nanoelectrospray mass spectrum.

2.3.1.1 Aerosol Generator

Dry aerosol particles were generated with a fluidized bed powder disperser (Model 3400, TSI, Shoreview, MN). This instrument is a general-purpose powder disperser that produces particles in the size range from 500 nm to 40 μm and in concentrations from 10 to 100 mg/cm^3. The fluidized bed aerosol generator is illustrated in Figure 2-7. This instrument is composed of a fluidized bed chamber and a powder reservoir. The fluidized bed contains 100 μm diameter bronze beads supported by a porous screen that allows dry air to flow through, yet prevents the passage of any powder. Powder is fed to the fluidized bed by a variable speed bead chain. Dry air flows through the porous screen causing the "boiling" of the bronze beads. The continuous motion of the bronze beads disperses the analyte powder into particles, which are then carried upward by the airflow through a vertical elutriator, a stainless steel tube with a length of 333 mm. At the top of the elutriator, a cyclone causes particles with high inertia to collide with the wall of the cyclone, thus preventing large particles from being dispersed. The particle size can be

controlled by adjusting the flow of air through the fluidized bed, and the particle concentration can be adjusted by changing the feed rate of powder into the fluidized bed chamber.

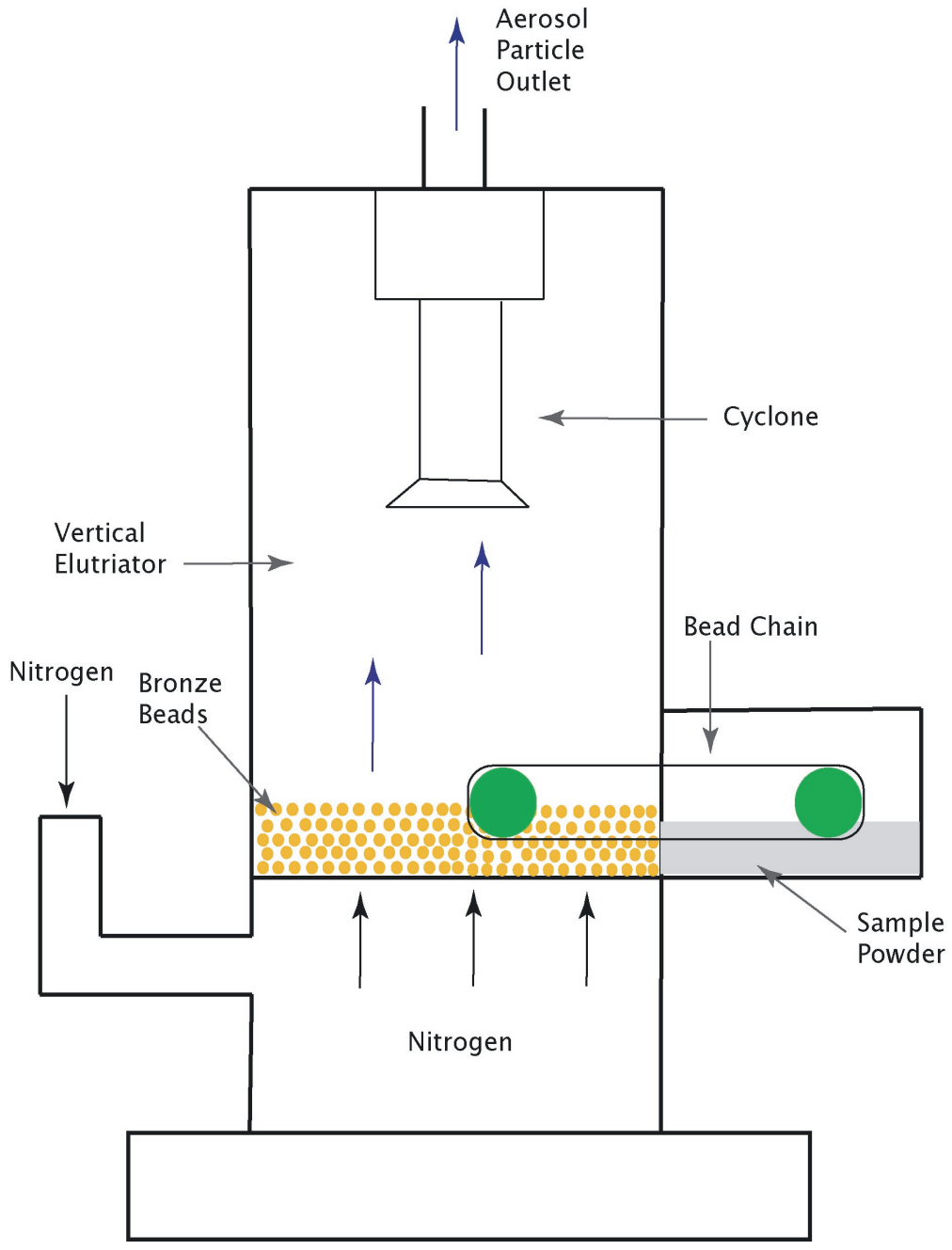

Figure 2-7. Fluidized bed aerosol generator.

In this research, nitrogen gas was used at a flow rate of 10 L/min. Between 3 and 4 grams of sample was required to fill the powder reservoir. At the set flow rate, the cyclone prevents particles larger than approximately 10 μm from exiting the particle generator. Silicon (platinum-cured) tubing (96410-15, Masterflex) 4.8 mm i.d. was connected to the outlet of the aerosol generator and extended to the mass spectrometer and the nanoelectrospray emitter. To allow a constant flow of particles, the aerosol generator was turned on for one minute before acquiring a mass spectrum.

2.3.1.2 Particle Sizer

An aerodynamic particle sizer (APS, Model 3321, TSI, Shoreview, MN) was used to measure the particle size and concentration. The APS measures the aerodynamic diameter and light-scattering intensity in real-time. Particles in the size range between 500 nm and 20 μm can be measured to a precision of 30 nm. Light-scattering intensity measurements are recorded for particles between 300 nm and 20 μm in size. Particle concentrations up to 10,000 particles/cm^3 can be measured. A detailed descriptions of its theory of operation can be found elsewhere.[82]

For dry particle measurement, particles exiting the particle generator were directed into the APS through a silicon tube connected to one side of a plastic Y connector. The other side of the Y connector was open to the air. The purpose of the Y connector was to balance the pressure inside the particle sizer. The sampling time for particle size and concentration measurements was 20 seconds. Figure 2-8 is the particle size distribution plot of erythromycin particles produced using the aerosol generator. Erythromycin particles were in the size range from 0.5 μm to 3 μm, and the mean particle size was around 1.0 μm. It can also be seen in the figure that erythromycin particles with sizes of 0.5 μm or smaller have the highest concentration of 250 particles/cm^3. However, note that particle size and count measurements below 500 nm are significantly less

precise. As the particle size increases from 0.5 μm to 3 μm, the particle concentration has a roughly Gaussian shape with a highest concentration of approximately 150 particles/cm^3 at the size of 0.8 μm.

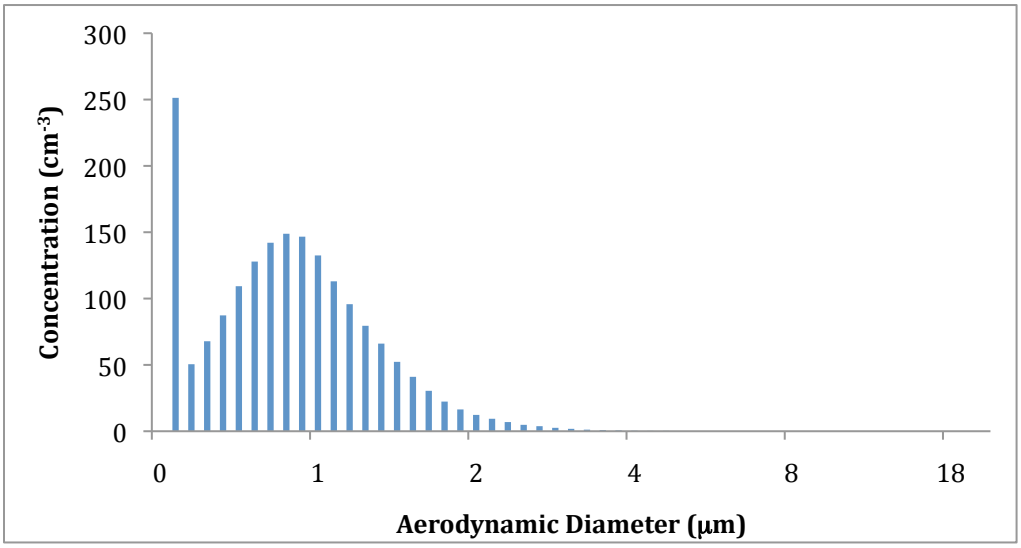

Figure 2-8. Particle size distribution plot of erythromycin particles generated from the aerosol generator.

2.3.1.3 Configuration of Dry Particle Merged Electrospray

The configuration of the dry particle merged electrospray ionization source is illustrated in Figure 2-9. Unlike the nanoelectrospray experiment discussed in Section 2.2, in which the nanoelectrospray emitter was perpendicular to the MS skimmer cone, the nanoelectrospray emitter was placed 4 mm away and at a 60° angle to the MS skimmer in this experiment. Silicon tubing connected the outlet of the aerosol generator to the mass spectrometer and the nanoelectrospray emitter. The angle between the silicon tubing and the nanoelectrospray emitter was 90°. The interaction of the dry particles from the aerosol generator and the charged solvent droplets occurred in front of the MS skimmer cone.

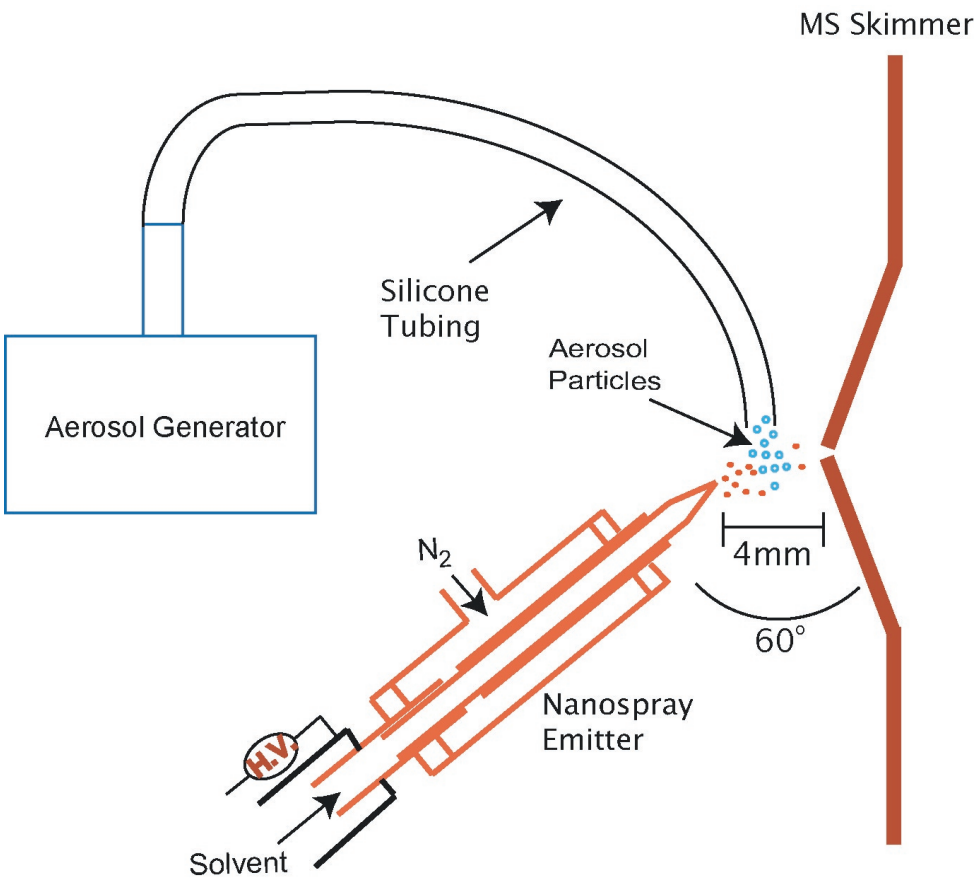

Figure 2-9. Schematic of the dry particle merged electrospray setup.

2.3.2 Combustion Source

Fuel-rich combustion was obtained using a home-built flame generator. The products from the flame were ionized directly by merging into the charged droplets from the nanoelectrospray source.

2.3.2.1 Flame Generator

The flame source consisted of a propane tank (Bernzomatic, Wilmington, OH) and a glass bubbler as illustrated in Figure 2-10. Propane gas with less than 1 ppm additive ethanethiol flowed through a brass valve (UL2317, Bernzomatic, Wilmington, OH), and a silicon tube was used to connect the tank to the bubbler inlet.

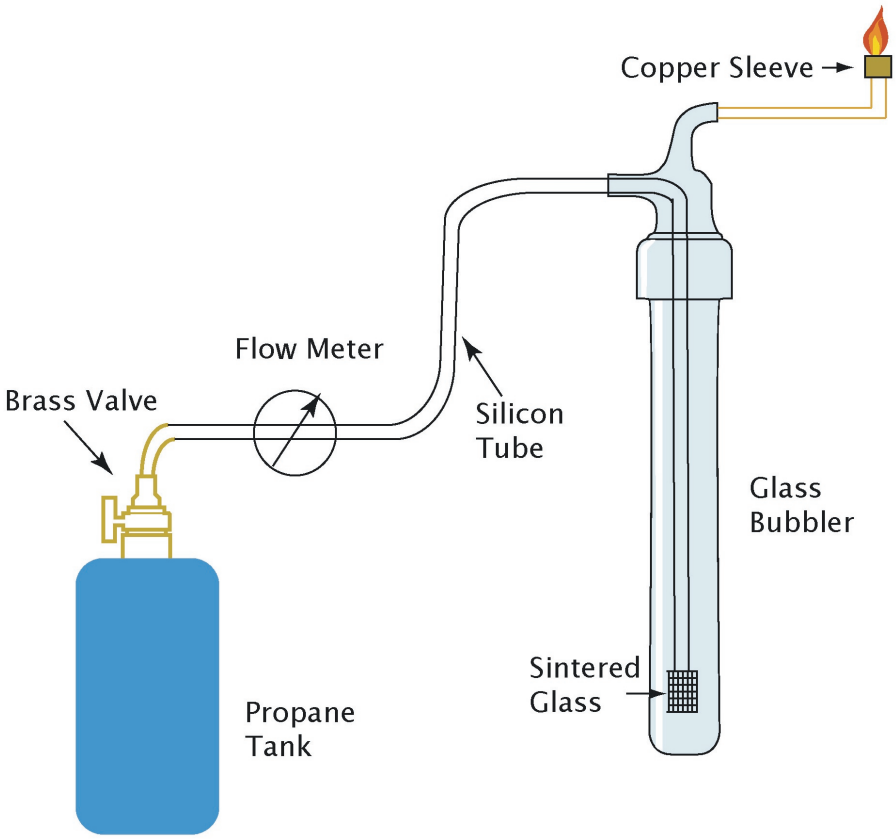

Figure 2-10. Schematic of the flame combustion source setup.

A flow meter controlled the flow rate of the propane gas. The end of the bubbler inlet was a porous sintered glass tip. Solvent or fuel was added to the bubbler to a level above the sintered glass tip. A mixture of propane and solvent or fuel vapor was generated due to the high vapor pressure of the liquid. The gas mixture flowed through copper tubing to the propane burner head. A copper sleeve covered the burner holes to control the air-to-fuel ratio. Fuel-rich combustion was achieved by limiting the air flow.

Particle combustion products generated from the flame source were measured with the APS described in section 2.3.1.2. A copper tee was placed above the flame to transfer the combustion products to the particle sizer. One side of the copper tee was connected to nitrogen,

and the other side was connected to a plastic tube (8889-224104, MG Scientific, Pleasant Prairie, WI) extending to the particle sizer through a Y connector. Figure 2-11 is the particle distribution plot of particles generated by combustion of the diesel fuel and propane gas mixture. Only the particles with the sizes greater than 0.5 μm are shown in the figure.

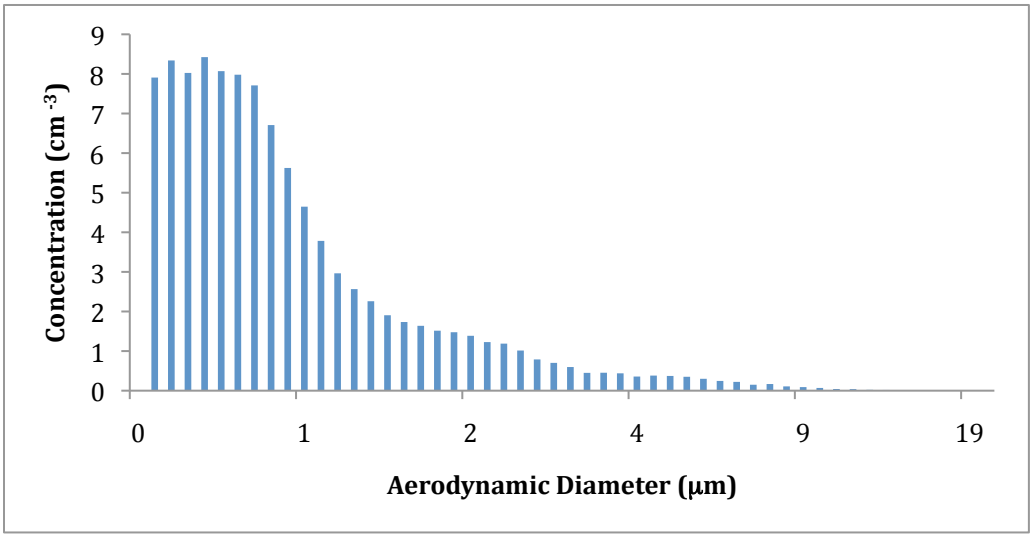

Figure 2-11. Particle distribution plot of diesel fuel and propane gas mixture combustion products.

2.3.2.2 Mass Spectrometer Configuration

The configuration of the flame source with the mass spectrometer is illustrated in Figure 2-12. A 1/2 in. inner diameter copper tee was placed above the flame to transfer the combustion products to the ion source. The flame position was around 2~3 cm inside the bottom of the copper tee. One side of the copper tee was connected to the nitrogen carrier gas and the exit was open and parallel to the MS skimmer cone and perpendicular to the nanoelectrospray emitter. A venturi section made from a 1/4 in. inner diameter stainless steel union tee (A-400-3, Swagelok) was placed inside the copper tee at the center. The nanoelectrospray emitter was held 8 mm away

from the MS skimmer cone. As a result of the venturi effect, combustion products were pulled from the flame and into the spray.

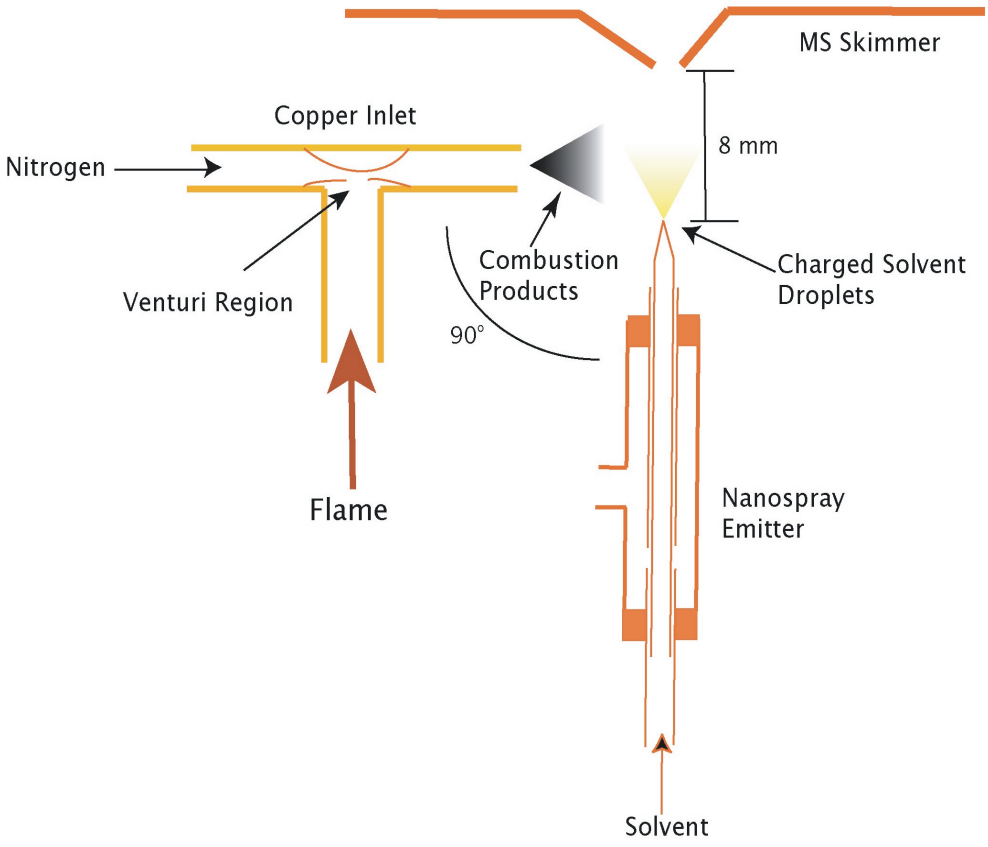

Figure 2-12. Configuration of the flame source with the mass spectrometer.

Smoke was also sampled directly. The smoke was generated directly from the combustion of cigarettes, incense or candles. While the smoke was generated, the burning material was placed between the nanoelectrospray emitter and the MS skimmer cone and around 5 cm below the emitter as illustrated in Figure 2-13. The smoke slowly passed through the path of the charged droplets.

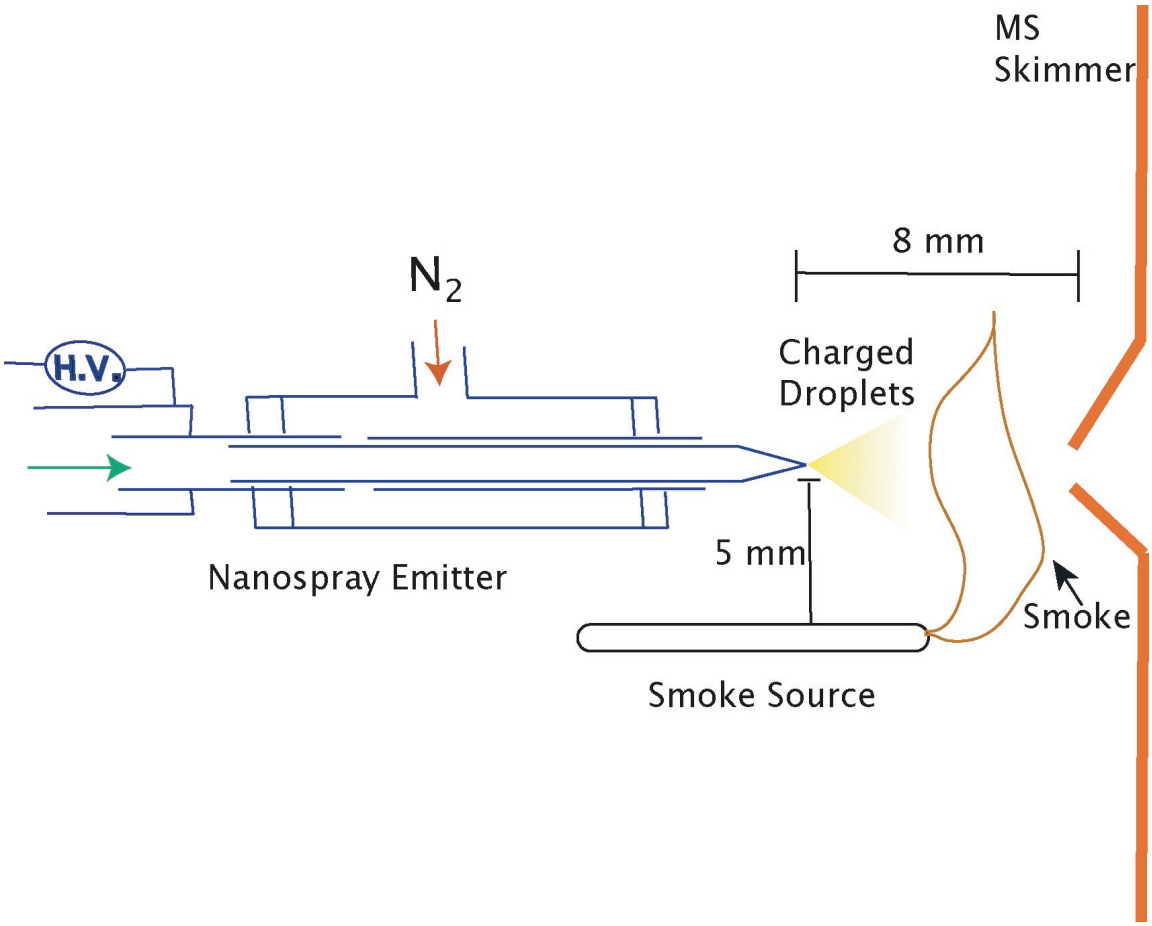

Figure 2-13. Configuration of the smoke source with the mass spectrometer.

2.3.2.3 Combustion Product Collection and Analysis

Diesel fuel combustion products were collected with an Andersen N6 single–stage impactor (Thermo Andersen, Smyrna, GA). The impactor is composed of an aluminum inlet cone, jet stage and a base plate held together with three spring clamps and sealed with an O-ring gasket as illustrated in Figure 2-14. The impactor is equipped with a 400 hole accelerator plate containing 0.26 mm diameter holes. Each holes serves as a separate impaction mini-jet. The impactor was operated at 28.3 L/min, and it uses a rotary vane pump specifically designed and

calibrated for this impactor. The impactor has a sharp cutoff diameter for particles greater than 0.6 μm.

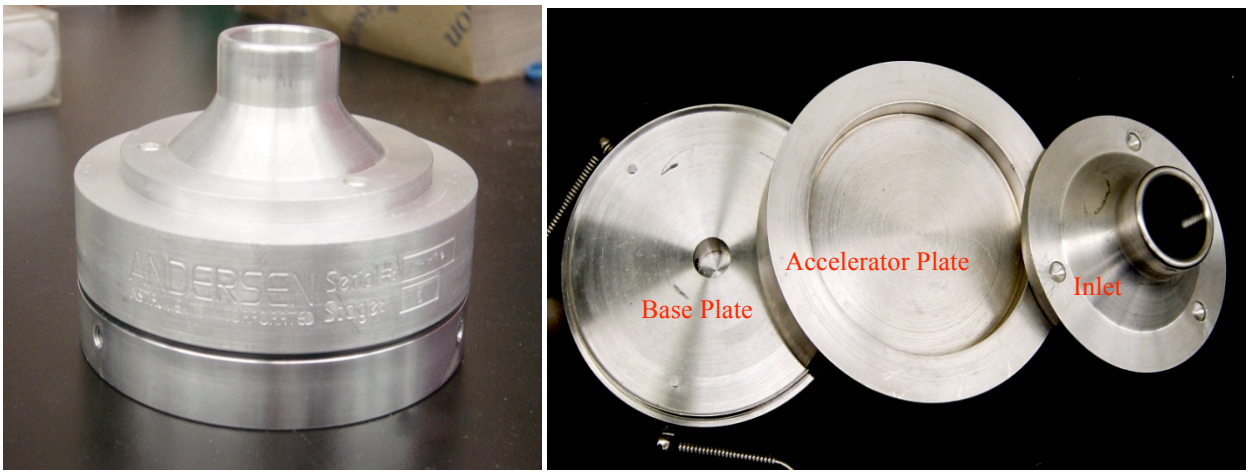

Figure 2-14. Image of assembled (left) and disassembled (right) Andersen N6 Single-stage Impactor.

Diesel fuel flame particulate was collected with the impactor for approximately 1 hr using the configuration illustrated in Figure 2-15. The flame products were directed through a copper inlet to a glass connector, and connected to the impactor inlet. For safety, the sample collection was performed in the fume hood. After 1 hr collection, approximately 0.5 mg of the collected samples were weighted, and transferred from the base plate of the impactor into a glass vial filled with 5 mL methanol and 0.2% acetic acid solution for the MALDI analysis.

The collected sample was analyzed with a MALDI-TOF mass spectrometer (Omniflex, Bruker, Billerica, MA). MALDI-TOF is equipped with a nitrogen laser (λ=337 nm, 3 ns pulse width) operated at 5 Hz. It can be operated in both linear and reflectron mode. In this work, no matrix was used for the analysis and the data was obtained in reflectron mode.

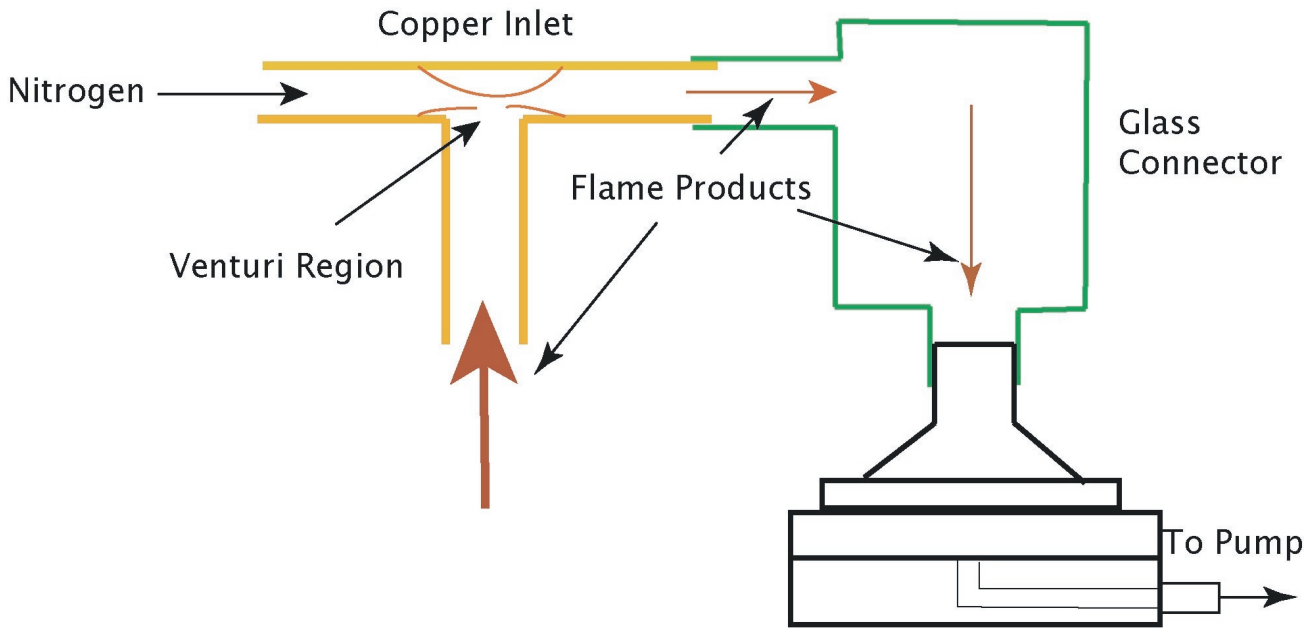

Figure 2-15. Configuration of the flame products collection by Andersen N6 impactor.

2.3.3 Infrared Laser Desorption Electrospray Ionization

In this experiment, the materials generated from IR laser desorption and ablation were merged and post-ionized by nanoelectrospray. Proteins, biological fluids and pharmaceuticals were tested with this system.

2.3.3.1 Laser Desorption and Ablation

Laser desorption and ablation is the process of removing material from a solid or liquid sample by irradiating with a pulsed laser. Both ultraviolet (UV) laser and infrared (IR) lasers can be used to ablate material from the sample. The amount of material removed with a single laser pulse depends on the material's optical properties and the laser wavelength. Laser pulses can vary over a wide range of durations and fluences and can be precisely controlled. A schematic (Figure 2-16) illustrates a common laser desorption and ablation setup. A stainless steel sample target is usually used for the sample deposition, and a thin layer of sample solution is placed on

this sample target. Laser light is directed through an attenuator and focusing lens onto the sample. Molecules, particles and droplets are produced by laser irradiation of the sample.

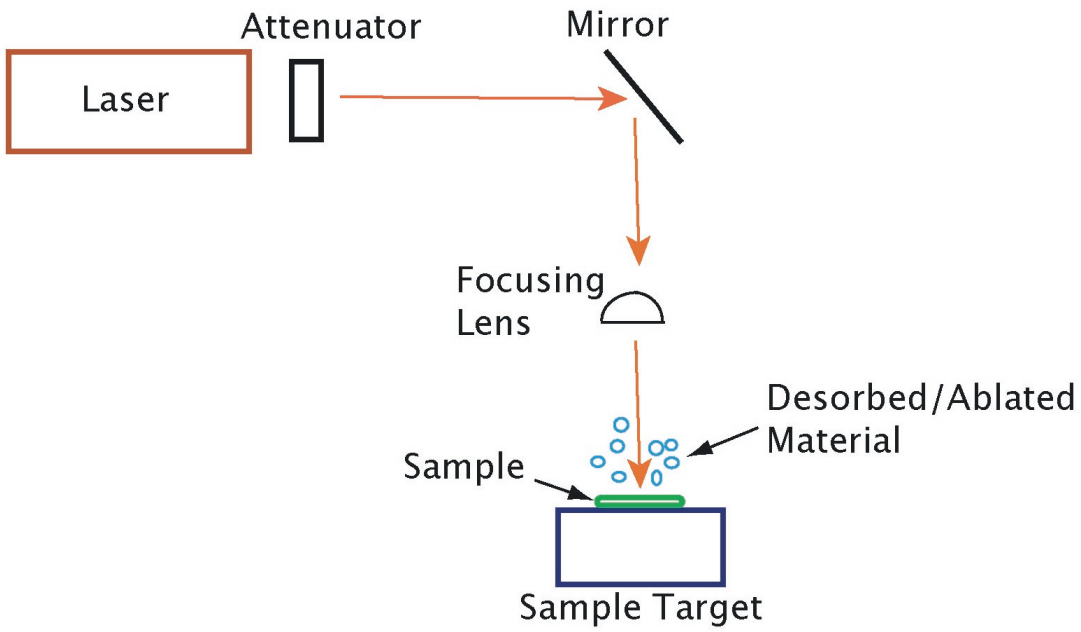

Figure 2-16. Laser desorption and ablation setup.

2.3.3.2 Er:YAG Laser

A pulsed solid-state Er:YAG laser (Bioptic Lasersysteme, Berlin, Germany) was used in this research. An Er:YAG laser emits light with a wavelength of 2.94 μm. The maximum pulse energy was 9 mJ with a pulse duration of 100 ns and a repetition rate of 10 Hz. Figure 2-17 is the schematic of the Er:YAG laser configuration. The laser was coupled into the instrument with a 50 mm focal length (25 mm diameter) CaF_2 plano-convex lens and a 450 μm core diameter germanium oxide optical fiber (Infrared Fiber Systems, Inc., Silver Spring, MD). The optical fiber provides an easy way to manipulate the laser light so that it can be delivered to the target in a safe and relatively simple fashion. The optical fiber was placed on a xyz translation stage (MT-XYZ; Newport) in front of the CaF_2 plano-convex lens. The output of the optical fiber was

collimated and focused on the sample surface using a 12.5 mm diameter CaF_2 plano-convex lenses with focal lengths of 50 and 20 mm respectively. Similar coupling of a pulsed IR laser with a sapphire optical fiber has been described previously.[96] The lenses at the output of the optic fiber were mounted on a xyz translation stage for focusing and aligning the laser with respect to the sample and nanoelectrospray. The laser beam was incident at 45° with respect to the sample target. The spot size of the laser beam at the target was approximately 200 μm as determined with burn paper. The laser energy at the output end of the optical fiber was 1.0 mJ/pulse. An additional 10 to 20% attenuation of the laser energy at the target is expected due to absorption and reflection losses in the remaining optical components.

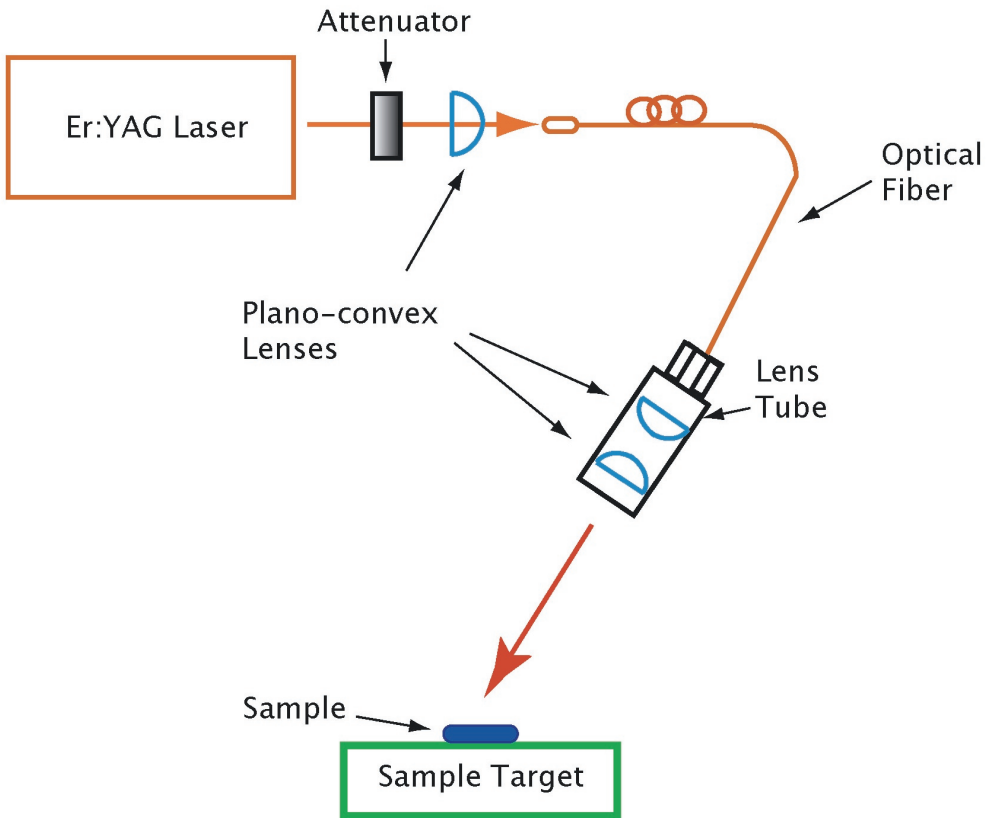

Figure 2-17. Er:YAG laser setup. The laser was focused onto the optical fiber by a 50 mm plano-convex lens. The output of the fiber was focused onto the sample using two plano-convex lenses with focal lengths of 50 and 20 mm respectively.

2.3.3.2 Infrared Laser Desorption Electrospray Ionization Source Configuration

Figure 2-18 shows a photograph and a schematic of the infrared laser desorption electrospray ionization sourc. The nanoelectrospray emitter was attached to a compact linear xyz translation stage. A stainless steel sample target was attached to a xyz translation stage, and was positioned between the MS skimmer cone and the nanoelectrospray emitter. The nanoelectrospray source was placed 6 mm from the skimmer cone and samples were placed 5 mm below the aperture. The pulsed laser was directed onto the sample so that the point of irradiation was at the mid point between the spray tip and the skimmer cone. Samples were deposited on the sample plate and irradiated with the laser. Material that was desorbed or ablated by the laser was ionized by interaction with the charged droplets in the ESI plume.

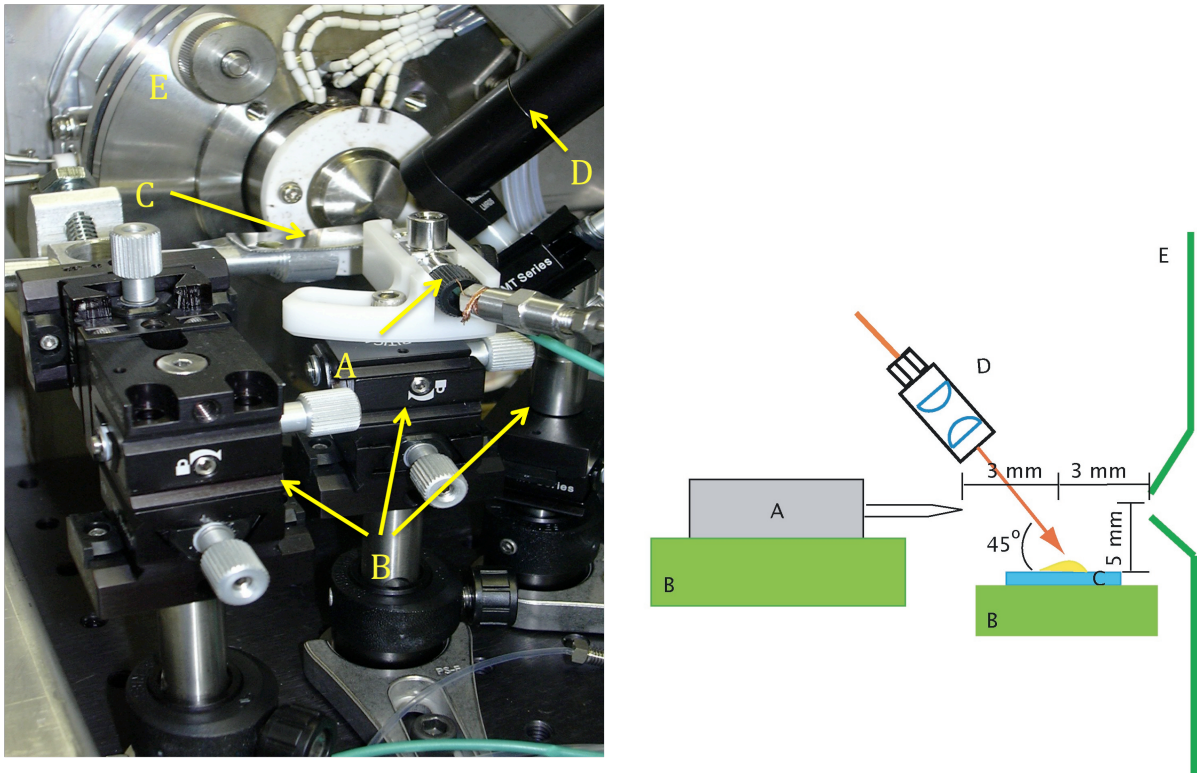

Figure 2-18. Photograph (left) and schematic (right) of the IR MALDESI ion source. A is the nanoelectrospray emitter, and it is placed on an xyz translation stage B. C is the sample target. D is the lens tube, which is used to hold the plano-convex lenses. E is the mass spectrometer skimmer.

2.4 Reagents and Chemicals

For the dry aerosol particle experiments, the reagents caffeine, lysine, asparagine and erythromycin A were used in powder form as obtained from the manufacturer (Sigma, St. Louis, MO). Commercial ibuprofen tablets (Nuprin) and artificial sweetener (Splenda) were ground into powder using a mortar and pestle. Instant cocoa powder (Starbucks) was used directly from the package. The solvents, HPLC grade acetonitrile and formic acid, were used as obtained from the manufacturer (Sigma) without further purification.

For the fuel-rich combustion experiments, toluene and m-xylene were used as obtained from the manufacturer (Sigma). Diesel fuel was purchased from a local Exxon Mobil gas station. Cigarettes (Camel), scented sandalwood incense sticks (Florasense), and paraffin wax candles were used directly from the package. The solvents HPLC grade methanol and acetic acid were used as obtained from the manufacturer (Sigma) without further purification.

For the IR laser assisted desorption electrospray ionization experiments, the peptide bradykinin and protein cytochrome c were purchased from Sigma-Aldrich (St. Louis, MO). Solubilized ibuprofen capsules (Advil LIQUI-GELS, Wyeth; Madison, NJ), cough syrup (Nyquil, Vicks; Procter & Gamble; Cincinnati, OH) and hydrocortisone cream (Cortizone, Pfizer Inc.; Morris Plains, NJ) were purchased from a local drug store. Blood was obtained from a volunteer using a lancet with the droplet directly transferred to a stainless steel target for analysis. Urine samples were collected using centrifuge tubes from two volunteers, a healthy person and a hypertension patient who had recently taken the drug atenolol. The urine samples were analyzed by depositing 3.0 μL directly onto the target without any sample pretreatment. HPLC grade methanol and acetic acid were obtained from Fisher Scientific (Pittsburgh, PA) and ultra-pure water (18 MΩ-cm, Barnstead E-pure System, Dubuque, IA) was used.

CHAPTER 3. MERGED ELECTROSPRAY OF AEROSOL PARTICLES*

Part of the work reported in this chapter has been published in *Rapid Communications in Mass Spectrometry*.[97]

3.1 Introduction

As described in Chapter 1, nebulized liquid sample particles and laser desorbed or ablated materials can be ionized by merging with electrospray under ambient conditions. In the research described in this chapter, this method has been extended by merging an electrospray with analytes in dry aerosol particles. Merging of the dry particles with the electrospray leads to the ionization of material in the dry particles.

The objective of this research was the development of an ionization method for the rapid analysis and detection of dry aerosol particles without collection and pretreatment. The effects of aerosols on human health, atmospheric chemistry, and climate are among the central topics in current environmental research,[98, 99] and the ability to rapidly analyze aerosols at ambient condition is an important goal in this area. The study of merged electrospray ionization for the analysis of dry aerosol particles will help to reach this goal. Further, the analysis of dry aerosol particles using merged electrospray ionization can aid in the understanding of laser desorption electrospray ionization described in Chapter 5. Laser desorption and ablation generates molecules and particles. Since dry particles can be directly ionized by electrospray, using electrospray to ionize laser-generated materials should also be applicable.

In this study, materials in dry powdered samples were ionized directly through the interaction with an electrospray of charged solvent droplets. Dry powder samples were loaded

*Reprinted by the permission of Wiley-Blackwell.

into a fluidized bed powder disperser and entrained in a flow of compressed nitrogen gas. The dry aerosol particles were merged with a solvent-only electrospray. Ions formed through the interaction of the electrosprayed droplets and dry particles were introduced into the ion trap mass spectrometer. Samples of powdered lysine, asparagine, caffeine, erythromycin, powdered cocoa mix, artificial sweetener and ibuprofen were tested with this method.

3.2 Experimental

The experimental configuration for dry particle merged electrospray was described in detail in Chapter 2, Section 2.3.1. The nanospray tip was held 4 mm away from the sampling cone of the mass spectrometer at a 60º angle from the skimmer cone axis. An equal volume mixture of acetonitrile and 0.2% formic acid was used as the spray solvent, which was pumped through a 50 μm i.d. silica capillary with a syringe pump at a flow rate of 500 nL/min. Nitrogen gas at 3 PSI (20 kPa) pressure was used as the pneumatic assist gas. The voltage applied to the needle and the sampling cone were +2.0 kV and +40 V, respectively. The angle between the 4.8 mm i.d. silicon tubing and the nanosprayer was approximately 90º for this work. However, no significant difference in the signal-to-noise ratio was observed when the angle was varied between 70º and 100º. Mass spectra were acquired in positive-ion mode and ions were accumulated for 100 ms in the trap. The reproducibility of the aerosol DESI spectra was verified by repeating experiments three times.

The size of the particulate from the fluidized bed aerosol generator varied somewhat depending on the grain size of the analyte powder. The mean aerodynamic diameters for the analytes used in this work were caffeine (1.3 μm), erythromycin A (1.0 μm), cocoa (2.9 μm), sweetener (1.3 μm), and ibuprofen (2.0 μm). The total mass concentration of the particles at the outlet varied between 0.2 and 2 mg/m^3.

Lysine and asparagine were used initially to test the applicability of this ionization method, and they were handled differently than the other samples. Samples of lysine and asparagine were ground into powders using a mortar and pestle. The sizes of the ground particles were approximately 100 μm in diameter measured with a direct measuring microscope (Edmund Scientific, Barrington, NJ). Note that this optical method is not efficient at detecting nm sized particulate. Then, the powder was placed in a micropipette tip that worked as a funnel, allowing the powder to drop through the tip under the influence of gravity when tapped. The micropipette was held 1 cm above the nanospray emitter, and lysine and asparagine powder were dispersed directly into the path of the nanospray solvent droplets. Other experimental conditions were the same as indicated above.

3.3 Results

The mass spectra generated by directly dispersing the lysine and asparagine powders into the nanoelectrospray are shown in Figure 3-1 and Figure 3-2, respectively.

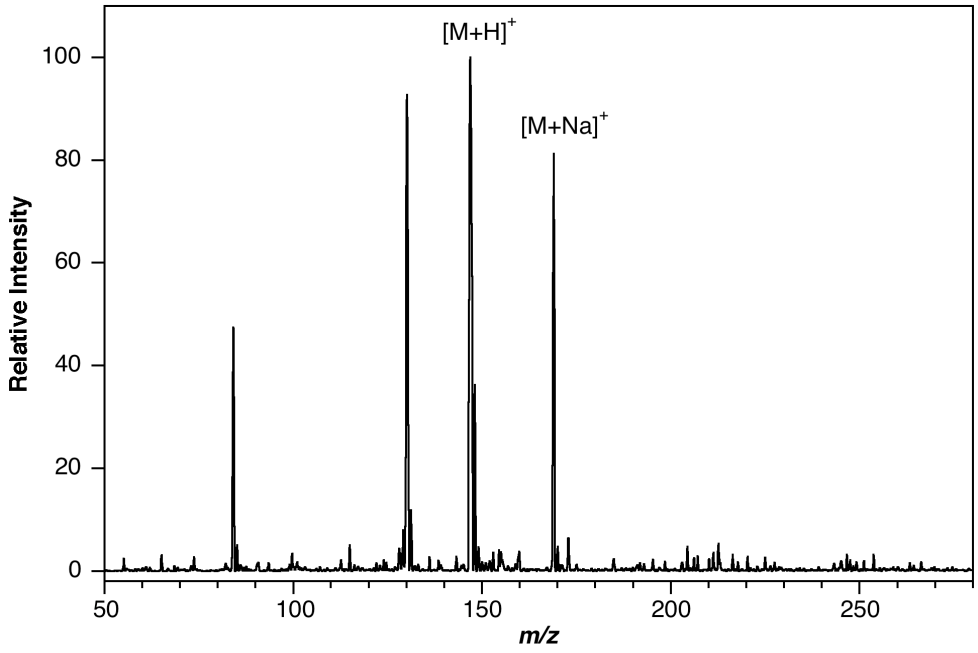

Figure 3-1. Positive-ion merged electrospray ionization mass spectrum of lysine.

For lysine (MW = 146 Da) particles, three intense peaks were observed in the spectrum. The peak at *m/z* 130 represents the protonated molecule after loss of a hydroxyl group (–OH). The peak at *m/z* 147 and the *m/z* 169 peak represent the protonated lysine molecule $[M + H]^+$, and the sodium-cationized lysine $[M + Na]^+$ ion. For the asparagine (MW 132) particles, the peaks observed at *m/z* 155 and 133 correspond to the sodium-cationized asparagine molecule $[M + Na]^+$ and the protonated asparagine molecule $[M + H]^+$, respectively. There are other peaks in the spectrum that are likely due to fragmentation or aggregation of the analyte molecules. These results suggest that charged droplets from the electrospray are able to directly ionize molecules in dry particles without completely dissolving them. Due to the relative large sizes of the particles, the ionization likely occurs through the brief interaction between the charged solvent droplets and the analyte dry particles. The solvent droplet may desorb the analyte molecule from the surface of the dry particle. However, it is possible that nm sized particles could participate in this process.

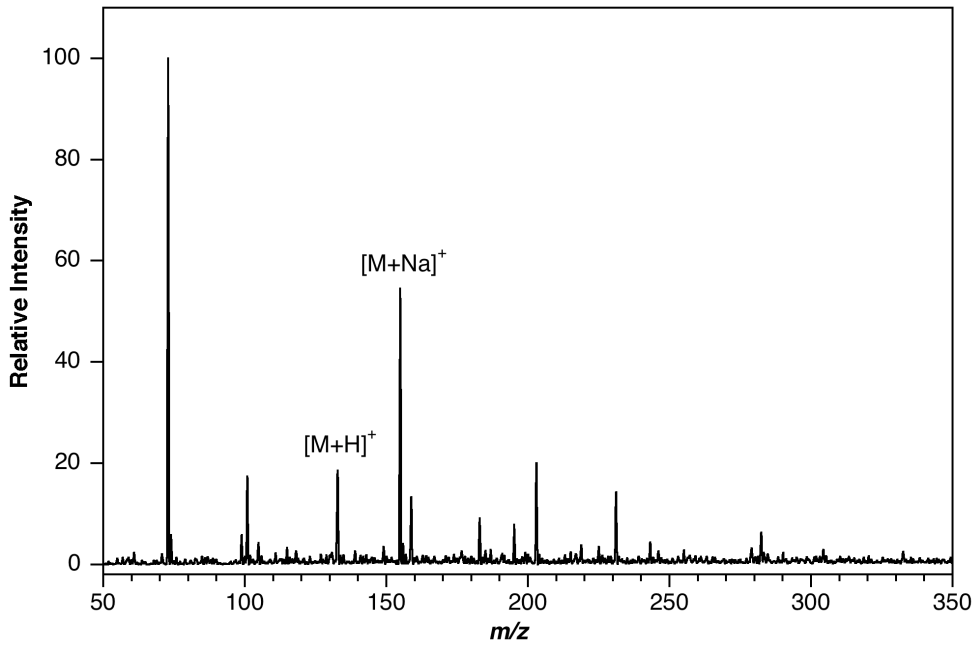

Figure 3-2. Positive-ion merged electrospray ionization mass spectrum of asparagine.

A mass spectrum obtained from direct ionization of caffeine powder dispersed using the aerosol generator is shown in Figure 3-3. The most intense peak in the spectrum corresponds to the protonated caffeine molecule, $[M + H]^+$, at *m/z* 195. A less intense peak at *m/z* 217 corresponds to sodium-cationized caffeine, $[M + Na]^+$. The spectrum is similar to the caffeine conventional ESI mass spectrum as shown in Figure 2-4 and Figure 2-6. This result shows that caffeine powder can be directly ionized by the charged solvent droplets. However, due to the high vapor pressure of caffeine, it is impossible to tell whether the MS signal comes from the particles or from the caffeine vapor.

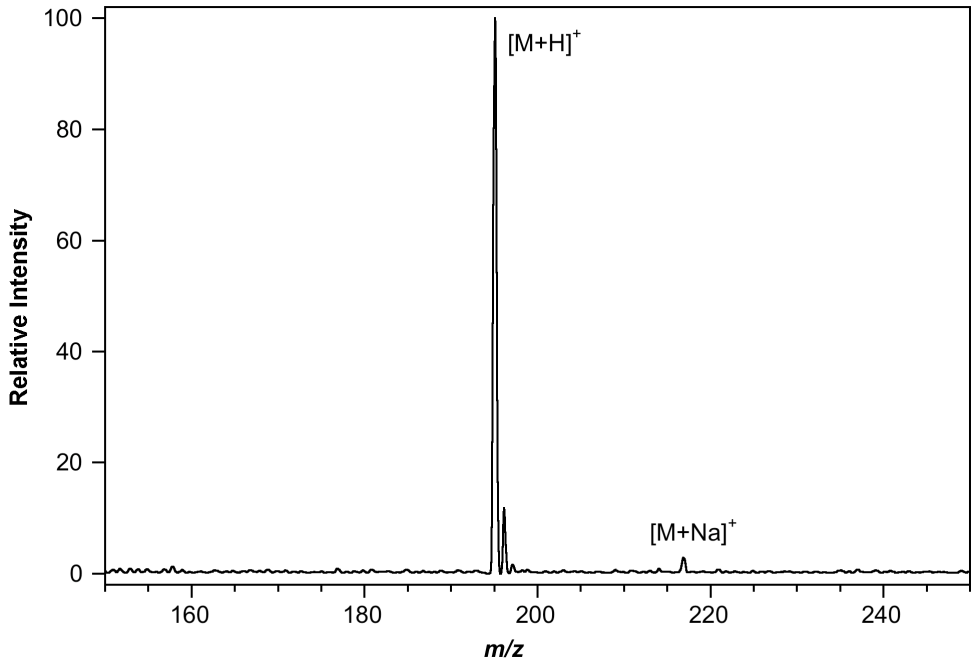

Figure 3-3. Positive-ion merged electrospray ionization mass spectrum of caffeine; the $[M + H]^+$ peak is at *m/z* 195.

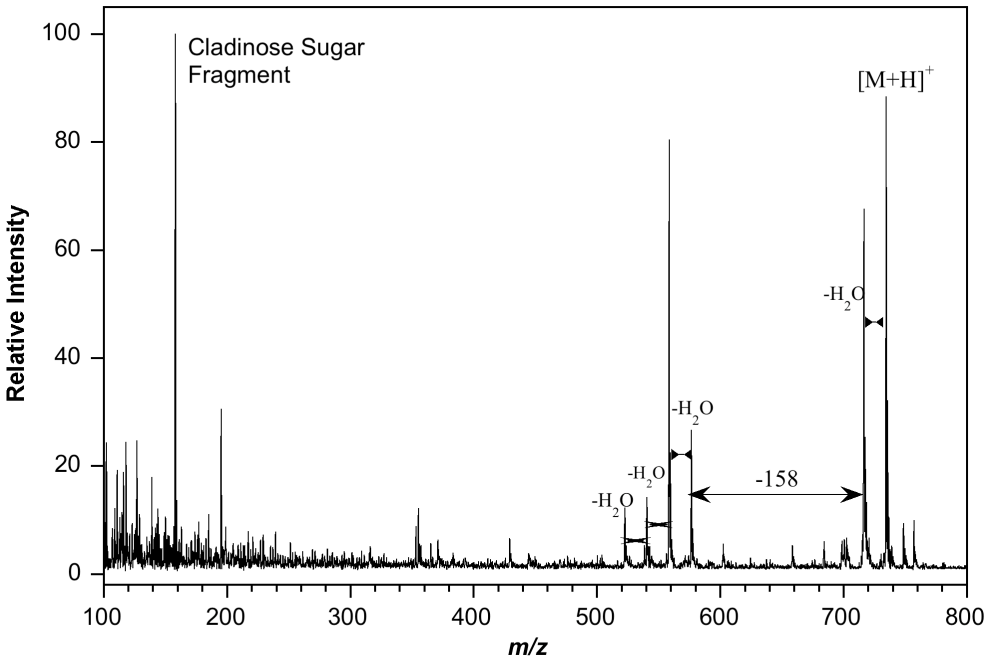

Figure 3-4. Positive-ion merged electrospray ionization mass spectrum of erythromycin; the $[M + H]^+$ peak is at *m/z* 734.

To further address this question, a higher mass and lower vapor pressure powdered sample, erythromycin, was tested under the same conditions as caffeine. Erythromycin A (EA) was dispersed using the aerosol generator and the resulting mass spectrum is shown in Figure 3-4. The peak corresponding to the protonated EA molecule is observed at *m/z* 734. The peaks at *m/z* 716 and 576 correspond to the loss of a water molecule and the loss of a cladinose sugar fragment (MW=158 Da) respectively. The peak at *m/z* 558 is assigned to the loss of both the cladinose sugar and the water molecule. The peaks at *m/z* 540 and 522 are assigned to the successive losses of one and two water molecules from the fragment of EA at *m/z* 558, respectively. The *m/z* 158 peak corresponds to the cladinose sugar residue. The observed mass spectrum is similar to the ESI mass spectra of EA previously reported.[100, 101] A similar mass spectrum, as shown in Figure 3-5, was observed with our instrument using standard electrospray

with 0.14 mM EA in 1:1 (v/v) acetonitrile and 0.2% aqueous formic acid sprayed at a flow rate of 3.3 µl/min. This result suggests that the MS signal obtained from direct analysis of powdered erythromycin may come from the particles due to its low vapor pressure. If there are no free erythromycin molecules, ionization must occur through the interaction of the electrospray droplets with the surface of the large erythromycin particles or the pick-up of nm sized erythromycin particles (if the latter are present).

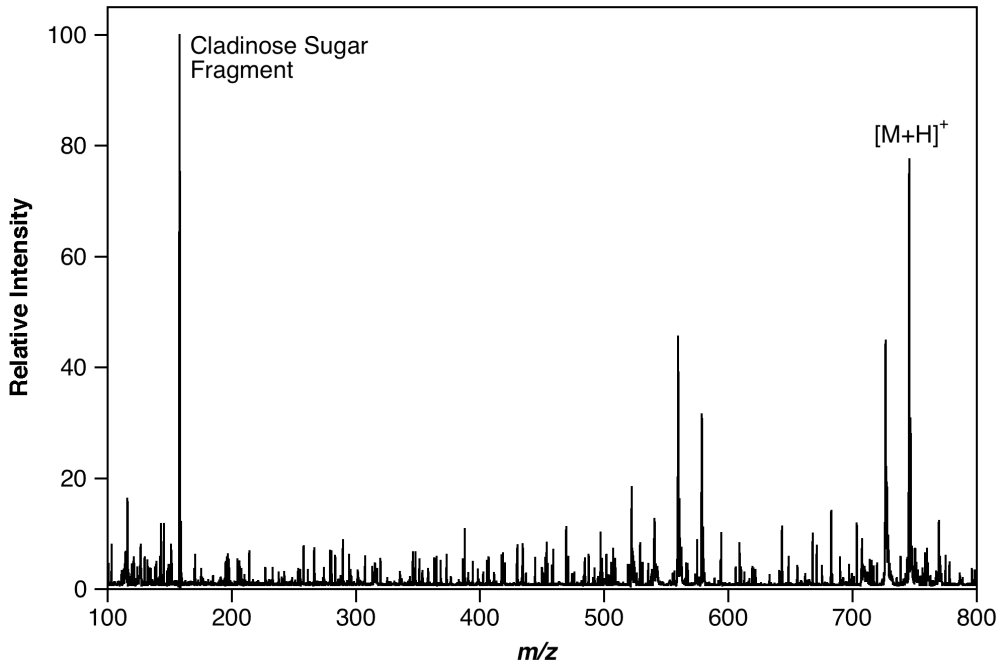

Figure 3-5. Positive-ion conventional electrospray mass spectrum of erythromycin A.

To further validate the dry particle merged electrospray ionization system, some commonly available powdered food and drug samples were tested. The mass spectrum obtained from dry instant cocoa powder is shown in Figure 3-6. Here the powder was added directly to the fluidized bed with no pretreatment. The dominant peak in the mass spectrum at *m/z* 181 is assigned to protonated theobromine, an alkaloid of the cacao tree (*Theobroma cacao)* and a

major component of cocoa. The peak at *m/z* 203 is assigned to sodium-cationized theobromine, $[M + Na]^+$. A peak corresponding to protonated caffeine appears at *m/z* 195 in the spectrum. Other peaks are not assigned, but likely represent other components in cocoa powder, such as phenols, flavonoids and sugars, as well as smaller molecular fragments of various compounds. This experiment shows that the predominant components in the food samples can be directly analyzed without any pretreatment.

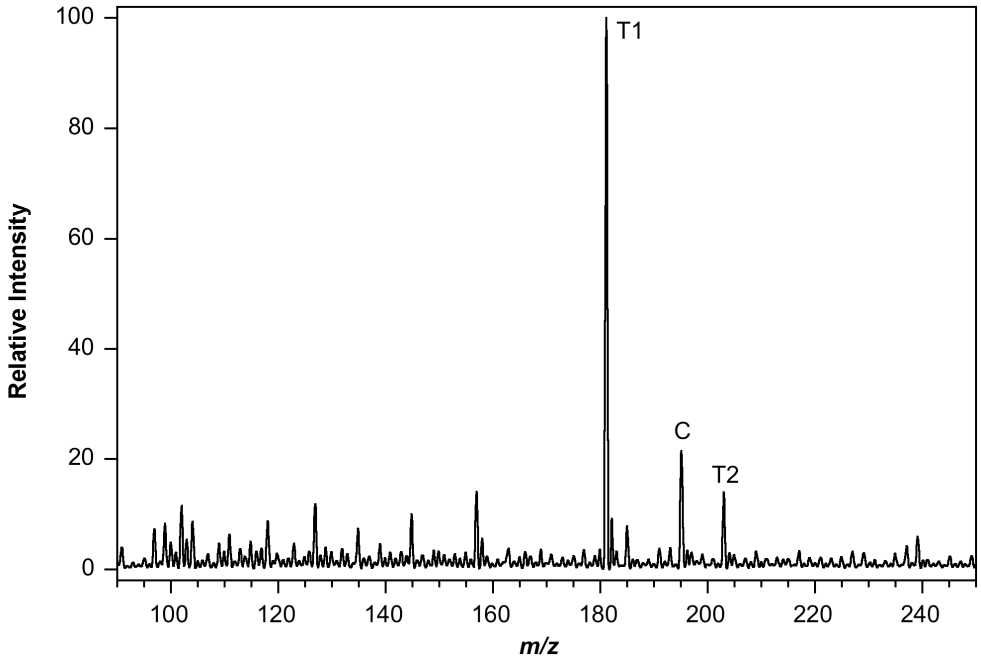

Figure 3-6. Positive-ion merged electrospray ionization mass spectrum of cocoa powder. The *m/z* 181 peak (T1) corresponds to protonated theobromine and the peak is at *m/z* 195 (C) is protonated caffeine. T2 is the peak corresponds to sodiated theobromine.

Figure 3-7 shows the mass spectrum of a powdered artificial sweetener, which is a mixture of sucralose ($C_{12}H_{19}Cl_3O_8$) and the bulking agents maltodextrin and glucose. The most intense peak observed in the spectrum corresponds to the sodium cation adduct of glucose at *m/z* 203. The glucose protonated molecule peak at *m/z* 181 is also observed in the spectrum.

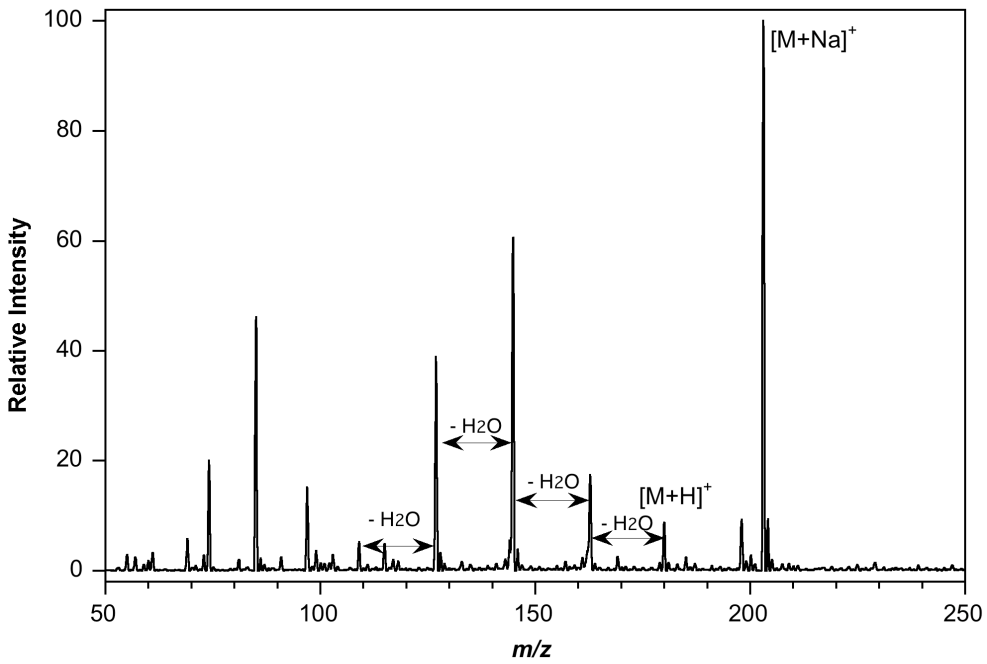

Figure 3-7. Positive-ion merged electrospray ionization mass spectrum of sweetener powder, the $[M + Na]^+$ and $[M + H]^+$ of glucose peaks are at *m/z* 203 and 181, respectively.

The *m/z* 163, 145, 127 and 109 peaks correspond to glucose that has lost one to four water molecules, respectively. There are other peaks in this spectrum, which may due to other ingredients in the sweetener such as carbohydrates and maltodextrin or their fragments. This spectrum is similar to the mass spectrum of merged electrospray of pure powdered glucose as shown in Figure 3-8. Figure 3-8 was obtained by dispersing pure glucose powder using the aerosol generator into the charged electrospray droplets. The most prominent peak in Figure 3-8 is also the sodium cation adduct of glucose at *m/z* 203. It is known that glucose forms adducts with sodium cation, and sodium chloride has been used to isolate pure glucose from impurities.[102] This explains why the most intense peak in the spectrum is the sodiated glucose peak. In addition, the sodium adduct of glucose observed in the spectrum suggests that the ion

was formed from a charged droplet. This supports the droplet pickup mechanism of the ionization method.

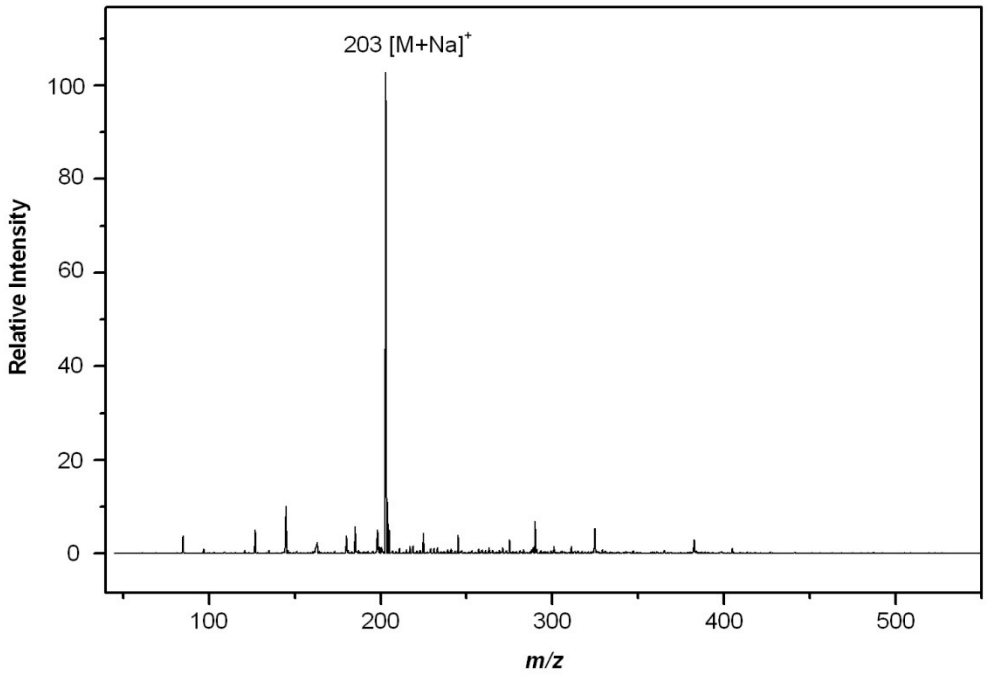

Figure 3-8. Positive-ion merged electrospray ionization mass spectrum of glucose powder, the $[M + Na]^+$ of glucose peak is at *m/z* 203.

Pharmaceutical analysis in complex matrixes is one of the most challenging topics in modern analytical chemistry. High-throughput pharmaceutical analysis was demonstrated using DESI-MS for solid tablets.[103] Besides tablets, many pharmaceutical products are in powder form. As a demonstration, direct analyses of the active components in a powdered drug were performed using merged electrospray ionization. The mass spectrum resulting from merging dry particles of a powdered ibuprofen tablet with the electrospray is shown in Figure 3-9. The tablets were ground into powder using a mortar and pestle, and then the powder was dispersed using the

aerosol generator. The ibuprofen tablet is a complex matrix. Its active ingredient is ibuprofen along with other additives. The ibuprofen is present in a relatively high concentration. In the spectrum, the *m/z* 207 peak corresponds to protonated ibuprofen and the *m/z* 229 peak corresponds to the ibuprofen sodium adduct. The *m/z* 177 is assigned to a fragment resulting from the loss of formaldehyde and the most intense peak at *m/z* 161 corresponds to ibuprofen that has lost its carboxylic acid group.

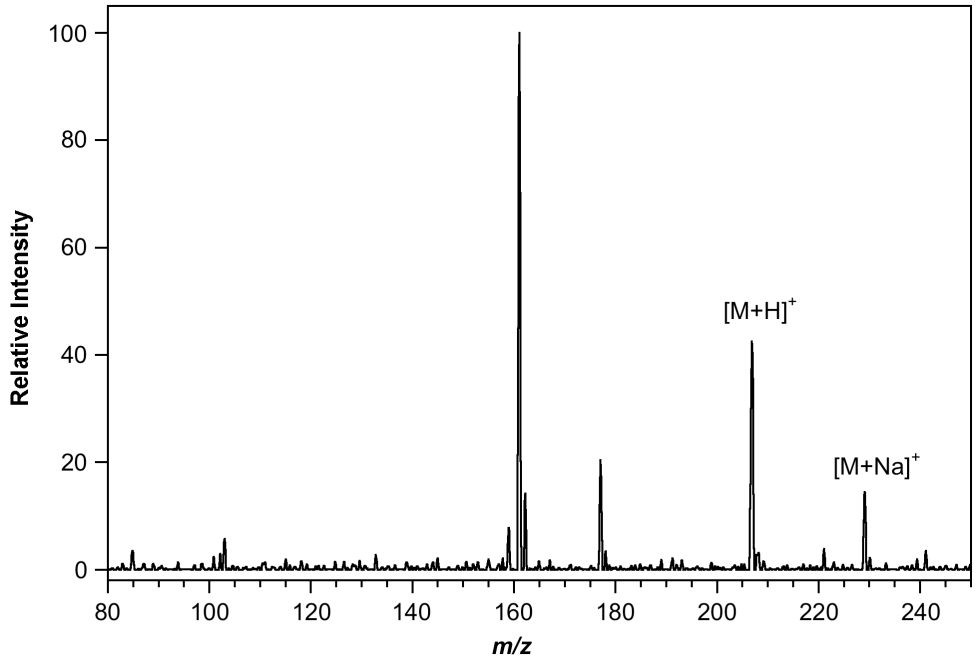

Figure 3-9. Positive-ion merged electrospray ionization mass spectrum of powdered ibuprophen tablets. The $[M + Na]^+$ and $[M + H]^+$ of ibuprofen are at *m/z* 229 and 207, respectively.

The molecular formulae of the identified peaks were confirmed by calculating the isotope peak percentage and considering the measured mass and mass accuracy. The selected peaks are either protonated or sodiated peaks of the ananlyte. The results are listed in Table 3-1. The theoretical isotope peak percentage can be calculated by use of the following formulas if only C, H, N, O, F, P and I are present,[104]

$$\%(M+1) \approx 1.1*\text{number of C atoms} + 0.36*\text{number of N atoms}$$

$$\%(M+2) \approx (1.1*\text{number of C atoms})^2/200 + 0.20*\text{number of O atoms}$$

As shown in the table, the mass accuracy of the measurements of pure sample caffeine and erythromycin is good relative to the resolution of the instrument, and the measured isotope peak percentages of these two analytes are also very close to their theoretical values (within 10%). For cocoa powder and artificial sweetener, the most intense peaks in the spectrum are assigned to the protonated theobromine and sodiated glucose. The mass accuracy of these two measurements is also good, and the isotope peak percentages are close to their theoretical values. However, the mass accuracy of the protonated ibuprofen peak is high value, and the measured isotope peak percentage is also off the theoretical value by approximately 50%. This may be due to the relatively low intensity for the ibuprofen peak and the fact that the isotope peaks are not well resolved. Since most of the experimental values of the isotope peak percentage are close to their corresponding theoretical values, and the mass accuracy of the assigned peaks are in the acceptable range for the ion trap mass spectrometer, this supports the assignment of the peaks observed in the experiments.

Table 3-1. Calculation of the mass accuracy and comparison of isotope peak percentage of some identified peaks.

Molecule	Measured m/z Value of $[M+H]^+$	Accurate Mass of the Molecule	Mass Difference (ppm)	Measured Isotope Peak Percentage	Theoretical Isotope Peak Percentage
Caffeine $[M+H]^+$	195.07	195.0877	90	11%	10%
Erythromycin $[M+H]^+$	734.51	734.4685	56	38%	41%

(**Table 3-1.** Cont.)

Theobromine $[M+H]^+$	181.14	181.0720	375	9%	9%
Glucose $[M+Na]^+$	203.07	203.0526	85	8%	7%
Ibuprofen $[M+H]^+$	206.94	207.138	955	7%	14%

3.4 Discussion

The ionization mechanism of merged electrospray ionization of dry particles has not been fully elucidated in this proof-of-principle study. However, we postulate that there are two likely mechanisms for the ionization of materials in dry aerosol particles. The first is a variation of the droplet pick-up mechanism for desorption electrospray ionization.[37] For DESI, the droplet pick-up process includes three steps: surface wetting by the solvent droplets, generation of the progeny droplets, and progeny droplets bouncing off the surface.[45, 105] For merged electrospray ionization of dry particles, droplets dispersed by electrospray impinging on a dry particle may extract analyte molecules during their brief contact time with the surface. The departing droplets retain the analyte molecules and subsequently form analyte ions by the standard electrospray mechanisms. Since the nanoelectrosprayed droplets are much smaller than the micrometer-sized dry particles,[94, 95] merging of the entire dry particles into the droplets will not likely lead to the ion formation. In addition, during the traveling process of the charged electrospray droplets from the nanospray emitter tip to the MS skimmer, the size of the droplets will become smaller due to the solvent evaporation. With an aerosol, the charged electrospray droplets may collide with the larger dry particles and extract material from the surface of the particles, and thereafter expel ions via the standard electrospray mechanism.

A second mechanism can occur when the analyte has sufficiently high vapor pressure. In this case, evaporation can occur followed by either gas phase ionization or merging of the gas

molecule in the droplet. Given the vapor pressure of caffeine, it is expected that a gas phase mechanism will be in effect for this molecule. However, the sodium adduct of caffeine observed in Figure 3-3 suggests that the ion was formed from a charged droplet. Thus, in this case, it seems likely that gas phase ionization or a combination of gas phase ionization and droplet pickup is occurring. Given the relatively large molar mass, the erythromycin sample is expected to have a much lower vapor pressure compared to caffeine and therefore it is anticipate that in this case, the ionization mechanism is dominated by droplet pick-up.

To completely elucidate the ionization mechanism of merged electrospray ionization of dry particles, much remains to be done, such as evaluating the mass spectra of various types of particulate samples and systematical measurement of the particle size (including the nm range) and its effects on the MS signal intensity.

3.5 Summary

The method of merged electrospray ionization has been extended to the analysis of dry aerosol particles. Ions are formed by interaction of the charged electrospray droplets and dry aerosol particles. It has been demonstrated that samples in powdered form can be analyzed directly without pretreatment or processing. Various samples were analyzed including pure samples and mixtures. Singly charged protonated molecule peaks of pure samples and singly charged protonated molecule peaks of major mixture constituents were observed. Fragment peaks were also observed in some samples. The ionization of low vapor pressure compounds indicates a mechanism similar to droplet pick-up suggested for DESI of surfaces.

Future studies will be directed at extending dry particle merged electrospray to compounds with larger molar masses such as proteins and lipids that are likely components of bioaerosols. A small-scale powder disperser will be used in these bioaerosol studies to limit

sample consumption due to limited sample availability. Standard biomolecules, such as bradykinin, insulin and cytochrome *c*, will be used initially. Bioaerosols, such as pollen and bacterial samples will then be studied.

CHAPTER 4. MERGED ELECTROSPRAY IONIZATION OF COMBUSTION PRODUCTS

4.1 Introduction

Combustion is an important environmental concern due to its toxic component emission during the combustion processes.[106, 107] In addition to the emission of gaseous pollutants, such as CO, NO_x, SO_x, or low mass volatile organic compounds, particulate matter is also emitted.[108] Fine and ultrafine soot particles with diameter smaller than 2.5 μm are dominant in combustion emissions.[108] Most importantly, these fine and ultrafine particles pose great health risks to humans because of their innate ability to deposit deep in the lungs.[109] Therefore, rapid detection of combustion products is important in the areas of environmental and human health.

Many techniques have been used for combustion products detection. Laser spectroscopy techniques such as laser induced fluorescence spectroscopy (LIF) and Raman spectroscopy have been used in combustion diagnostics.[110, 111] LIF is an emission spectroscopy technique used to analyze combustion products and is sensitive and reliable.[112] However, the sample pretreatment is time-consuming, and the data interpretation is complicated. Raman spectroscopy[113] provides simple data interpretation and multi-species analysis of combustion products. However, the Raman scattering process is extremely weak, and Raman spectroscopy suffers from poor sensitivity.

Mass spectrometry has been an effective technique for obtaining the chemical information of combustion products. Examples of techniques are laser microprobe mass spectrometry (LAMMA),[108] MALDI,[114] atmospheric-pressure chemical ionization (APCI) and GC-MS.[115] However, these methods all require analyte collection and extraction or dissolution of the sample or other preparation steps. Such processes are time-consuming. Recently, rapid

analysis of PAHs in atmospheric aerosols without extraction or pre-concentration using DESI was reported.[116, 117] However, sample collection is still a requirement. A major advantage of merged electrospray ionization for the analysis of combustion products is that no sample collection or treatment is required. The analysis can be performed on combustion products in real time.

An important consideration in this research was whether the signal arises from particles or gas phase molecules when using merged electrospray ionization. In order to test this, we analyzed several combustion products using this method. Initially, smoke samples from cigarettes, incense and candles were analyzed by direct merging into the nanoelectrospray. Next, incomplete combustion products of hydrocarbon fuels, such as toluene, xylene and diesel fuel, were tested using this ionization method. Incomplete combustion was achieved using a home-built flame source. The flame products were transferred through a copper tee into the nanoelectrospray region and detected with the ion trap mass spectrometer. Using this ionization method, no sample collection is needed and a mass spectrum can be obtained in seconds.

4.2 Experimental

The experimental configuration for merged electrospray of combustion products was described in detail in Chapter 2, Section 2.3.2. For smoke analysis, a 4:1 (v/v) mixture of methanol and 0.2% acetic acid was used as the spray solvent and was pumped through a 50 μm i.d. silica capillary tubing with a syringe pump at a flow rate of 500 nL/min. Smoke samples were directly passed through the path of the spray. Different methanol and water ratios for the electrospray solvent were tested, and no significant difference in the signal-to-noise ratio was observed when changing the solvent composition.

For fuel combustion analysis, a 1:1 (v/v) mixture of methanol and 0.2% acetic acid was used as the spray solvent at a flow rate of 833 nL/min. The flame was controlled by setting the flow rate of propane to approximately 0.03 m^3/h, and by controlling the air-to-fuel ratio. The fuel is a mixture of propane and the solvent vapor. The ratio of the propane and the solvent vapor is determined by the vapor pressure of the solvent at room temperature and atmospheric pressure. The vapor pressure of toluene is 25 mm Hg, which is two times higher than xylene. Flame products were transferred to the spray region due to the venturi effect in the tee. The flow of nitrogen gas, which was connected to one side of the tee, was set at approximately 0.06 m^3/h.

The voltage applied at the nanospray emitter and the sampling cone were +3.0 kV and +40 V, respectively. No pneumatic gas was used for this experiment. Mass spectra were acquired in positive-ion mode and ions were accumulated for 100 ms in the trap.

4.3 Results and Discussion

4.3.1 Direct Analysis of Smoke

Smoke is usually an unwanted by-product of combustion that contains solid and liquid particulate and gases. Cigarettes, stick incense and candles can be easily used as smoke sources. In this study, smoke samples were analyzed without any pretreatment with merged electrospray ionization. Once these tests proved successful, a more sophisticated combustion source was built.

The spectra obtained from cigarette smoke and sandalwood-scented stick incense smoke are shown in Figure 4-1 and 4-2 respectively. It has been reported that nicotine (M_R = 162) is the major component in cigarette sidestream smoke with a number of other small molecular weight components detected by GC-MS, such as phenol, limonene, hexamethylenetetramine, 3-vinylpyridine, and high molecular weight components such as polycyclic aromatic hydrocarbons (PAHs).[118-120] The assignment of the peaks in the cigarette smoke mass spectrum is carried out

by consulting literature data for compounds present including their expected yields, and by the compounds' chemical properties, *i.e.* ionization potentials under electrospray condition.

In Figure 4-1, the most intense peak is assigned to the nicotine $[M + H]^+$ peak observed at *m/z* 163. The high intensity of the nicotine peak is due to its high concentration in the smoke, and the fact that it is easily ionized by protonation. The (M+1) isotope peak percentage of nicotine, which is denoted by the arrow in the insert graph, is measured as 12% in the spectrum. It is identical to the theoretical isotope peak percentage of nicotine calculated as 12%. This comparison confirms the assignment of the nicotine peak.

Other less intense peaks in the low mass range may be due to the other components in the smoke. The peak at *m/z* 95 is tentatively assigned to the protonated phenol, and the peak at *m/z* 141 is tentatively assigned to the protonated hexamethylenetetramine that has been reported to be present in the particulate phase of sidestream of cigarette and is formed by the reaction of ammonia and formaldehyde.[121] However, due to the relatively low intensity in the spectrum and possibility to overlap with other nearby peaks, the measured value of the isotope peak percentage for these two peaks cannot confirm the assignment. To confirm the identified peaks and further identify other low intensity peaks, tandem MS or a high-resolution mass spectrometer is necessary. Further, due to the high intensity of the nicotine peak, peaks from some other components such as PAHs, which has been detected at trace levels in the cigarette smoke by GC-MS,[118, 122] are obscured and cannot be identified in the spectrum.

Nicotine has been reported to be 50-80% in the gaseous phase of the cigarette smoke sidestream,[123] while other researchers report its presence almost entirely in the particulate phase.[124] In spite of its particulate phase, nicotine will readily evaporate from the particles due to

its the high vapor pressure. Thus, in this experiment, it is likely that ionization occurs by pick up of gas molecules by the electrospray droplet.

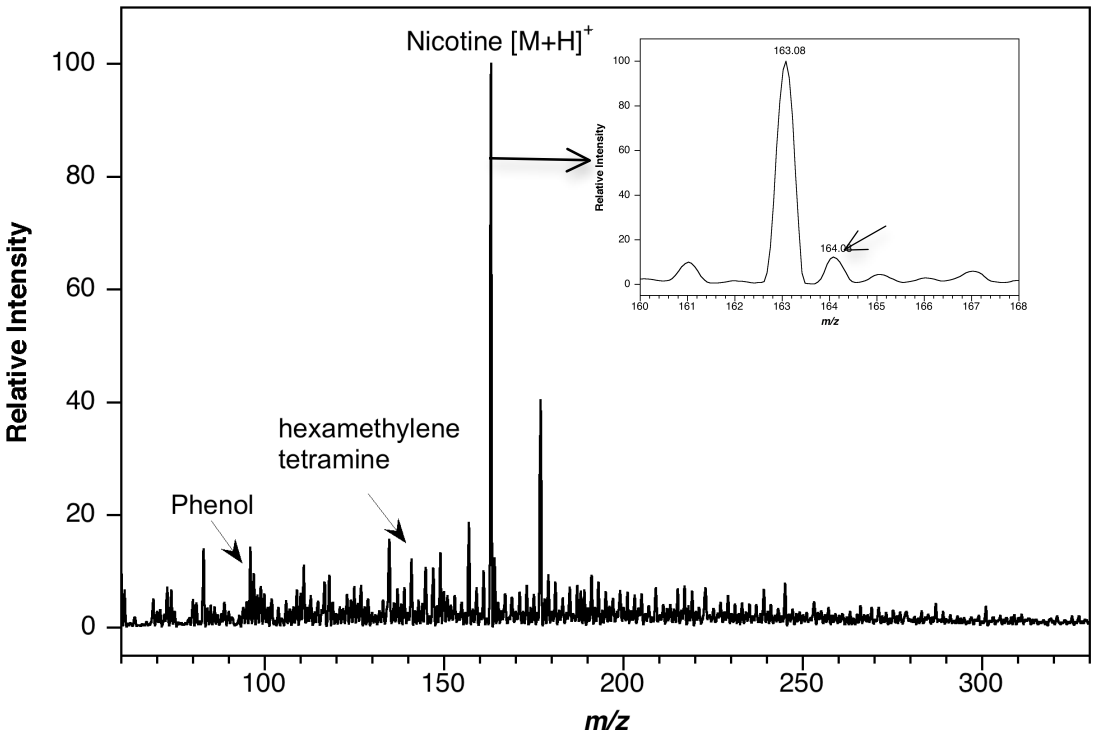

Figure 4-1. Positive-ion cigarette smoke merged electrospray ionization mass spectrum. The insert graph is the enlargement of the most intense protonated nicotine peak.

Incense smoke is another source of smoke particulate.[125, 126] It has been reported that burning of incense generates accumulation mode and coarse mode particulate. [127] Incense smoke has been studied extensively by using GC-MS, 2-dimentional GC-MS and LC-MS, and many components have been identified such as PAHs and metals.[127, 128]

The incense used in this experiment was sandalwood incense. In Figure 4-2, the peak at *m/z* 222 was assigned to the protonated santalol molecule ($C_{15}H_{24}O$), which is the main component of sandalwood oil and likely to be generated during the combustion of the incense.

The *m/z* 244 peak corresponds to sodium-cationized santalol, $[M + Na]^+$. The most intense peak is at *m/z* 177, which may correspond to the fragment of santalol molecule. To confirm these assignments, the isotope peak percentage of peak at *m/z* 222 was also measured and shown in the insert graph of Figure 4-2. The theoretical values of santalol (M+1) isotope peak and (M+2) isotope peak are calculated as 16% and 1.5% respectively. In comparison with the theoretical values, the measured values are off by -23% for the (M+1) isotope peak and +53% for the (M+2) isotope peak. This may be due to the fact that the peak is broad and not sufficiently intense to be measured accurately, or it may be that the assignment of the peak to the santalol is incorrect. To confirm this assignment, a high-resolution mass spectrometer is necessary. There are other low mass peaks in this spectrum not assigned, which may be due to minor components in the incense. By examining the isotope peak patter of all the peaks in the figure, no metal containing compounds, which have been detected in the incense smoke using other techniques, were identified. It may be that the metal containing compounds are not easily ionized under electrospray conditions. No significant peaks were observed at mass range above *m/z* 300 in Figure 4-2.

In the cigarette and incense smoke experiments, only low mass components in the cigarette and incense smoke were detected using our method. This may be due to the low concentration or low ionization efficiency of the higher mass components. If ions forming from low vapor pressure molecules can be detected using merged electrospray ionization, they are suggestive of ions formed from particles. Additional experiments described below were performed in order to address this issue of ion formation from particulate.

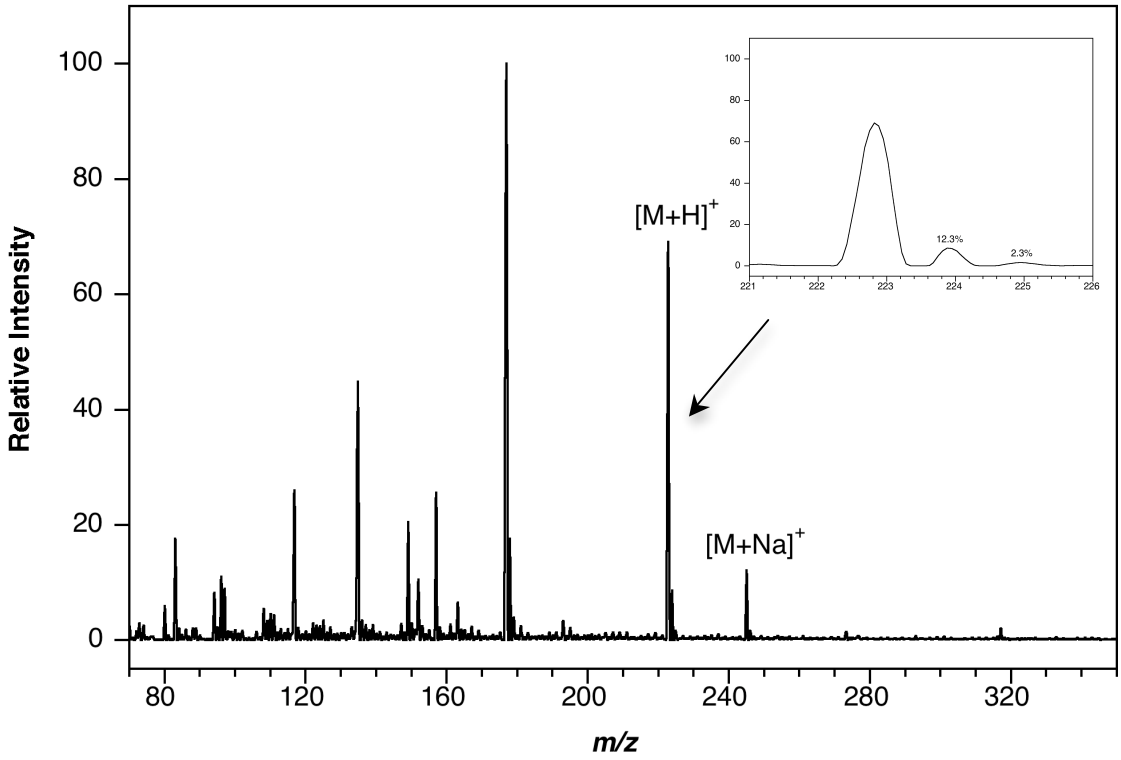

Figure 4-2. Positive-ion incense smoke merged elecrospray ionization mass spectrum. $[M + H]^+$ and $[M + Na]^+$ are protonated and sodiated santalol peaks, respectively. The insert graph is the enlargement of the protonated santalol peak.

Candle smoke was analyzed because it was found to be a highly variable source of particles, and the burning manner of the candle affected its particle emissions.[129] For this experiment, an ordinary white candle, which is composed of paraffin wax and a cotton wick, was used. The burning was under ambient laboratory conditions for each measurement. The smoke was generated directly after extinguishing candle, and a black smoke could be seen with the unaided eye.

Paraffin wax consists of the alkane hydrocarbon solids with the general formula $C_n H_{2n+2}$ (n = 20 - 40). When the candle wax is heated, the hydrocarbon chain molecules break down. The mass spectrum collected from candle smoke using merged electrospray ionization is shown in Figure 4-3. No signals could be observed when the electrospray was run without the smoke or

when the smoke was generated without the electrospray. Fine *et. al.* have demonstrated using GC-MS that approximately 95% products from burning of paraffin candle are hydrocarbons, including alkanes, alkenes, and cyclic hydrocarbons.[130] Thus, the series of peaks from around *m/z* 200 to *m/z* 600 with a 14 *m/z* spacing are likely to be the alkanes or alkenes with different number of CH_2 groups. Since alkanes and alkenes are not easy ionized under electrospray conditions, we tentatively assigned the detected peaks to the protonated aromatic hydrocarbons, some with an alkane side chains.

To confirm the assignment of the peaks, the most intense peaks in the 480-500 *m/z* range in the spectrum were enlarged and analyzed. This group of peaks is shown in the insert graph in Figure 4-3. The intense peaks in the inset graph denoted by the red dots are separated by *m/z* 2, which is likely to be the dehydrogenation ($-H_2$) or hydrogenation ($+H_2$) on the alkane chain. Each of the intense peaks has a low intensity (M+1) isotope peak, which are denoted by asterisks in the inset graph. Table 4-1 lists the *m/z* values and intensities of these peaks and their isotope peaks. The measured isotope peak percentages are listed in the table. If the molecule of these corresponding to the peak at m/z 493.7 contains only carbon and hydrogen atoms, the corresponding molecular formula is $C_{35}H_{72}$. The theoretical isotope peak percentage of $C_{35}H_{72}$ is calculated as 39%, which is much higher than the measured value. The difference between the theoretical value and measured value may be due to the relatively low resolution of the instrument, which leads to the inaccurate measurement of the isotope peak intensity. Also, in the insert figure, a peak at *m/z* 495.6 (denoted by the arrow) is likely to be the (M+2) isotope peak of the peak at *m/z* 493.7. If this is the case, the corresponding molecule of this peak may contain oxygen atoms or sulfur atoms, which is possible because the oxygen is rich in the air and sulfur

may exist in the candle wick. Thus, the assignment of the peak to the protonated aromatic hydrocarbons with an alkane side chain is not conclusive.

In addition, the observed peaks may be the radical cations instead of protonated molecules. A comparison experiment was performed with a deuterated solvent (50% CH_3OD + 50% D_2O + 0.1% AA) as the electrospray solvent. If the peaks are from the protonated molecules, then by using the deuterated solvent, the (M+1) peak intensity should increase significantly. However, this was not observed. The reason may be that the acetic acid used was not deuterated, and the proton for the ionization mainly comes mainly from the acid. However, the deuterium atom from CH_3OD or D_2O should still lead to the increase of the (M+1) peak intensity. Thus, it cannot be excluded that the observed peaks may come from the radical cations of the hydrocarbons generated during the candle combustion.

Table 4-1. The *m/z* value and intensity of the peaks in the insert graph of Figure 4-3.

m/z	485.7	486.7	487.8	488.8	489.6	490.6	491.7	492.7	493.7	494.7
Intensity	20.557	5.168	37.985	9.832	52.330	12.174	63.603	16.286	77.228	21.921
Isotope Peak Percentage	25%		26%		23%		26%		28%	

Since it is difficult to affirmatively assign the peaks observed from the candle smoke, it is difficult to infer information about the ionization mechanism in this experiment. However, the high mass peaks up to *m/z* 600 observed in the spectrum suggests that the ions may be generated from particulates instead of from gas molecules due to the low vapor pressure of high mass compounds.

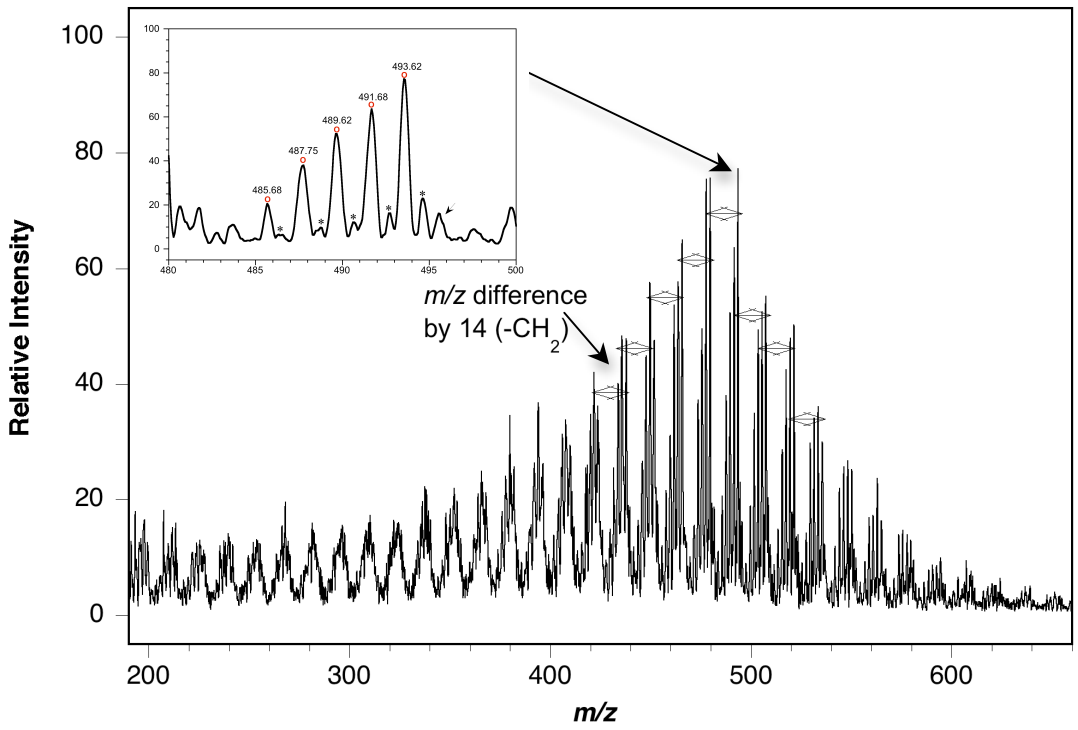

Figure 4-3. Positive-ion candle smoke merged electrospray ionization mass spectrum. The insert graph is the enlargement of the most intense peak group at *m/z* 493.

4.3.2 Direct Analysis of Flames

Based on the success of the smoke analysis, a flame source was constructed and the analysis of fuel-rich combustion products with merged electrospray ionization was performed. Fuel-rich combustion generates soot particles and higher concentration PAHs in comparison to the smoke samples.[131] The observation of signals from soot particles and higher mass PAHs, which are more likely physically absorbed or chemically bonded on the surface of the soot particles instead of in the gas-phase,[132] would be indicative of a particle ionization mechanism.

Pure toluene was used as a model fuel in this study. Combustion products of a toluene and propane gas mixture were directly analyzed using the experimental setup described in Chapter 2. Propane gas was used to assist in generating toluene vapor and transferring the vapor

out from the glass bubbler. These fuels were burned under fuel-rich conditions as indicated by the presence of a yellow flame. Soot particles were observed from the flame of burning of propane and toluene gas mixture. The mass spectrum generated from the combustion of propane and the mass spectrum generated from the combustion of propane and toluene gas mixture were compared.

The mass spectrum collected from fuel-rich combustion of propane only is shown in Figure 4-4. No significant signal is observed relative to the background in this spectrum. However, in Figure 4-5, a series of peaks corresponding to a series of protonated PAH molecules are observed in the spectrum of the combustion of toluene and propane mixture. In order to compare the spectra, the intensity of mass spectra is shown on the same scale and in total ion counts. The assignment of the peaks in this spectrum is based on the detected *m/z* and previous research on pyrolysis of toluene.[133, 134] The peaks have a spacing of 14 *m/z* (CH_2), and each group is composed of several peaks with different intensities and a spacing of 2 *m/z* (H_2). It should be noted that PAH ions with equal molecular weight and different chemical structures will be observed at the same *m/z* value. For simplicity, only one compound of the related set of compounds at certain *m/z* value was listed to represent the corresponding peak.

The most prominent peak group from *m/z* 179 to *m/z* 185 is assigned to the methylphenalene $[M + H]^+$ peak and its hydrogenation/dehydrogenation products. The 2 *m/z* peak separation is attributed to ring condensation and ring fusion leading to dehydrogenation ($-H_2$) or hydrogenation ($+H_2$).[135] This assignment is also supported by the comparison of the measured isotope peak percentage (13%) with the theoretical isotope peak percentage (15%).

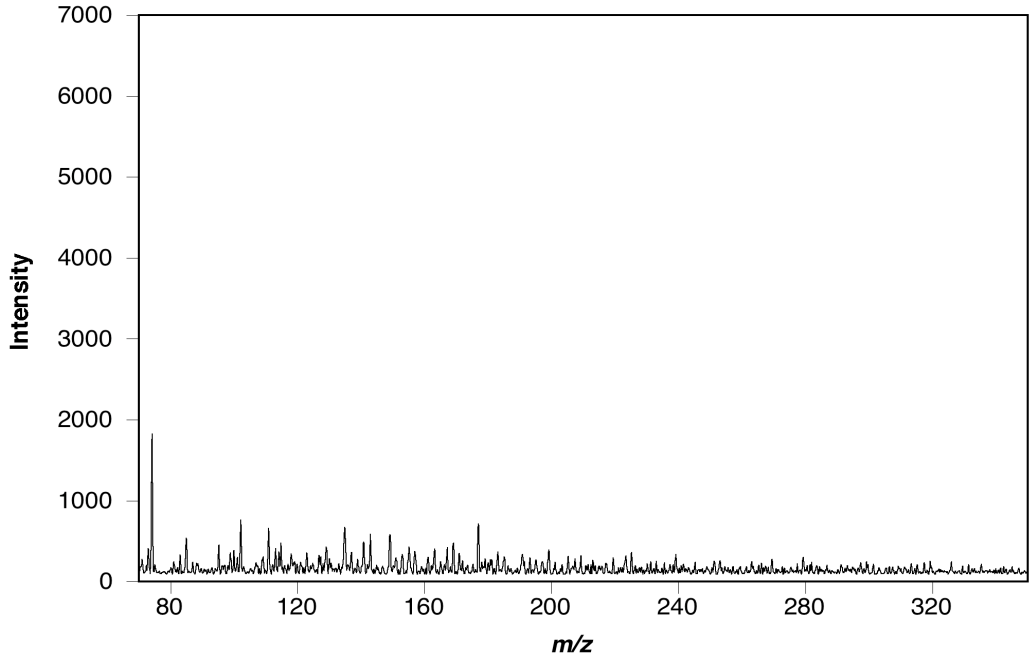

Figure 4-4. Positive-ion propane flame products merged electrospray ionization mass spectrum.

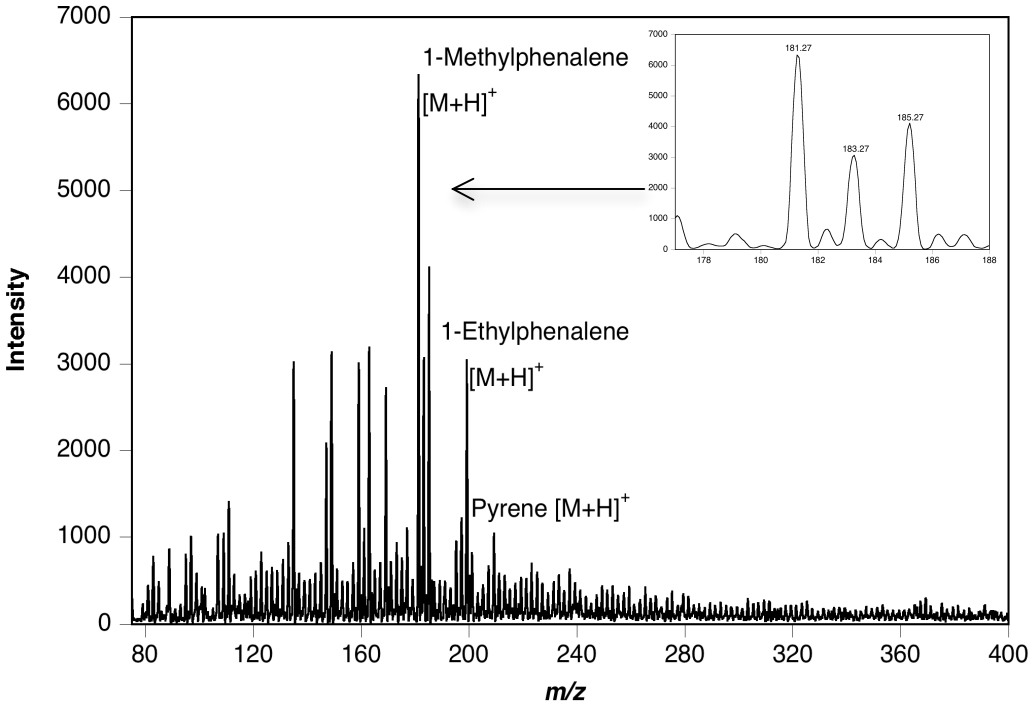

Figure 4-5. Positive-ion toluene and propane flame products merged electrospray ionization mass spectrum. The insert figure is the enlargement of the most intense peak group denoted by the arrow.

Toluene combustion or pyrolysis has been studied extensively and it is known that radical species play an important role in the formation of PAHs in aromatic fuel combustion.[135-138] The radical species produced depend on the type of fuel and combustion conditions, including pressure and flame temperature.[135] It has been demonstrated that the radical species generated from toluene flame under fuel-rich combustion conditions are methyl radical ($\bullet CH_3$), phenyl radical, and benzyl radical.[139] In our case, it is possible that the PAHs form through the methyl radical polymerization, phenyl radical addition, or benzyl radical addition with lower molecular weight PAHs leading to the formation of higher molecular weight PAHs; eventually soot particles form through this polymerization. There are radicals, PAHs molecules, and soot particles with PAHs intermediates absorbed on the surface generated in the process of the fuel-rich combustion of toluene. From our results, no significant signals are observed at *m/z* 77 (phenyl radical) and *m/z* 91 (benzyl radical). Methyl radical *m/z* value is not in the measurable *m/z* range of our instrument. The reason for no significant signals from radicals may be due to their short lifetime in the flame. The ionization process in this experiment may be the charged solvent droplets desorbing the PAHs on the surface of the soot particles or merging of gas phase PAHs with the electrospray. Due to the low vapor pressure of PAHs, the pick-up of PAH molecules on the surface of the soot particles by the electrospray droplets may explain the ionization process.

Xylene is another model fuel tested in the same way as toluene. Xylene has lower vapor pressure than toluene, therefore the proportion of xylene in the gas mixture was lower. In Figure 4-6, the observed peaks of the flame products of an m-xylene and propane mixture are less intense than in Figure 4-5. It seems that the proportion of the aromatic fuel affects the concentration of the generated products. Xylene has a similar chemical structure to toluene with

an additional CH_3 group. Therefore, it is not surprising that the products of xylene and propane mixture flame are similar to those for toluene.

In the xylene combustion spectrum, more PAHs are observed from *m/z* 100 to *m/z* 500. This may be due to the less intense protonated methyl-phenalene peak at *m/z* 181 in this spectrum. Thus, larger PAH peaks with lower intensity are not obscured by the more intense peak. In the xylene spectrum, the most prominent peak group is shifted to the *m/z* 167 range, and is assigned to the fluorene $[M + H]^+$ peak and its hydrogenation/dehydrogenation products. Other peaks are assigned to the same products as in Figure 4-5.

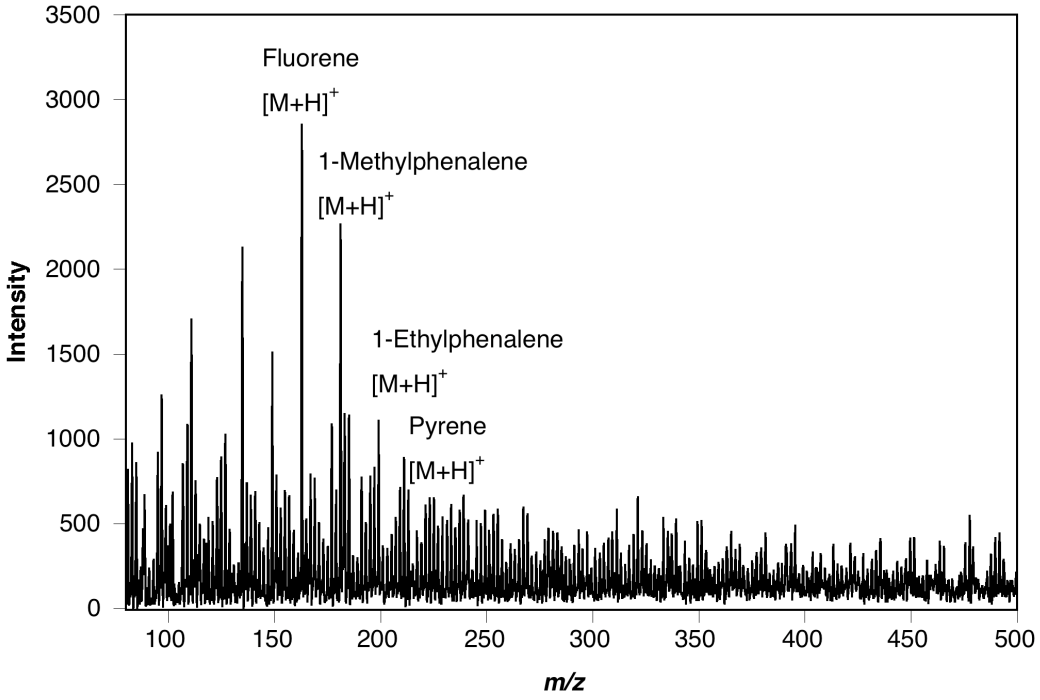

Figure 4-6. Positive-ion xylene and propane flame products merged electrospray ionization mass spectrum.

Diesel fuel is a more complex sample that was also tested in this study. Diesel fuel is composed of about 75% saturated hydrocarbons (primarily paraffin) and 25% aromatic hydrocarbons. The spectrum from the combustion of diesel fuel and propane is shown in Figure

4-7. The spectrum is similar to that shown in Figure 4-5 and Figure 4-6 due to the aromatic hydrocarbon component in the diesel fuel, which is important for PAH and soot particle formation. It was noticeable that the diesel fuel generated more soot than the model fuels. This may be due to the complex contents of diesel oil that may generate more radicals and cause the soot formation, which could lead to more PAH peaks observed in its spectrum. The most intense peak in Figure 4-7 is assigned to methylphenanthrene $[M + H]^+$ peak and its hydrogenation and dehydrogenation products, which is the same as that observed in the toluene flame results. The other series of grouped peaks from *m/z* 100 to *m/z* 500 are also assigned to the corresponding PAHs with the addition of the methyl or phenol radical to the low mass PAHs. Since the tandem MS data was not collected, the assignment of the PAHs was not confirmed, and only some peaks are labeled in the spectrum.

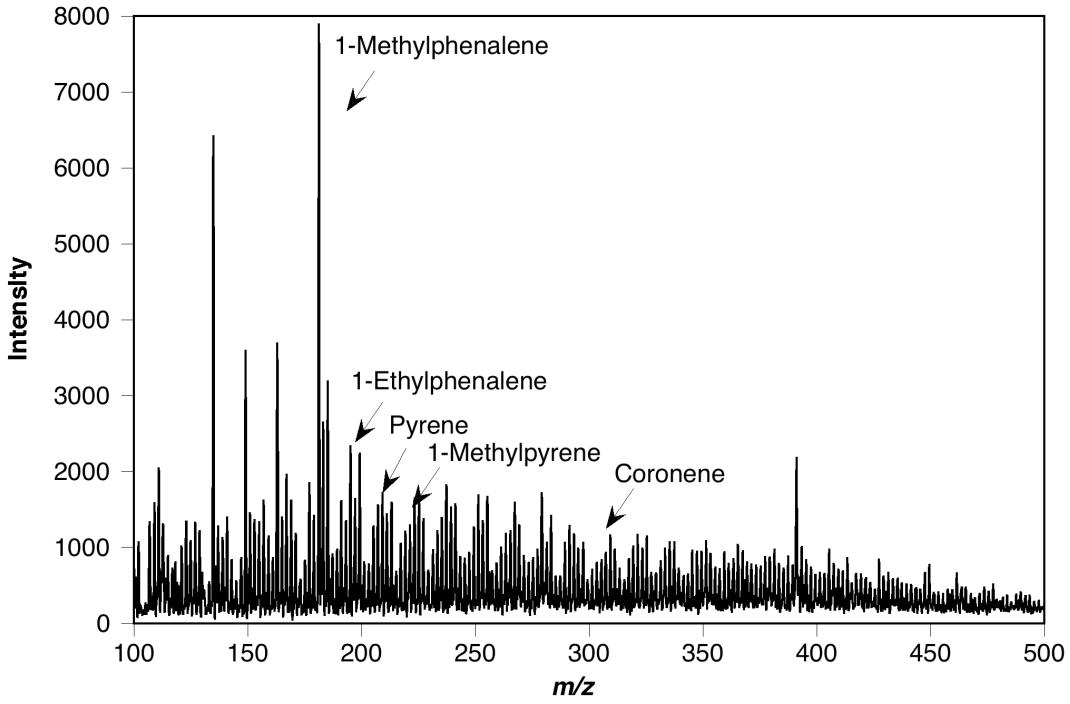

Figure 4-7. Positive-ion diesel fuel and propane flame products merged electrospray ionization mass spectrum.

In order to further understand whether particulate or gas phase molecules were responsible for the merged electrospray ionization signal, flame products of diesel fuel were collected and analyzed with a commercial MALDI-TOF mass spectrometer. The mass spectrum obtained without a MALDI matrix is shown in Figure 4-8. Different spectral patterns are observed from the LDI of collected flame products compared to the merged electrospray ionization. However, some peaks observed in Figure 4-7 are also observed in Figure 4-8, such as protonated methylphenalene peak at *m/z* 181 and the protonated coronene $[M + H]^+$ peak at *m/z* 301. The differences in the results may be due to the differences between the direct analysis and the collected samples, or the particle size discrimination of the impactor. It is also possible that merged electrospray ionizes mainly PAHs in the gas phase, while MALDI only ionizes PAHs deposit on the particles. From this result, it is difficult to distinguish between a particle and gas phase mechanism.

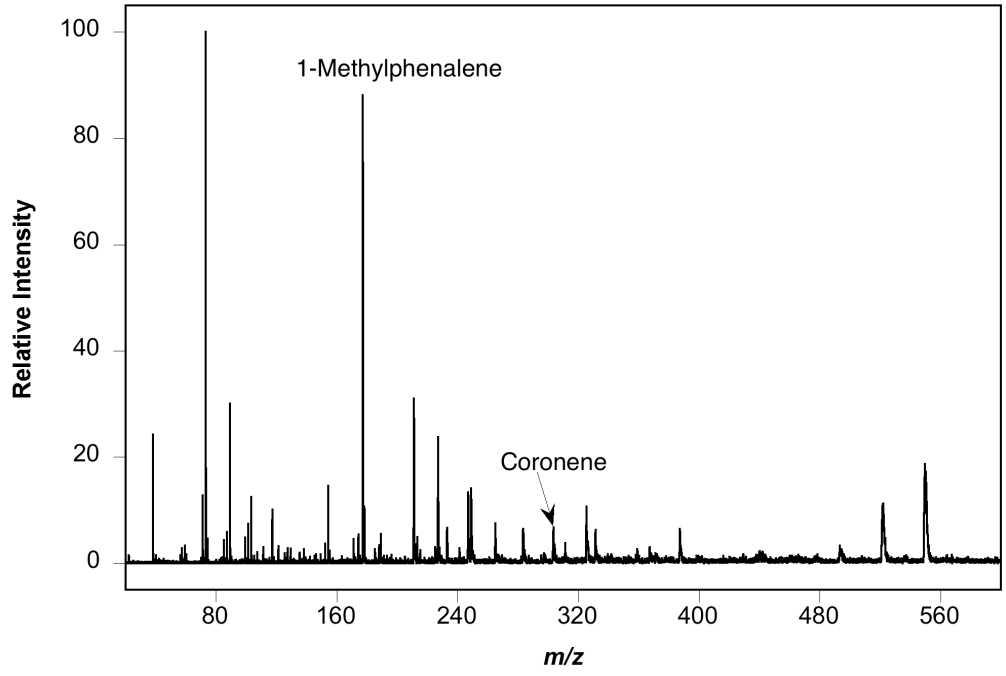

Figure 4-8. Positive-ion MALDI mass spectrum of collected diesel flame products.

A filter experiment was performed to aid the understanding of the ionization mechanism. The filter is used to block the particles coming out from the flame. A HEPA filter capable of blocking 99.9% of particles as small as 300 nm in diameter was placed at the output side of the copper tee to block particles produced by the flame.

The spectra of the toluene flame collected without (Figure 4-9a) and with (Figure 4-9b) the filter under the same combustion conditions are shown for comparison. The background signal (Figure 4-9c) was also collected with electrospray of the solvent. The spectrum of the toluene flame products without filtering is the same as shown in Figure 4-5. However, in the spectrum of the toluene flame with the filter, almost no signal is observed relative to the background. The ionization signal decreased approximately 99% following filtration. However, the HEPA filter also affects the gas flow rate. It was found using a flow meter that the HEPA filter blocks approximately 60% of the gas flow. Since the PAH signal was lost completely, this indicates either that particles are important for the ionization process or that the gas phase PAHs are adsorbed on the filter. Much remains to be done in order to elucidate the mechanism fully, such as using a virtual impactor that will only remove the particles and will not trap the gas molecules.

4.4 Summary

In this study, combustion generated materials were detected using merged electrospray ionization. It is important to elucidate the ionization mechanism of merged electrospray ionization technique. Through the understanding of the mechanism, the figures of merits of the technique can be further improved. Thus, the method can be widely applied to different research areas.

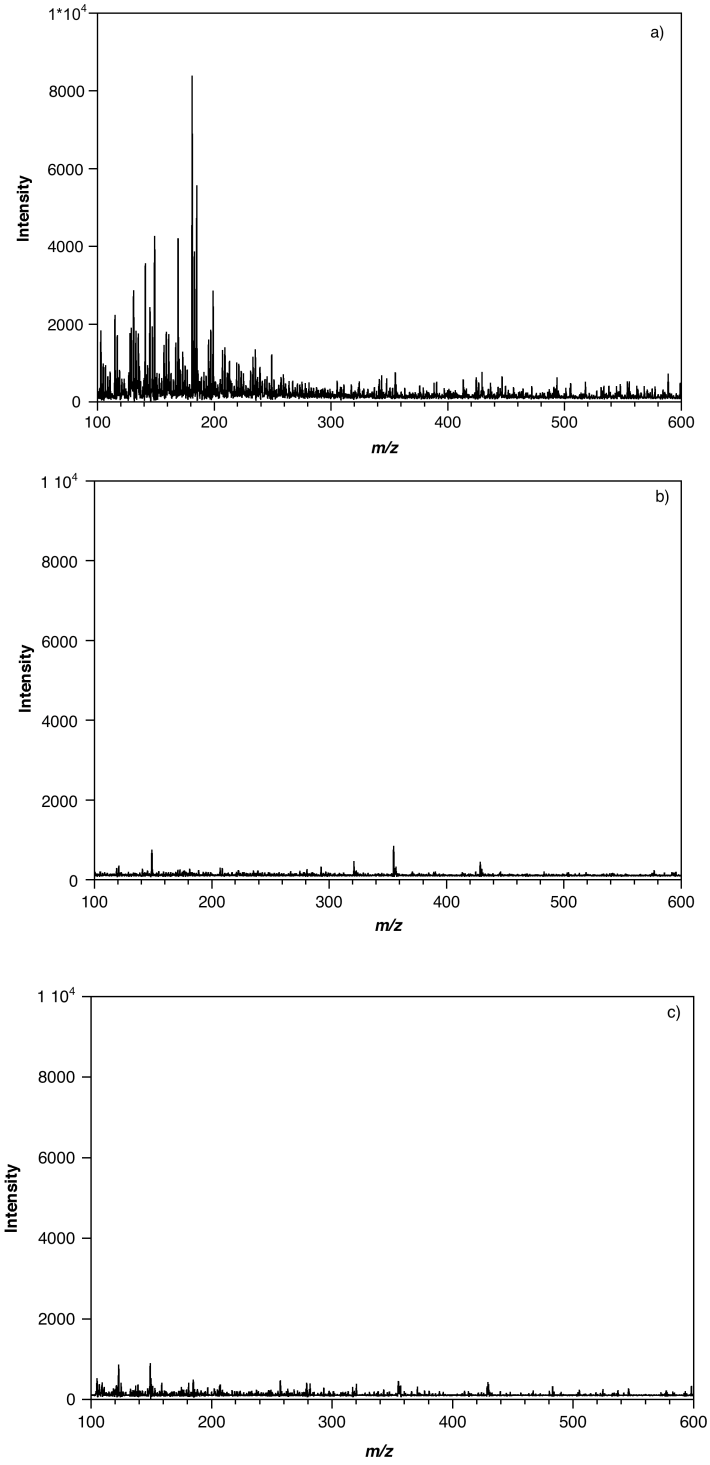

Figure 4-9. The comparison of toluene and propane mixture flame mass spectra a) without HEPA filter, b) with HEPA filter, and c) background.

In this study, we observed signal from smoke and flame products using merged electrospray ionization. The ionization may be based on the charged solvent droplets pickup analyte molecules from the surface of particles, but this mechanism has not been fully confirmed. It is also possible that gas-phase pick-up is the major contribution to the generation of the ions from the combustion products. If in this case, the application of merged electrospray ionization will be limited, because large molecules will be difficult to detect.

This study demonstrates that merged electrospray ionization can be used to directly analyze combustion products from smoke and flame sources without sample collection and pretreatment. The major components in cigarette smoke, incense smoke and candle smoke were detected in seconds. Several PAHs generated from fuel-rich combustion were also analyzed in real-time without sample collection, extraction or pre-concentration, which prevents any information loss or change of the analytes. However, the mass spectra obtained by this method do not appear to represent all the combustion products. To obtain complete information of the combustion products, use with other methods such as LDI is necessary.

Future experiments using a more controlled flame source for the fuel-rich combustion study appear to be necessary to obtain consistent results among analyses and to compare with other results in the literature. The flame temperature and the oxygen/fuel ratio should be controlled. The size and concentration of the particles generated by the combustion source (including nm sized particles) should be precisely measured. In addition, coupling the ionization source to a high-resolution mass analyzer, such as a Fourier transform ion cyclotron resonance (FT-ICR) or orthogonal time-of-flight (Q-TOF) MS, will improve the accuracy of peak identification and provide tandem MS ability. These results will be helpful to understand the mechanism of merged electrospray ionization of combustion products.

CHAPTER 5. INFRARED MATRIX-ASSISTED LASER DESORPTION ELECTROSPRAY IONIZATION*

The work reported in this chapter has been published in the *Analyst*.[140]

5.1 Introduction

Matrix-assisted laser desorption electrospray ionization (MALDESI) was described in detail in the first chapter.[71, 72] A pulsed 337 ultraviolet (UV) laser was used in previous studies. In the research described in this chapter, an infrared (IR) laser was used for the removal of the material that was ionized by interaction with an electrospray. It has been reported that laser desorption and ablation of the materials generates a large number of particles and clusters and a small amount of ions.[141] Thus, this method is a subset of merged electrospray ionization. In order to differentiate this approach from the ionization of dry particles without laser assistance introduced in the previous chapters, merged electrospray ionization of IR desorbed and ablated materials is called IR matrix-assisted laser desorption electrospray ionization (IR MALDESI).

The characteristics of IR lasers for desorption has been previously described.[142] Compared to UV lasers, an IR laser has three main advantages. First, the penetration depth of an IR laser under MALDI conditions is approximately 1 μm, which is several orders of magnitude larger than for UV lasers.[143] This characteristic enables an IR laser to remove deeply embedded analytes from materials such as thin layer chromatography plates, polyacrylamide gels, and tissue.[144-146] Second, an IR laser has the ability to remove large molecules without the need for an added matrix. It has been reported that existing natural components in the sample, for example, water, can act as a matrix in the infrared.[147] Therefore, an IR laser is good for the analysis of

*Reprinted by the permission of the Royal Society of Chemistry. Dr. Yohannes Rezenom built the laser system, and the author and Dr. Rezenom performed all the experiments together.

analytes with high water content, such as biological fluids and tissue samples. Third, it is possible to tune the IR laser energy, pulse width, and wavelength to control the desorption conditions and thereby control the generation of particles.[148] This feature is useful for changing the form of the removed material.

In this chapter, we describe the use of an IR laser for the desorption and ablation of samples with electrospray ionization. The IR MALDESI technique was performed by modifying the ion trap mass spectrometer to include a 2.94 μm Er:YAG laser for desorption and a nanoelectrospray source for ionization. Peptide and protein standards were used to characterize the system. In addition, blood, urine, and pharmaceutical products were analyzed without any sample pretreatment to demonstrate the system with complex mixtures.

5.2 Experimental

The experimental configuration of IR MALDESI was described in detail in Chapter 2, Section 2.3.3. The nanoelectrspray source was used to spray a 1:1 (v/v) solution of methanol and 0.2% acetic acid directly into the mass spectrometer. The solution flow rate was 500 nL/min using a syringe pump and a fused-silica capillary. No nebulizing gas was used. The nanoelectrospray needle was held at 2.5 kV, and the sample plate was at ground. The solution was sprayed continuously. Samples were deposited from 1 to 3 μL of aqueous analyte solutions onto the sample plate. The pulsed Er:YAG laser irradiated the liquid sample at the mid point between the spray tip and the skimmer cone. Mass spectra were acquired in positive ion mode and ions were accumulated for 100 ms.

5.3 Results

Standard peptides and proteins were used to test the IR MALDESI system. Samples in the liquid state were deposited from aqueous solutions onto the metal target. Then, the IR laser

was used to irradiate the sample to desorb and ablate material for interaction with the electrospray. No peptide or protein signals could be achieved when the laser was operated without the electrospray or when the electrospray was run without the laser. Also, no peptide or protein signal was obtained from dry sample deposits. After several minutes of exposure to the air, the water evaporated from the sample deposit, and it was no longer possible to obtain mass spectra. Signal could be recovered by adding water to the sample deposit.

The mass spectrum of the peptide bradykinin (M_R=1060) obtained using our system is shown in Figure 5-1. The doubly protonated bradykinin molecule peak is observed at *m/z* 531 in the spectrum. The singly protonated molecule peak of bradykinin is too weak to be distinguished from the background. Caffeine at 0.6 mM was used as an internal standard in the deposited solution and the protonated caffeine molecule peak is observed at *m/z* 195. The peaks below the caffeine peak are attributed to the electrospray solution. The mass spectrum is similar to that obtained from conventional ESI of bradykinin using the same instrument.

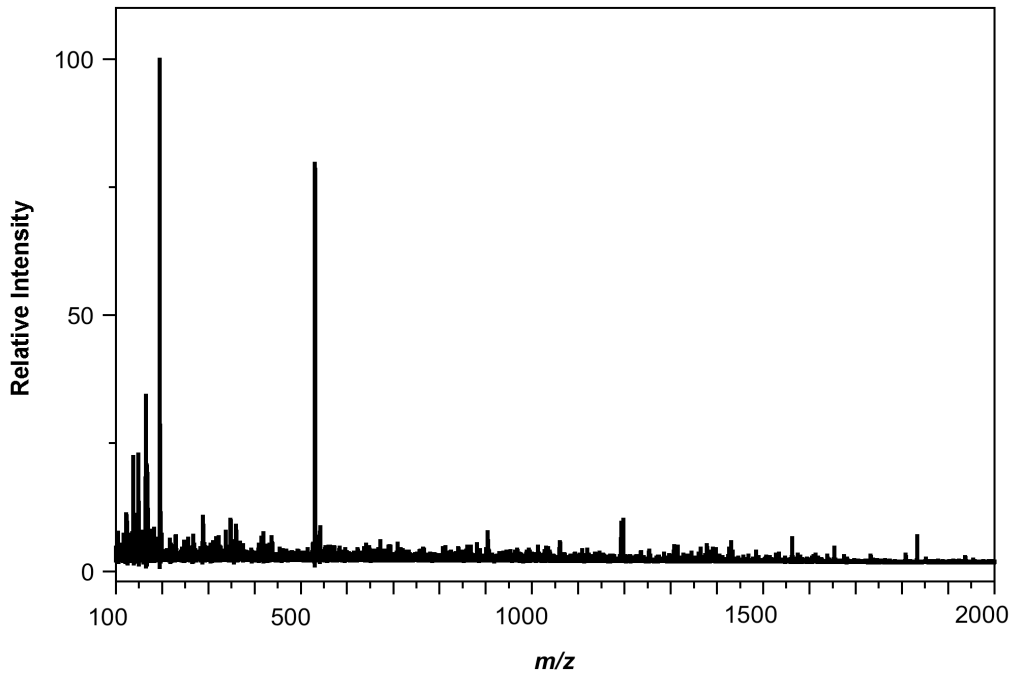

Figure 5-1. IR MALDESI mass spectrum of bradykinin.

An IR MALDESI mass spectrum of the protein cytochrome *c* is shown in Figure 5-2. It has been found that the observed charge states can provide information on the structure of the protein.[149] Native proteins that are compact, and thus some of the basic groups are inaccessible, and therefore show lower degrees of protonation than the denatured species.[149-151] The apparent bimodal peak intensity distribution in Figure 5-2 suggests the presence of both denatured and native cytochrome *c*. In the mass spectrum, a local maximum at $[M + 11H]^{11+}$ corresponds to the denatured protein, and a local maximum at $[M + 8H]^{8+}$corresponds to the native protein, respectively. This spectrum is similar to that obtained with conventional ESI and contains multiply protonated cytochrome *c* ions from $[M + 7H]^{7+}$ to $[M + 15H]^{+15}$. The mass spectrum is also similar to that of a cytochrome *c* dried deposit[152] and aqueous cytochrome *c* mixed with matrix,[153] which were irradiated with a UV laser and entrained into an electrospray.

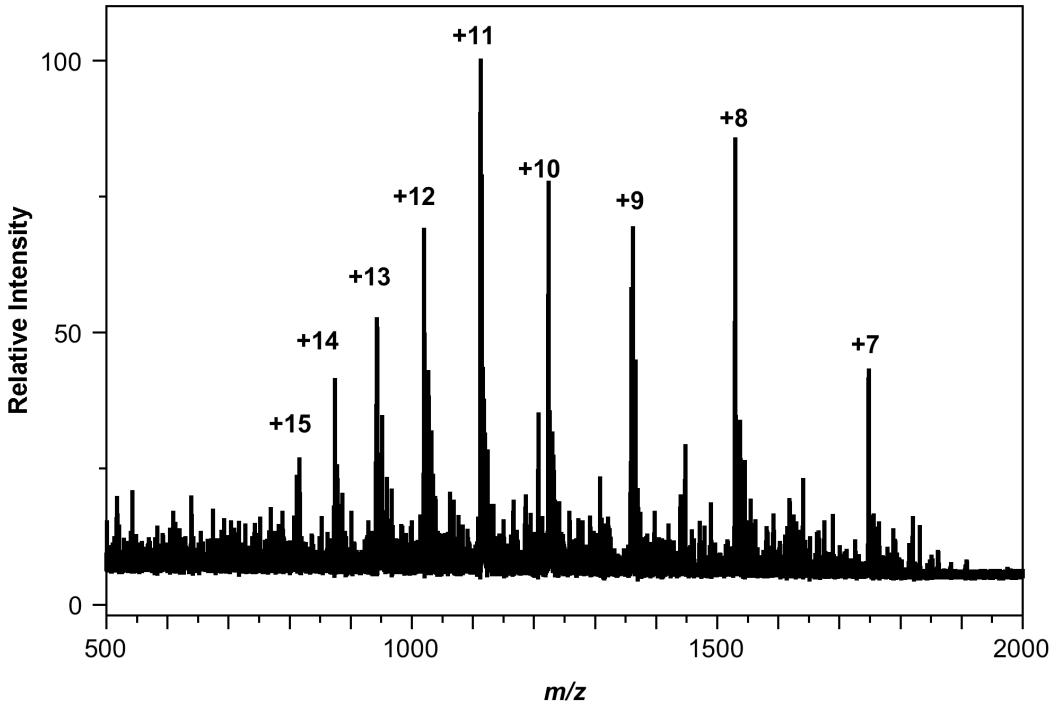

Figure 5-2. IR MALDESI mass spectrum of bovine cytochrome *c*.

In a previous report of UV-MALDESI, native cytochrome *c* was detected with a charge state maximum at $[M + 9H]^{+9}$ using α-cyano-4-hydroxycinnamic acid as the matrix, and denatured cytochrome *c* was detected using the same electrospray solution but without matrix.[152] The electrospray solution was a 1:1 (v/v) mixture of methanol and 0.1% acetic acid. However, in the absence of both matrix and acetic acid, peaks from both denatured and native cytochrome *c* with maxima at $[M + 16H]^{+16}$, $[M + 17H]^{+17}$ and $[M + 9H]^{+9}$, were observed. The consistency of our result with the previous work shows that our IR laser system can be applied to protein analysis. Different charge distributions of the multiply charged cytochrome *c* peaks obtained using our IR laser system in comparison with DESI and UV-MALDESI also shows that it is possible to obtain additional information about the sample. Future work can now exploit the advantages of our IR laser system.

To test the ability of IR MALDESI to analyze complex mixtures in biological fluids, a direct analysis of whole blood was performed. Figure 5-3 is the IR MALDESI spectrum of a fresh whole blood sample. Several peaks corresponding to multiply charged ions were observed, which are corresponding to hemoglobin α and β chains. Ionized heme at *m/z* 617 was also observed in the spectrum. Dried human blood was previously analyzed directly at ambient conditions using both DESI[48] and UV-LDESI.[154] These reports also demonstrated the detection of α and β chain hemoglobin. The spectrum of dryied whole blood obtained using UV-LDESI showed hemoglobin ion distribution from $[M + 11H]^{+11}$ to $[M + 18H]^{+18}$, which is similar to the IR MALDESI results shown here. However, in the DESI spectrum, ions corresponding to heme and hemoglobin α and β at *m/z* between $[M + 8H]^{+8}$ and $[M + 11H]^{+11}$ were observed.[48] This comparison shows that DESI is a softer desorption method than MALDESI, since the hemoglobin peaks detected by MALDESI came from denatured forms, while using DESI they

were in their native form. Although only α and β chain hemoglobin were detected from whole blood, the analysis of serum using UV-LDESI demonstrated the detection of albumin and other intact proteins.[154] This experiment shows that using our IR MALDESI system, the predominant proteins in biological fluids can be directly analyzed without drying. This approach reduces the possibility of the protein conformational change caused by drying or sample treatment.

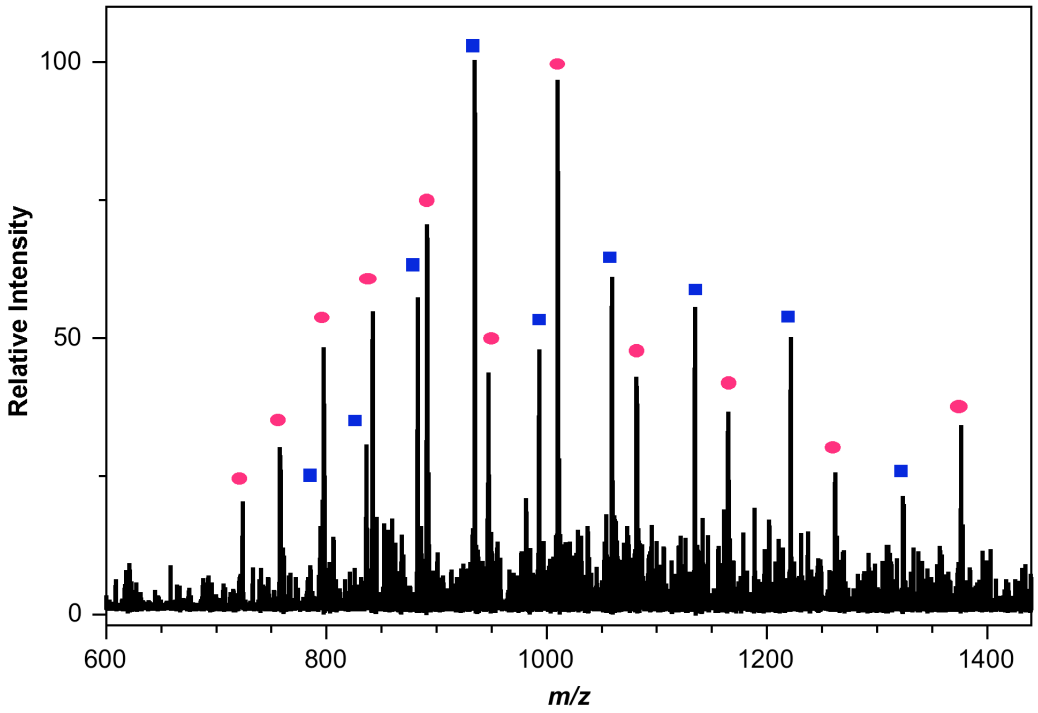

Figure 5-3. IR MALDESI mass spectrum of human whole blood. The blood droplet was deposited on a stainless steel surface and ablated with IR laser before it was dried. Peaks identified as ■, α-chain and ●, β-chain hemoglobin.

To further illustrate the application of IR MALDESI to the direct analysis of biological fluids, urine samples from two individuals (healthy and medicated) were analyzed and compared. Three μL of urine without any treatment was transferred onto the target and irradiated by the IR laser for electrospray ionization.

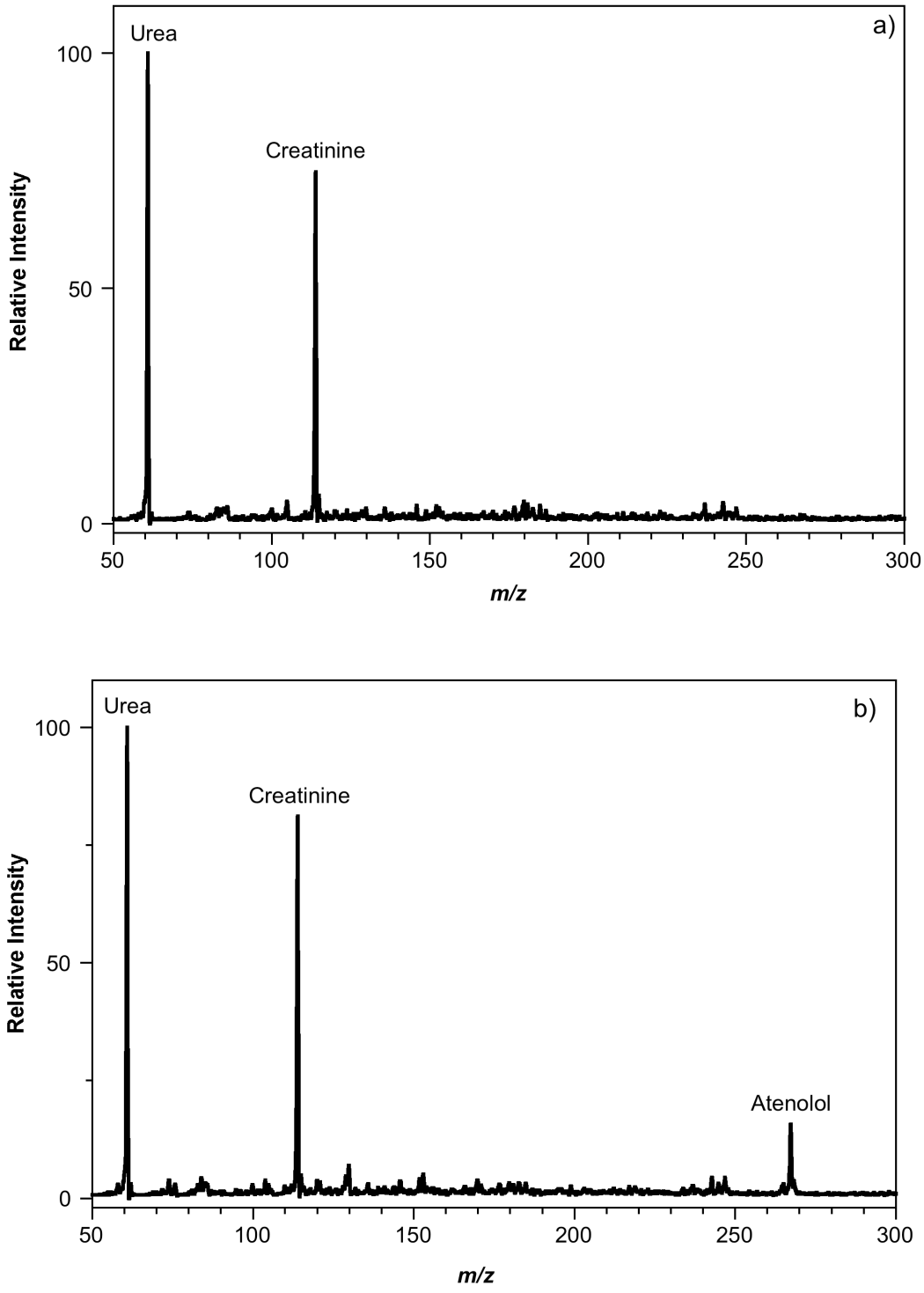

Figure 5-4. IR MALDESI mass spectrum of a urine sample of a) healthy and b) medicated individuals.

The spectrum shown in Figure 5-4a was obtained from the urine of the healthy individual. In this spectrum, the most intense peak is at *m/z* 61, and is attributed to protonated urea. Protonated creatinine at *m/z* 114 is also observed. It has been reported previously that using DESI, both urea and creatinine were detected from human urine.[155] Unlike the DESI result, no sodium adducts of the major urine constituent were observed using IR MALDESI. The IR MALDESI mass spectrum of urine obtained from a person who had been medicated the drug atenolol (100 mg daily) is shown in Figure 5-4b. Atenolol is a β-adrenoreceptor blocking drug used to treat hypertension.[156]The mass spectrum in Figure 5-4b is similar to Figure 5-4a with an additional peak at *m/z* 267, which corresponds to protonated atenolol. Previously, metabolism studies of atenolol have shown that only 10% of the drug is absorbed by the body and metabolized; the remaining material is excreted unchanged.[156, 157] The observation of an intense signal from the unmodified atenolol is consistent with this study. However, the major metabolite component of atenolol, 1-[4-(C-carbamoylhydroxymethyl)phenoxy]-3-isopropylaminopropan-2-ol,[157] obtained by hydroxylation of methyl carbon of the acetamide moiety by liver[156] was not detected under our current experimental conditions. This results shows that it is possible to use this method for the analysis of metabolites of drugs in biological fluids.

Several over-the-counter pharmaceutical products were directly analyzed using IR MALDESI. The liquid contents of a gel coated ibuprofen tablet were transferred onto the sample target without any additional treatment and laser ablated into the ESI plume. The tablet contained a viscous liquid with 200 mg of solubilized ibuprofen as well as other inactive ingredients such as dyes, gelatin, mineral oil, polyethylene glycol, and sugars.

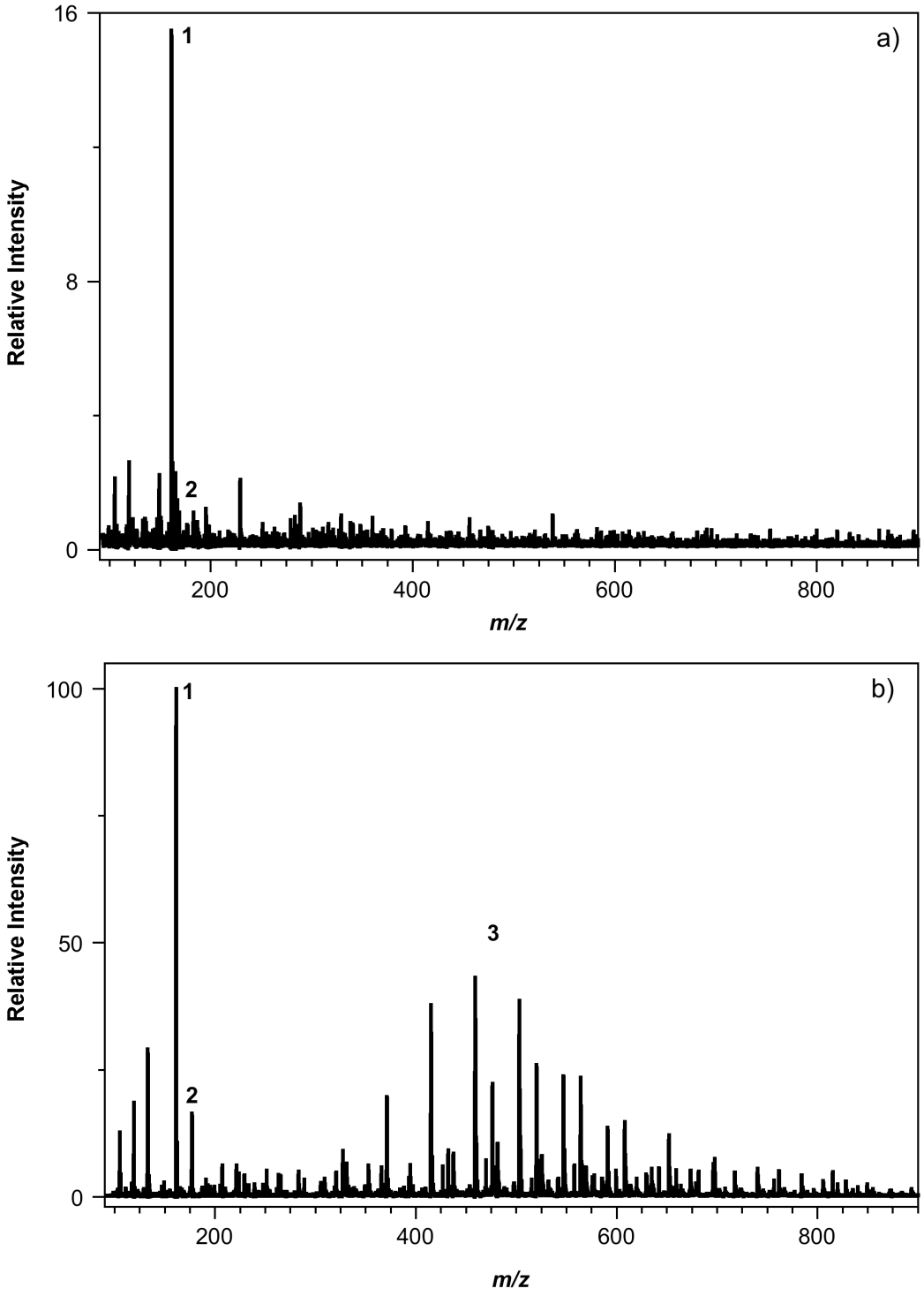

Figure 5-5. IR MALDESI mass spectrum of a gel form ibuprophen tablet a) without adding water and b) after addition of 4.0 μL of water. The intensity of a) is normalized relative to the base peak intensity (at *m/z* 161) of b); 1 and 2 are the protonated fragment of ibuprophen, 3 is the group of peaks from the polyethylene glycol.

Figure 5-5a is the spectrum obtained from this sample without any treatment. The peak at *m/z* 177 corresponds to a protonated fragment of ibuprofen with the loss of formaldehyde and the base peak at *m/z* 161 corresponds to ibuprofen that has lost the carboxylic acid group. A relatively weak signal at *m/z* at 207 corresponds to the protonated ibuprofen peak. Figure 5-5b is the spectrum obtained from the same ibuprofen gel after addition of 4 μL of water to the sample target. From the spectrum, we can see that the signals of the protonated ibuprofen and its fragments were enhanced by the presence of water. In addition to the detection of ibuprofen and its fragments, ions from polyethylene glycol were also observed after adding water. This result shows that water is important for the ionization, and it plays the role of a matrix.

Figure 5-6 shows the IR MALDESI analysis of a cold medicine with multiple active ingredients, such as acetaminophen (30 mg/mL), sedating antihistamine (doxylamine succinate, 0.4 mg/mL), and antitussive (dextromethorphan, 1 mg/mL). The protonated acetaminophen peak is observed at *m/z* 152. The peak observed at *m/z* 110 corresponds to protonated acetaminophen with loss of ketene. Weak signals from protonated doxylamine (<8% relative intensity) at *m/z* 271, and its fragments by successive loss of $[C(C_6H_5)(C_5H_4N)(CH_3)]^+$ group and $[C(C_6H_5)(C_5H_4N)]^+$ group were observed at *m/z* 182 and 167 respectively. A peak at *m/z* 272 was assigned to the protonated molecule of the third active ingredient, dextromethorphan. The cluster of peaks observed between 262 and 650 *m/z* correspond to protonated PEG. Also, the sodium adduct of fructose is observed at m/z 203. A sodium adduct was not observed in any of the other samples run using IR MALDESI. This suggests that the presence of sodiated fructose in the spectrum is due to the greater quantity of sodium presents in the cold medicine or due to the fact that sugars tend to form adducts with sodium.[102]

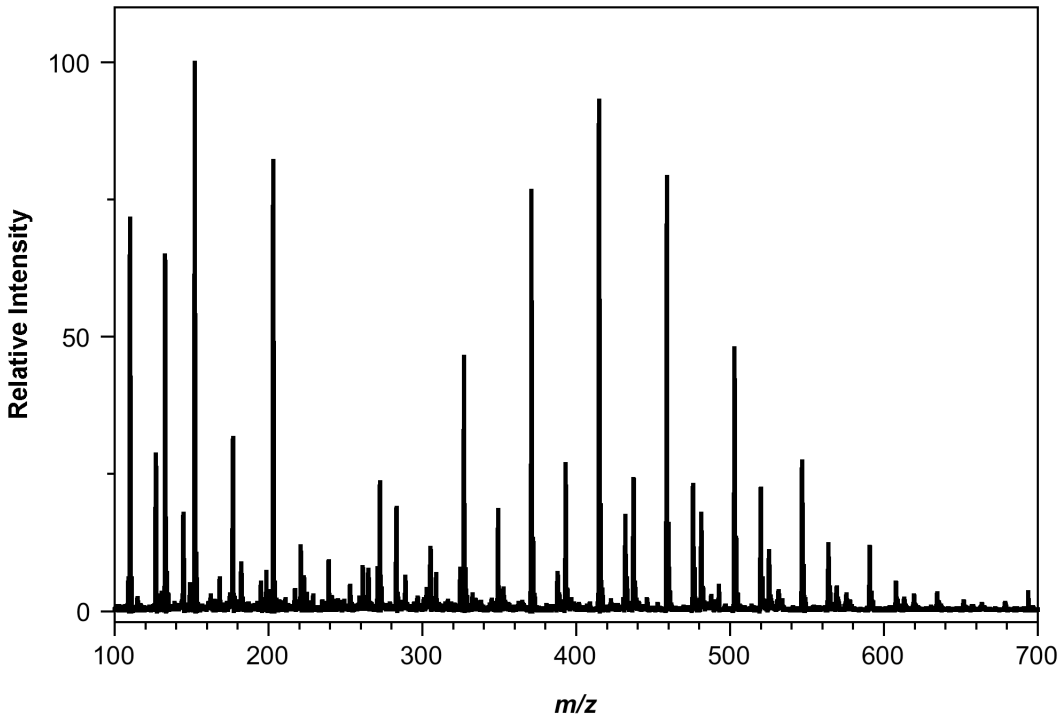

Figure 5-6. IR MALDESI of a liquid cold medicine.

Pharmaceutical products in ointment form were also analyzed using IR MALDESI. A small amount of the ointment (approximately 1- 2 mg) was spread on a stainless steel platform and was exposed to the pulsed laser. A mass spectrum obtained from the ointment (1% hydrocortisone cream) is shown in Figure 5-7. The most intense peak at *m/z* 363 corresponds to protonated hydrocortisone. The several peaks below *m/z* of 360 are tentatively assigned to sugars. The peaks observed between 560 and 760 *m/z* with a 29 *m/z* spacing, suggest the loss of an ethyl group from an oil or wax component of the sample. Earlier, it was demonstrated that hydrocortisone ointment was weakly ionized by DESI in positive ion mode.[158, 159] From the result above, the ionization of hydrocortisone was enhanced using our IR MALDESI system.

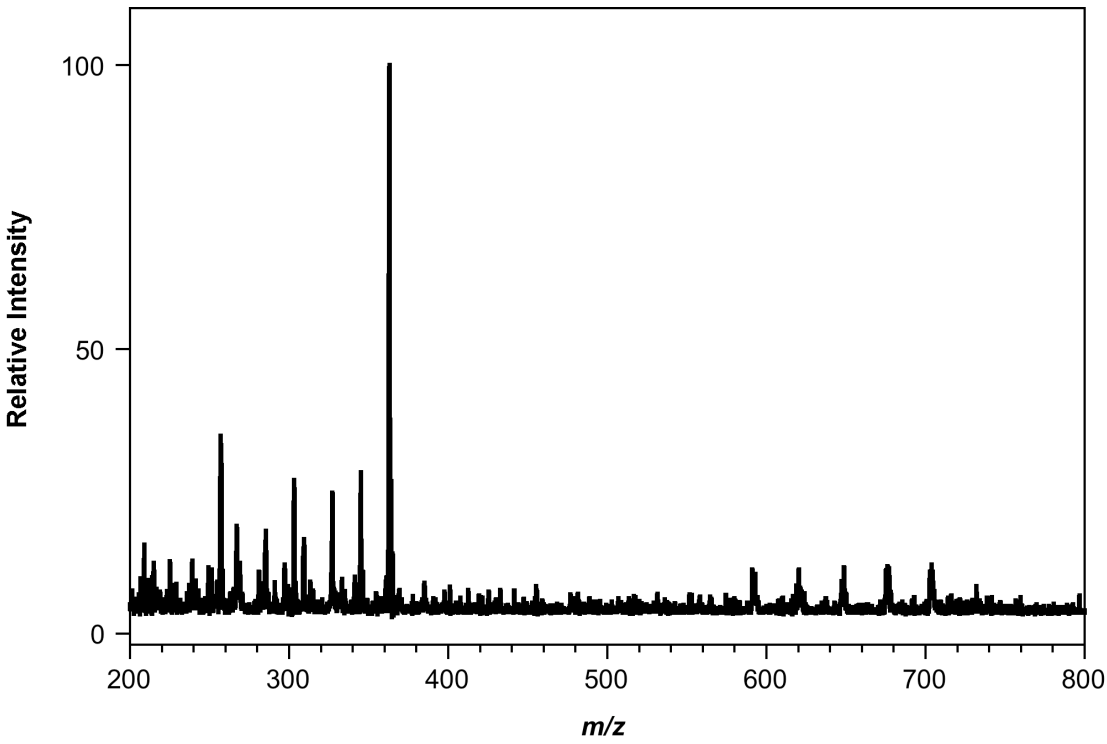

Figure 5-7. IR MALDESI mass spectrum of 1% hydrocortisone cream.

5.4 Discussion

The exact mechanism of combining laser desorption and electrospray ionization is yet not fully understood. It has been postulated that gas-phase analyte molecules desorbed by the laser are post-ionized by their fusion with charged solvent droplets followed by the subsequent ESI processes from the newly formed droplet.[85, 86] However, in the referenced study, a UV laser was used, and the experimental geometries, such as the distances between the electrospray, sample target, and the MS skimmer, were different from our design. These parameters are important factors that can affect the ionization. Also, in the previous study of the MALDI mechanism, it has been reported that desorption or ablation of analyte material occurs before analyte ionization, and laser desorption or ablation removes more material as clusters and particles than as ions.[82, 160] Therefore, we postulate that material ablated from the target in the form of particulate

interacts with the ESI droplets, which pick up the analyte material in a similar manner to the electrospray droplets in a DESI source, where the analyte molecule is picked up from a solid target. This mechanism is also similar to that postulated for dry particles in Chapter 3, in which electrospray droplets pick up analyte molecule from particulate material. It has been demonstrated that a large fraction of IR ablated material is in the form of particles, which are larger than the nanoelectrosprayed droplets.[94] The small electrospray droplets collide with these larger particles, extract material and thereafter expel ions via the standard electrospray mechanism. For more volatile materials, a second mechanism may occur in which the analyte is desorbed as free molecules and is thereby incorporated in the electrospray droplets.[161] The ionization of the low molecular weight materials most likely proceeds by this mechanism. A systematic study of the effect of parameters of the experimental geometry on signal intensity as well as some computer simulation methods used to study MALDI and DESI mechanism such as molecular dynamics simulation[162] may provide useful information to further elucidate the mechanism.

In addition, the above results indicate the importance of water for desorption of material using an infrared laser. The O-H stretch of water has a strong IR absorption between the wavelengths of 2.8 and 3.2 μm, and readily absorbs the laser pulse energy leading to the ejection of a microscopic volume of the sample in the form of neutral particles and molecules.[163, 164] Water has been employed as a matrix in IR MALDI both under vacuum[165] and in atmospheric pressure MALDI.[166, 167] Recently, water mixed with glycerol has also been used as matrix, in which multiply-charged proteins were observed in atmospheric pressure MALDI.[168] It has been suggested that the ionization mechanism is similar to electrospray and involves the ejection of highly charged particles from the glycerol that evaporate to form ions. This speculation is

supported by high-speed photography[169] and studies of IR laser particle formation from a glycerol matrix.[170]

5.5 Summary

This study demonstrates biological and pharmaceutical samples can be directly analyzed without any sample treatment using IR MALDESI under ambient conditions. Water in the sample appears to act as an endogenous matrix. In IR MALDESI, the laser desorbs material from the sample that then interacts with the electrospray to form ions. It is postulated that the ablated particles interact with the multiply charged electrospray droplets, which extract the analyte molecules and form ions by the standard electrospray mechanism.

Our results indicate that water facilitates the desorption process. This bodes well for the application of IR MALDESI for direct analysis of body fluids for the study of both drug metabolism and pharmacokinetics. Biological fluids from urine and blood can be used for direct monitoring of drug metabolites. In addition, because the water content in biological tissue is significant, IR MALDESI has some potential for tissue imaging under ambient conditions. For convenience, it is also possible to re-arrange the experimental configuration and develop an IR laser remote probe by using an optical fiber for imaging analysis.

The ionization process of IR MALDESI can be affected by several factors, including laser wavelength and energy, electrospray solution, and the geometry of the experimental configuration. Although a detailed study of optimization conditions for ionization was not performed, laser wavelength and energy will play a critical role in increasing the amount of material removed. In addition to these parameters, coupling of IR MALDESI to different mass analyzers, such as Fourier transform ion cyclotron resonance mass spectrometer (FT-ICR)[171] and

orthogonal time of flight (Q-TOF), will benefit the technique in terms of resolution and mass range of detection.

CHAPTER 6. CONCLUSIONS AND FUTURE DIRECTIONS

In this dissertation, we configured merged electrospray ionization with various sample sources for diverse applications. Using this technique, dry aerosol particles, combustion products, and IR laser desorbed and ablated materials were analyzed under ambient conditions. This work is a proof-of-principle study. The significance of this work is that it opens up a new way to analyze samples in various states without sample collection or pretreatment.

One of the promising results of this study is the ability to directly analyze dry aerosol particles of powdered samples generated from an aerosol generator. As shown in Chapter 3, major components in powdered samples can be directly detected through the interaction of the particles with the electrospray charged droplets. This study was the fundamental part of this entire research. Previously, charged droplets from eletrospray had been used to directly ionize neutral liquid particles, such as in EESI,[70] and particles and molecules desorbed by a pulsed laser, such as in UV-MALDESI.[71, 72] In this work, dry particles were shown to be directly ionized by charged droplets. This result indicates that particles in various states can interact with charged droplets from an electrospray source, and generates ions that can be analyzed by a mass spectrometer. In addition, dry particles containing large molecules can be analyzed by this method. Thus, it may be possible to use merged electrospray ionization to monitor bioaerosols. Bioaerosols are the primary dissemination mechanism of biological warfare and terrorism. Therefore, fast and accurate detection and identification of bioaerosols is imperative. The merged electrospray ionization technique matches this criterion.

An application of the merged electrospray ionization technique was the direct analysis of combustion products generated from fuel combustion and smoke. As shown in Chapter 4, a

home-build flame source and some smoke sources were configured with merged electrospray ionization. The major components from smoke and fuel combustion flames can be directly detected by interacting with the electrospray charged droplets. This part of work shows that real-world materials generated from the smoke and fuel combustion can be ionized by this method. Even though, we still cannot confirm whether particles or molecules play a more important role in the ionization, it points the direction for future studies. In addition, the implication of this study includes the application of this method to air quality control and monitoring of combustion products and other pollutants. The information obtained by merged electrospray ionization complements the results obtained using the traditional MS techniques, such as LDI and GC-MS that can affirmatively identify additional products from the mass spectra. We believe that with further modifications to the apparatus and using a higher resolution mass spectrometer, the results will be improved.

Another important extended study is using electrospray to ionize materials desorbed or ablated by an IR laser. It was shown in Chapter 5 that biological and pharmaceutical samples can be directly analyzed by combining IR laser desorption or ablation and electrospray ionization. Multiply charged peaks for protein samples were observed using this method. Major components in biological fluids and multiple components in pharmaceutical samples were detected without any treatment. This approach separates the location of desorption from that of ion formation, in comparison with methods such as DESI and DART that deliver charged species to the sample. Thus, this method makes it easier to create a remote analysis probe since the umbilical cord that connects the sampler to the instrument requires only a gas flow and a fiber optic rather than liquid, gas and high voltage. Also, the IR laser shows several advantages compared to the UV laser. With the greater penetration depth of the IR laser and the direct ionization of the sample

materials with their endogenous matrix (such as water) combining an IR laser with electrospray ionization shows potential for application to tissue imaging and the analysis of biological fluids. This system also has the potential to be interfaced with continuous flow sample introduction with potential applications in interfacing this IR MALDESI system with a microfluidic chip. With the development of a micro-fluidic chip interface,[172] such as on chip cell lysing and proteolytic digestion, it may be possible to monitor protein digestion and biological reactions on the chip using the IR MALDESI system.

REFERENCES

1. Dass, C., Principles and Practice of Biological Mass spectrometry. *John Wiley&Sons, Inc.* **2001,** Chapter 1&2, 1-58.

2. Vestal, M. L., Methods of ion generation. *Chem. Rev.* **2001,** *101* (2), 361-75.

3. Busch, K. L., Mass spectrometry forum electron ionization: more ins and outs. *Spectroscopy (Duluth, MN, U. S.)* **2006,** *21* (10), 14, 16, 18-19.

4. Baldwin, M. A., Mass spectrometers for the analysis of biomolecules. *Methods Enzymol.* **2005,** *402* (Biological Mass Spectrometry), 3-48.

5. Munson, M. S. B.; Field, F. H., Chemical ionization mass spectrometry. I. General introduction. *J. Am. Chem. Soc.* **1966,** *88* (12), 2621-30.

6. Barber, M.; Bordoli, R. S.; Sedgwick, R. D.; Tyler, A. N., Fast atom bombardment of solids (F.A.B.): a new ion source for mass spectrometry. *J. Chem. Soc., Chem. Commun.* **1981,** (7), 325-7.

7. Torgerson, D. F.; Skowronski, R. P.; Macfarlane, R. D., New approach to the mass spectroscopy of non-volatile compounds. *Biochem. Biophys. Res. Commun.* **1974,** *60* (2), 616-21.

8. Aduru, S.; Chait, B. T., Californium-252 plasma desorption mass spectrometry of oligosaccharides and glycoconjugates: control of ionization and fragmentation. *Anal. Chem.* **1991,** *63* (15), 1621-5.

9. Dass, C.; Desiderio, D. M., Fast atom bombardment mass spectrometry analysis of opioid peptides. *Anal. Biochem.* **1987,** *163* (1), 52-66.

10. Barber, M.; Green, B. N., The analysis of small proteins in the molecular weight range 10-24 kDa by magnetic sector mass spectrometry. *Rapid Commun. Mass Spectrom.* **1987,** *1* (5), 80-3.

11. Fenn, J. B.; Mann, M.; Meng, C. K.; Wong, S. F.; Whitehouse, C. M., Electrospray ionization for mass spectrometry of large biomolecules. *Science* **1989,** *246* (4926), 64-71.

12. Karas, M.; Bachmann, D.; Hillenkamp, F., Influence of the wavelength in high-irradiance ultraviolet laser desorption mass spectrometry of organic molecules. *Anal. Chem.* **1985,** *57* (14), 2935-9.

13. Fenn, J. B.; Mann, M.; Meng, C. K.; Wong, S. F.; Whitehouse, C. M., Electrospray ionization-principles and practice. *Mass Spectrom. Rev.* **1990,** *9* (1), 37-70.

14. Taylor, G. I., Disintegration of water drops in an electric field. *Proc. R. Soc. London Ser. A* **1964,** *280*.

15. Kebarle, P., A brief overview of the present status of the mechanisms involved in electrospray mass spectrometry. *J. Mass Spectrom.* **2000,** *35* (7), 804-17.

16. Manisali, I.; Chen, D. D. Y.; Schneider, B. B., Electrospray ionization source geometry for mass spectrometry: past, present, and future. *Trac-Trends Anal. Chem.* **2006,** *25* (3), 243-256.

17. Iribarne, J. V.; Thomson, B. A., On the evaporation of small ions from charged droplets. *J. Chem. Phys.* **1976,** *64* (6), 2287-94.

18. Dole, M.; Mack, L. L.; Hines, R. L.; Mobley, R. C.; Ferguson, L. D.; Alice, M. B., Molecular beams of macroions. *J. Chem. Phys.* **1968,** *49* (5), 2240-9.

19. Mann, M.; Shen, S.; Fenn, J. B., Electrospray mass spectrometry. *NATO ASI Ser., Ser. C* **1992,** *353* (Mass Spectrom. Biol. Sci.: Tutorial), 145-63.

20. Kaltashov, I. A.; Mohimen, A., Estimates of Protein Surface Areas in Solution by Electrospray Ionization Mass Spectrometry. *Anal. Chem.* **2005,** *77* (16), 5370-5379.

21. Dass, C., Recent developments and applications of high-performance liquid chromatography-electrospray ionization mass spectrometry. *Curr. Org. Chem.* **1999,** *3* (2), 193-209.

22. Herrero, M.; Ibanez, E.; Cifuentes, A., Capillary electrophoresis-electrospray-mass spectrometry in peptide analysis and peptidomics. *Electrophoresis* **2008,** *29* (10), 2148-2160.

23. El-Aneed, A.; Cohen, A.; Banoub, J., Mass Spectrometry, Review of the Basics: Electrospray, MALDI, and Commonly Used Mass Analyzers. *Appl. Spectrosc. Rev.* **2009,** *44* (3), 210-230.

24. Karas, M.; Bahr, U.; Hillenkamp, F., UV laser matrix desorption/ionization mass spectrometry of proteins in the 100,000 Dalton range. *Int. J. Mass Spectrom. Ion Proesses* **1989,** *92*, 231-42.

25. Tanaka, K.; Waki, H.; Ido, Y.; Akita, S.; Yoshida, Y.; Yohida, T., Protein and polymer analyses up to m/z 100,000 by laser ionization time-of-flight mass spectrometry. *Rapid Commun. Mass Spectrom.* **1988,** *2* (8), 151-3.

26. Siuzdak, G., Mass spectrometry for Biotechnology. **1999,** Chapter 2.

27. Knochenmuss, R., Ion formation mechanisms in UV-MALDI. *Analyst* **2006,** *131* (9), 966-986.

28. Chang Wei, C.; Huang Ling Chu, L.; Wang, Y.-S.; Peng, W.-P.; Chang Huan, C.; Hsu Nien, Y.; Yang Wen, B.; Chen Chung, H., Matrix-assisted laser desorption/ionization (MALDI) mechanism revisited. *Anal. Chim. Acta* **2007,** *582* (1), 1-9.

29. Karas, M.; Gluckmann, M.; Schafer, J., Ionization in matrix-assisted laser desorption/ionization: singly charged molecular ions are the lucky survivors. *J. Mass. Spectrom.* **2000,** *35* (1), 1-12.

30. Tabb, D. L.; McDonald, W. H.; Yates, J. R., 3rd, DTASelect and Contrast: tools for assembling and comparing protein identifications from shotgun proteomics. *J. Proteome Res.* **2002,** *1* (1), 21-6.

31. Karas, M.; Ingendoh, A.; Bahr, U.; Hillenkamp, F., Ultraviolet-laser desorption/ionization mass spectrometry of femtomolar amounts of large proteins. *Biomed. Environ. Mass Spectrom.* **1989,** *18* (9), 841-3.

32. Tang, K.; Taranenko, N. I.; Allman, S. L.; Chen, C. H.; Chang, L. Y.; Jacobson, K. B., Picolinic acid as a matrix for laser mass spectrometry of nucleic acids and proteins. *Rapid Commun. Mass Spectrom.* **1994,** *8* (9), 673-7.

33. Hsu, N.-Y.; Yang, W.-B.; Wong, C.-H.; Lee, Y.-C.; Lee, R. T.; Wang, Y.-S.; Chen, C.-H., Matrix-assisted laser desorption/ionization mass spectrometry of polysaccharides with 2',4',6'-trihydroxy-acetophenone as matrix. *Rapid Commun. Mass Spectrom.* **2007,** *21* (13), 2137-46.

34. Hedrich, H. C.; Isobe, K.; Stahl, B.; Nokihara, K.; Kordel, M.; Schmid, R. D.; Karas, M.; Hillenkamp, F.; Spener, F., Matrix-assisted ultraviolet laser desorption/ionization mass spectrometry applied to multiple forms of lipases. *Anal. Biochem.* **1993,** *211* (2), 288-92.

35. Tang, X.; Dreifuss, P. A.; Vertes, A., New matrixes and accelerating voltage effects in matrix-assisted laser desorption/ionization of synthetic polymers. *Rapid Commun. Mass Spectrom.* **1995,** *9* (12), 1141-7.

36. Montaudo, G.; Montaudo, M. S.; Puglisi, C.; Samperi, F., Determination of Absolute Mass Values in MALDI-TOF of Polymeric Materials by a Method of Self-Calibration of the Spectra. *Anal. Chem.* **1994,** *66* (23), 4366-9.

37. Cooks, R. G.; Ouyang, Z.; Takats, Z.; Wiseman, J. M., Detection Technologies. Ambient mass spectrometry. *Science* **2006,** *311* (5767), 1566-70.

38. Harris, G. A.; Nyadong, L.; Fernandez, F. M., Recent developments in ambient ionization techniques for analytical mass spectrometry. *Analyst* **2008,** *133* (10), 1297-301.

39. Venter, A.; Nefliu, M.; Cooks, R. G., Ambient desorption ionization mass spectrometry. *TrAC-Trends Anal. Chem.* **2008,** *27* (4), 284-90.

40. Laiko, V. V.; Baldwin, M. A.; Burlingame, A. L., Atmospheric pressure matrix-assisted laser desorption/ionization mass spectrometry. *Anal. Chem.* **2000,** *72* (4), 652-7.

41. Laiko, V. V.; Moyer, S. C.; Cotter, R. J., Atmospheric pressure MALDI/ion trap mass spectrometry. *Anal. Chem.* **2000,** *72* (21), 5239-43.

42. Daniel, J. M.; Laiko, V. V.; Doroshenko, V. M.; Zenobi, R., Interfacing liquid chromatography with atmospheric pressure MALDI-MS. *Anal. Bioanal. Chem.* **2005,** *383* (6), 895-902.

43. Daniel, J. M.; Ehala, S.; Friess, S. D.; Zenobi, R., On-line atmospheric pressure matrix-assisted laser desorption/ionization mass spectrometry. *Analyst* **2004,** *129* (7), 574-8.

44. Takats, Z.; Wiseman, J. M.; Gologan, B.; Cooks, R. G., Mass spectrometry sampling under ambient conditions with desorption electrospray ionization. *Science* **2004,** *306* (5695), 471-3.

45. Venter, A.; Sojka, P. E.; Cooks, R. G., Droplet dynamics and ionization mechanisms in desorption electrospray ionization mass spectrometry. *Anal. Chem.* **2006,** *78* (24), 8549-55.

46. Costa, A. B.; Cooks, R. G., Simulation of atmospheric transport and droplet-thin film collisions in desorption electrospray ionization. *Chem. Commun. (Camb)* **2007,** (38), 3915-7.

47. Volny, M.; Venter, A.; Smith, S. A.; Pazzi, M.; Cooks, R. G., Surface effects and electrochemical cell capacitance in desorption electrospray ionization. *Analyst* **2008,** *133* (4), 525-31.

48. Takats, Z.; Wiseman, J. M.; Cooks, R. G., Ambient mass spectrometry using desorption electrospray ionization (DESI): instrumentation, mechanisms and applications in forensics, chemistry, and biology. *J. Mass Spectrom.* **2005,** *40* (10), 1261-75.

49. Kasi, S. R.; Kang, H.; Sass, C. S.; Rabalais, J. W., Inelastic processes in low-energy ion-surface collisions. *Surf. Sci. Rep.* **1989,** *10* (1-2), 1-104.

50. Chen, H.; Talaty, N. N.; Takats, Z.; Cooks, R. G., Desorption electrospray ionization mass spectrometry for high-throughput analysis of pharmaceutical samples in the ambient environment. *Anal. Chem.* **2005,** *77* (21), 6915-27.

51. Fernandez, F. M.; Cody, R. B.; Green, M. D.; Hampton, C. Y.; McGready, R.; Sengaloundeth, S.; White, N. J.; Newton, P. N., Characterization of solid counterfeit drug samples by desorption electrospray ionization and direct-analysis-in-real-time coupled to time-of-flight mass spectrometry. *Chemmedchem.* **2006,** *1* (7), 702.

52. Shin, Y. S.; Drolet, B.; Mayer, R.; Dolence, K.; Basile, F., Desorption Electrospray Ionization-Mass Spectrometry of Proteins. *Anal. Chem.* **2007,** *79*, 3514-18.

53. Wiseman, J. M.; Puolitaival, S. M.; Takats, Z.; Cooks, R. G.; Caprioli, R. M., Mass spectrometric profiling of intact biological tissue by using desorption electrospray ionization. *Ange. Chem. Int. Ed.* **2005,** *44* (43), 7094-97.

54. Kaur-Atwal, G.; Weston, D. J.; Green, P. S.; Crosland, S.; Bonner, P. L.; Creaser, C. S., Analysis of tryptic peptides using desorption electrospray ionisation combined with ion mobility spectrometry/mass spectrometry. *Rapid Commun. Mass Spectrom.* **2007,** *21* (7), 1131-8.

55. Bereman, M. S.; Nyadong, L.; Fernandez, F. M.; Muddiman, D. C., Direct high-resolution peptide and protein analysis by desorption electrospray ionization Fourier transform ion cyclotron resonance mass spectrometry. *Rapid Commun. Mass Spectrom.* **2006,** *20* (22), 3409-11.

56. D'Agostino, P. A.; Chenier, C. L.; Hancock, J. R.; Lepage, C. R., Desorption electrospray ionisation mass spectrometric analysis of chemical warfare agents from solid-phase microextraction fibers. *Rapid Commun. Mass Spectrom.* **2007,** *21* (4), 543-9.

57. Cotte-Rodriguez, I.; Takats, Z.; Talaty, N.; Chen, H.; Cooks, R. G., Desorption electrospray ionization of explosives on surfaces: sensitivity and selectivity enhancement by reactive desorption electrospray ionization. *Anal. Chem.* **2005,** *77* (21), 6755-64.

58. Takats, Z.; Cotte-Rodriguez, I.; Talaty, N.; Chen, H.; Cooks, R. G., Direct, trace level detection of explosives on ambient surfaces by desorption electrospray ionization mass spectrometry. *Chem Commun. (Camb)* **2005,** (15), 1950-2.

59. Justes, D. R.; Talaty, N.; Cotte-Rodriguez, I.; Cooks, R. G., Detection of explosives on skin using ambient ionization mass spectrometry. *Chem. Commun.* **2007,** (21), 2142-44.

60. Song, Y.; Talaty, N.; Tao, W. A.; Pan, Z.; Cooks, R. G., Rapid ambient mass spectrometric profiling of intact, untreated bacteria using desorption electrospray ionization. *Chem. Commun. (Camb)* **2007,** (1), 61-3.

61. Meetani, M. A.; Shin, Y. S.; Zhang, S.; Mayer, R.; Basile, F., Desorption electrospray ionization mass spectrometry of intact bacteria. *J. Mass Spectrom.* **2007,** *42* (9), 1186-93.

62. Nefliu, M.; Venter, A.; Cooks, R. G., Desorption electrospray ionization and electrosonic spray ionization for solid- and solution-phase analysis of industrial polymers. *Chem. Commun. (Camb)* **2006,** (8), 888-90.

63. Wiseman, J. M.; Ifa, D. R.; Song, Q. Y.; Cooks, R. G., Tissue imaging at atmospheric pressure using desorption electrospray ionization (DESI) mass spectrometry. *Ange. Chem. Int. Ed.* **2006,** *45* (43), 7188-92.

64. Van Berkel, G. J.; Kertesz, V., Automated sampling and imaging of analytes separated on thin-layer chromatography plates using desorption electrospray ionization mass spectrometry. *Anal. Chem.* **2006,** *78* (14), 4938-44.

65. Cody, R. B.; Laramee, J. A.; Durst, H. D., Versatile new ion source for the analysis of materials in open air under ambient Conditions. *Anal. Chem.* **2005,** *77* (8), 2297-302.

66. Penning, F. M., Ionization by metastable atoms. *Naturwissenschaften* **1927,** *15*, 818.

67. Nilles, J. M.; Connell, T. R.; Durst, H. D., Quantitation of Chemical Warfare Agents Using the Direct Analysis in Real Time (DART) Technique. *Anal. Chem.* **2009,** *81* (16), 6744-49.

68. Sparkman, O. D.; Jones, P. R.; Curtis, M., Accurate mass measurements with a reflectron time-of-flight mass spectrometer and the direct analysis in real time (DART) interface for the identification of unknown compounds below masses of 500 DA. *Chem. Anal.* **2009,** *173*, 229-45.

69. Williams, J. P.; Patel, V. J.; Holland, R.; Scrivens, J. H., The use of recently described ionisation techniques for the rapid analysis of some common drugs and samples of biological origin. *Rapid Commun. Mass Spectrom.* **2006,** *20* (9), 1447-56.

70. Chen, H.; Venter, A.; Cooks, R., Extractive electrospray ionization for direct analysis of undiluted urine, milk and other complex mixtures without sample preparation. *Chem. Commun.* **2006,** (19), 2042-4.

71. Shiea, J.; Huang, M. Z.; Hsu, H. J.; Lee, C. Y.; Yuan, C. H.; Beech, I.; Sunner, J., Electrospray-assisted laser desorption/ionization mass spectrometry for direct ambient analysis of solids. *Rapid Commun. Mass Spectrom.* **2005,** *19* (24), 3701-4.

72. Sampson, J. S.; Hawkridge, A. M.; Muddiman, D. C., Generation and detection of multiply-charged peptides and proteins by matrix-assisted laser desorption electrospray ionization (MALDESI) Fourier transform ion cyclotron resonance mass spectrometry. *J. Am. Soc. Mass Spectrom.* **2006,** *17* (12), 1712-6.

73. Chang, D. Y.; Lee, C. C.; Shiea, J., Detecting large biomolecules from high-salt solutions by fused-droplet electrospray ionization mass spectrometry. *Anal. Chem.* **2002,** *74* (11), 2465-9.

74. Hong, C. M.; Tsai, F. C.; Shiea, J., A multiple channel electrospray source used to detect highly reactive ketenes from a flow pyrolyzer. *Anal. Chem.* **2000,** *72* (6), 1175-1178.

75. Shiea, J.; Chang, D. Y.; Lin, C. H.; Jiang, S. J., Generating multiply charged protein ions by ultrasonic nebulization/multiple channel-electrospray ionization mass spectrometry. *Anal. Chem.* **2001,** *73* (20), 4983-7.

76. Shieh, I. F.; Lee, C. Y.; Shiea, J., Eliminating the interferences from TRIS buffer and SDS in protein analysis by fused-droplet electrospray ionization mass spectrometry. *J. Proteome Res.* **2005,** *4* (2), 606-12.

77. Chen, H.; Wortmann, A.; Zenobi, R., Neutral desorption sampling coupled to extractive electrospray ionization mass spectrometry for rapid differentiation of biosamples by metabolomic fingerprinting. *J. Mass Spectrom.* **2007,** *42* (9), 1123-35.

78. Lee, C. Y.; Shiea, J., Gas chromatography connected to multiple channel electrospray ionization mass spectrometry for the detection of volatile organic compounds. *Anal. Chem.* **1998,** *70* (13), 2757-61.

79. Chen, H.; Yang, S.; Wortmann, A.; Zenobi, R., Neutral desorption sampling of living objects for rapid analysis by extractive electrospray ionization mass spectrometry. *Angew. Chem. Int. Ed. Engl.* **2007,** *46* (40), 7591-4.

80. Alves, S.; Kalberer, M.; Zenobi, R., Direct detection of particles formed by laser ablation of matrices during matrix-assisted laser desorption/ionization. *Rapid Commun. Mass Spectrom.* **2003,** *17* (18), 2034-38.

81. Leisner, A.; Rohlfing, A.; Rohling, U.; Dreisewerd, K.; Hillenkamp, F., Time-resolved imaging of the plume dynamics in infrared matrix-assisted laser desorption/ionization with a glycerol matrix. *J. Phys. Chem. B* **2005,** *109* (23), 11661-6.

82. Jackson, S. N.; Mishra, S.; Murray, K. K., Characterization of coarse particles formed by laser ablation of MALDI matrixes. *J. Phys. Chem. B* **2003,** *107* (47), 13106-10.

83. Jackson, S. N.; Kim, J. K.; Laboy, J. L.; Murray, K. K., Particle formation by infrared laser ablation of glycerol: implications for ion formation. *Rapid Commun. Mass Spectrom.* **2006,** *20* (8), 1299-304.

84. Overberg, A.; Fischer, F., Effect of magnetic field on 3A1u -> 1A1g luminescence of lead(2+) in calcium fluoride and strontium fluoride and of gold(1-) in sodium chloride. *Phys. Status Solidi B* **1988,** *147* (2), 811-21.

85. Huang, M. Z.; Hsu, H. J.; Lee, J. Y.; Jeng, J.; Shiea, J., Direct protein detection from biological media through electrospray-assisted laser desorption ionization/mass spectrometry. *J. Proteome Res.* **2006,** *5* (5), 1107-16.

86. Huang, M. Z.; Hsu, H. J.; Wu, C. I.; Lin, S. Y.; Ma, Y. L.; Cheng, T. L.; Shiea, J., Characterization of the chemical components on the surface of different solids with electrospray-assisted laser desorption ionization mass spectrometry. *Rapid Commun. Mass Spectrom.* **2007,** *21* (11), 1767-75.

87. Sampson, J. S.; Hawkridge, A. M.; Muddiman, D. C., Direct characterization of intact polypeptides by matrix-assisted laser desorption electrospray ionization quadrupole Fourier transform ion cyclotron resonance mass spectrometry. *Rapid Commun. Mass Spectrom.* **2007,** *21* (7), 1150-4.

88. Ifa, D. R.; Wiseman, J. M.; Song, Q.; Cooks, R. G., Development of capabilities for imaging mass spectrometry under ambient conditions with desorption electrospray ionization (DESI). *Int. J. Mass Spectrom.* **2007,** *259* (1-3), 8-15.

89. Li, Y.; Shrestha, B.; Vertes, A., Atmospheric pressure molecular imaging by infrared MALDI mass spectrometry. *Anal. Chem.* **2007,** *79* (2), 523-32.

90. March, R. E., An introduction to quadrupole ion trap mass spectrometry. *J. Mass Spectrom.* **1997,** *32* (4), 351-69.

91. March, R. E.; Todd, J. F. J.; Editors, Practical Aspects of Ion Trap Mass Spectrometry; Volume III: Chemical, Environmental and Biomedical Applications. **1995**; 518.

92. Mathieu, E., *J. Math. Pure Appl. (J. Liouville)* **1868,** *13*, 137.

93. Stafford, G. C., Jr.; Kelley, P. E.; Syka, J. E. P.; Reynolds, W. E.; Todd, J. F. J., Recent improvements in and analytical applications of advanced ion trap technology. *Int. J. Mass Spectrom. Ion Processes* **1984,** *60*, 85-98.

94. Wilm, M.; Mann, M., Analytical properties of the nanoelectrospray ion source. *Anal. Chem.* **1996,** *68* (1), 1-8.

95. Wilm, M. S.; Mann, M., Electrospray and Taylor-Cone Theory, Doles Beam of Macromolecules at Last. *Int. J. Mass Spectrom. Ion Processes* **1994,** *136* (2-3), 167-180.

96. Feldhaus, D., Menzel, C., Berkenkamp, S., Hillenkamp, F., and Dreisewerd, K. , *J. Mass Spectrom.* **2000,** *35*, 1320-8.

97. Dong, J.; Rezenom, Y. H.; Murray, K. K., Desorption electrospray ionization of aerosol particles. *Rapid Commun. Mass Spectrom.* **2007,** *21* (24), 3995-4000.

98. Hinds, W. C., Aerosol Technology-Properties, Behavior, and Measurement. *John Wiley&Sons: New York, NY* **1982,** Chapter 1.

99. Poschl, U., Aerosol particle analysis: challenges and progress. *Anal. Bioanal. Chem.* **2003,** *375* (1), 30-2.

100. Gates, P. J.; Kearney, G. C.; Jones, R.; Leadlay, P. F.; Staunton, J., Structural elucidation studies of erythromycins by electrospray tandem mass spectrometry. *Rapid Commun. Mass Spectrom.* **1999,** *13* (4), 242-6.

101. Deubel, A.; Fandino, A. S.; Sorgel, F.; Holzgrabe, U., Determination of erythromycin and related substances in commercial samples using liquid chromatography/ion trap mass spectrometry. *J. Chromatogr. A* **2006,** *1136* (1), 39-47.

102. Hara, K. Refining dextrose. Application No. JP 67-40757, Patent No. 46024056, **1971**.

103. Leuthold, L. A.; Mandscheff, J.-F.; Fathi, M.; Giroud, C.; Augsburger, M.; Varesio, E.; Hopfgartner, G., Desorption electrospray ionization mass spectrometry: Direct toxicological screening and analysis of illicit Ecstasy tablets. *Rapid Commun. Mass Spectrom.* **2005,** *20* (2), 103-10.

104. Silverstein, R. M.; Webster, F. X.; Kiemie, D., Spectrometric Identification of Organic Compounds, 7th Edition, **2002**, Chapter1, 490.

105. Costa, A. B., Cooks, R. G. , Simulated splashes: Elucidating the mechanism of desorption electrospray ionization mass spectrometry. *Chem. Phys. Lett.* **2008,** *464* (1-3), 1-8.

106. Moller, P.; Folkmann, J. K.; Forchhammer, L.; Brauner, E. V.; Danielsen, P. H.; Risom, L.; Loft, S., Air pollution, oxidative damage to DNA, and carcinogenesis. *Cancer Lett.* **2008,** *266* (1), 84-97.

107. de Kok, T.; Driece, H. A. L.; Hogervorst, J. G. F.; Briede, J. J., Toxicological assessment of ambient and traffic-related particulate matter: A review of recent studies. *Mutat. Res., Rev. Mutat. Res.* **2006,** *613* (2-3), 103-22.

108. Zimmermann, R., Vaeck, L. V., Davidovic, M., Beckmann, M., Adams, F., Analysis of polycyclic aromatic hydrocarbons (PAH) adsorbed on soot particles by Fourier transform laser microprobe mass spectrometry (FT LMMS): Variation of the PAH patterns at different positions in the combustion chamber of an incineration plant. *Environ. Sci. Technol.* **2000,** *34*, 4780-88.

109. Dockery, D. W., Epidemiologic study design for investigating respiratory health effects of complex air pollution mixtures. *Environ. Health Perspect.* **1993,** *101 Suppl 4*, 187-91.

110. Wolfrum, J., Use of excimer and dye lasers for analysis of combustion processes. *VDI-Ber.* **1986,** *617*, 301-18.

111. Alden, M., Laser spectroscopic techniques for combustion diagnostics. *Combust. Sci. Technol.* **1999,** *149* (1-6), 1-18.

112. Crosley, D. R., Laser-induced fluorescence measurement of combustion chemistry intermediates. *High Temp. Mater. Processes* **1986,** *7* (1), 41-54.

113. Eckbreth, A. C., Nonlinear Raman spectroscopy for combustion diagnostics. *J. Quant. Spectrosc. Radiat. Transfer* **1988,** *40* (3), 369-83.

114. Przybilla, L.; Brand, J. D.; Yoshimura, K.; Rader, H. J.; Mullen, K., MALDI-TOF mass spectrometry of insoluble giant polycyclic aromatic hydrocarbons by a new method of sample preparation. *Anal. Chem.* **2000,** *72* (19), 4591-7.

115. Caslavsky, J.; Kotlarikova, P., Analysis of high-molecular-weight polycyclic aromatic hydrocarbons by laser desorption-ionisation/time-of-flight mass spectrometry and liquid

chromatography/atmospheric pressure chemical ionization mass spectrometry. *Environ. Chem.* **2005**, 393-408.

116. Chen, H.; Li, M.; Zhang, Y. P.; Yang, X.; Lian, J. J.; Chen, J. M., Rapid analysis of SVOC in aerosols by desorption electrospray ionization mass spectrometry. *J. Am. Soc. Mass Spectrom.* **2008,** *19* (3), 450-4.

117. Li, M.; Chen, H.; Wang, B.-F.; Yang, X.; Lian, J.-J.; Chen, J.-M., Direct quantification of PAHs in biomass burning aerosols by desorption electrospray ionization mass spectrometry. *Int. J. Mass Spectrom.* **2009,** *281* (1-2), 31-6.

118. Culea, M.; Cozar, O.; Culea, E., PAHs in cigarette smoke by gas chromatography-mass spectrometry. *Indoor Built Environ.* **2005,** *14* (3-4), 283-92.

119. Harris, J. E., Cigarette Smoke Components and Disease: Cigarette Smoke Is More Than a Triad of Tar, Nicotine, and Carbon Monoxide. *Smoking and Tobacco Control Monograph No. 7* **1996**, Chapter 5, 59-75.

120. Adams, J. D.; O'Mara-Adams, K. J.; Hoffmann, D., Toxic and carcinogenic agents in undiluted mainstream smoke and sidestream smoke of different types of cigarettes. *Carcinogenesis* **1987,** *8* (5), 729-31.

121. Gonzales, J. M., Sarabia, J. , An interesting compound of the sidestream tobacco smoke: Hexamethylenetetraamine. *Proc. CORESTA Congr.* **1992**, 127-41.

122. Ostafe, R.; Brumaru, C.; Papoe, G.; Lupsa, I.; Ostafe, V., Assessment using HPLC analysis of influence of tobacco brand, type of filter and smoking habits on PAHs concentration in cigarette smoke. *Ann. West Univ. Timisoara, Ser. Chem.* **2006,** *15* (1), 33-44.

123. Johnson, W. R.; Hale, R. W.; Nedlock, J. W.; Grubbs, H. J.; Powell, D. H., Distribution of products between mainstream and sidestream smoke. *Tob. Sci.* **1973,** *17*, 141-4.

124. Proctor, C. J.; Martin, C.; Beven, J. L.; Dymond, H. F., Evaluation of an apparatus designed for the collection of sidestream tobacco smoke. *Analyst* **1988,** *113* (10), 1509-13.

125. Chang, Y. C.; Lee, H. W.; Tseng, H. H., The formation of incense smoke. *J. Aerosol Sci.* **2007,** *38* (1), 39-51.

126. Chen, C. C.; Lee, H., Genotoxicity and DNA adduct formation of incense smoke condensates: Comparison with environmental tobacco smoke condensates. *Mutat. Res., Genet. Toxicol.* **1996,** *367* (3), 105-14.

127. Tran, T. C.; Marriott, P. J., Comprehensive two-dimensional gas chromatography - time-of-flight mass spectrometry and simultaneous electron capture detection/nitrogen phosphorous detection for incense analysis. *Atmos. Environ.* **2008,** *42* (32), 7360-72.

128. Tran, T. C.; Marriott, P. J., Characterization of incense smoke by solid phase microextraction - Comprehensive two-dimensional gas chromatography (GC Ã— GC). *Atmos. Environ.* **2007,** *41* (27), 5756-68.

129. Ott, W. R.; Siegmann, H. C., Using multiple continuous fine particle monitors to characterize tobacco, incense, candle, cooking, wood burning, and vehicular sources in indoor, outdoor, and in-transit settings. *Atmos. Environ.* **2006,** *40* (5), 821-43.

130. Fine, P. M.; Cass, G. R.; Simoneit, B. R. T., Characterization of fine particle emissions from burning church candles. *Environ. Sci. Tech.* **1999,** *33* (14), 2352-62.

131. Atakan, B.; Boehm, H.; Kohse-Hoeinghaus, K., Fuel-rich chemistry and soot precursors. *Appl. Combust. Diagn.* **2002**, 289-316.

132. Pan, S.; Wu, T.; Yao, Q.; Jia, C., Estimation of vapor pressure of polynuclear aromatic hydrocarbons by gas chromatography. *Fenxi Huaxue* **1996,** *24* (8), 906-9.

133. McClaine, J. W.; Ona, J. O.; Wornat, M. J., Identification of a new C28H14 polycyclic aromatic hydrocarbon as a product of supercritical fuel pyrolysis: Tribenzo[cd,ghi,lm]perylene. *J. Chromatogr. A* **2007,** *1138* (1-2), 175-83.

134. McClaine, J. W.; Wornat, M. J., Reaction Mechanisms Governing the Formation of Polycyclic Aromatic Hydrocarbons in the Supercritical Pyrolysis of Toluene: C28H14 Isomers. *J. Phys. Chem. C* **2007,** *111* (1), 86-95.

135. Richter, H.; Howard, J. B. In Formation of polycyclic aromatic hydrocarbons and their growth to soot - a review of chemical reaction pathways. *Prog. Energy Combust. Sci.* **2000;** 565-608.

136. Somers, M. L.; McClaine, J. W.; Wornat, M. J., The formation of polycyclic aromatic hydrocarbons from the supercritical pyrolysis of 1-methylnaphthalene. *Proc. Combust. Inst.* **2007,** *31*, 501-9.

137. Richter, H.; Benish, T. G.; Mazyar, O. A.; Green, W. H.; Howard, J. B. In Formation of polycyclic aromatic hydrocarbons and their radicals in a nearly sooting premixed benzene flame. *Proc. Combust. Inst.* **2000**; 2609-18.

138. Shukla, B.; Susa, A.; Miyoshi, A.; Koshi, M., In situ direct sampling mass spectrometric study on formation of polycyclic aromatic hydrocarbons in toluene pyrolysis. *J. Phys. Chem. A* **2007,** *111* (34), 8308-24.

139. Da Silva, G.; Chen, C.-C.; Bozzelli, J. W., Toluene Combustion: Reaction Paths, Thermochemical Properties, and Kinetic Analysis for the Methylphenyl Radical + O2 Reaction. *J. Phys. Chem. A* **2007,** *111* (35), 8663-76.

140. Rezenom, Y. H.; Dong, J.; Murray, K. K., Infrared laser-assisted desorption electrospray ionization mass spectrometry. *Analyst* **2008,** *133* (2), 226-32.

141. Handschuh, M.; Nettesheim, S.; Zenobi, R., Laser-induced molecular desorption and particle ejection from organic films. *Appl. Surf. Sci.* **1999,** *137* (1-4), 125-35.

142. Murray, K. K., Infrared MALDI. *Encyclopedia of Mass Spectrometry* **2006,** *6*, 701-6.

143. Dreisewerd, K.; Berkenkamp, S.; Leisner, A.; Rohlfing, A.; Menzel, C., Fundamentals of matrix-assisted laser desorption/ionization mass spectrometry with pulsed infrared lasers. *Int. J. Mass Spectrom.* **2003,** *226* (1), 189-209.

144. Dreisewerd, K.; Muthing, J.; Rohlfing, A.; Meisen, I.; Vukelic, Z.; Peter-Katalinic, J.; Hillenkamp, F.; Berkenkamp, S., Analysis of gangliosides directly from thin-layer chromatography plates by infrared matrix-assisted laser desorption/ionization orthogonal time-of-flight mass spectrometry with a glycerol matrix. *Anal. Chem.* **2005,** *77* (13), 4098-107.

145. Xu, Y.; Little, M. W.; Murray, K. K., Interfacing capillary gel microfluidic chips with infrared laser desorption mass spectrometry. *J. Am. Soc. Mass Spectrom.* **2006,** *17* (3), 469-74.

146. Dreisewerd, K.; Lemaire, R.; Pohlentz, G.; Salzet, M.; Wisztorski, M.; Berkenkamp, S.; Fournier, I., Molecular Profiling of Native and Matrix-Coated Tissue Slices from Rat Brain by Infrared and Ultraviolet Laser Desorption/Ionization Orthogonal Time-of-Flight Mass Spectrometry. *Anal. Chem.* **2007,** *79* (6), 2463-71.

147. Berkenkamp, S.; Karas, M.; Hillenkamp, F., Ice as a matrix for IR-matrix-assisted laser desorption/ionization: mass spectra from a protein single crystal. *Proc. Natl. Acad. Sci. U. S. A.* **1996,** *93* (14), 7003-7.

148. Fan, X.; Little, M. W.; Murray, K. K., Infrared laser wavelength dependence of particles ablated from glycerol. *App. Sur. Sci.* **2008,** *255* (5), 1699-704.

149. Chowdhury, S. K.; Katta, V.; Chait, B. T., An electrospray-ionization mass spectrometer with new features. *Rapid Commun. Mass Spectrom.* **1990,** *4* (3), 81-7.

150. Gatlin, C. L.; Turecek, F.; Vaisar, T., Determination of Soluble Cu(I) and Cu(II) Species in Jet Fuel by Electrospray Ionization Mass Spectrometry. *Anal. Chem.* **1994,** *66* (22), 3950-8.

151. Shiea, J.; Yuan, C.-H.; Huang, M.-Z.; Cheng, S.-C.; Ma, Y.-L.; Tseng, W.-L.; Chang, H.-C.; Hung, W.-C., Detection of native protein ions in aqueous solution under ambient conditions by electrospray laser desorption/ionization mass spectrometry. *Anal. Chem.* **2008,** *80* (13), 4845-52.

152. Shiea, J.; Huang, M. Z.; Hsu, H. J.; Lee, C. Y.; Yuan, C. H.; Beech, I.; Sunner, J., Electrospray-assisted laser desorption/ionization mass spectrometry for direct ambient analysis of solids. *Rapid Commun. Mass Spectrom.* **2005,** *19* (24), 3701- 4.

153. Peng, I. X.; Shiea, J.; Loo, R. R. O.; Loo, J. A., Electrospray-assisted laser desorption/ionization and tandem mass spectrometry of peptides and proteins. *Rapid Commun. Mass Spectrom.* **2007,** *21* (16), 2541- 6.

154. Huang, M. Z.; Hsu, H. J.; Lee, L. Y.; Jeng, J. Y.; Shiea, L. T., Direct protein detection from biological media through electrospray-assisted laser desorption ionization/mass spectrometry. *J. Proteome Res.* **2006,** *5* (5), 1107-16.

155. Takats, Z.; Wiseman, J. M.; Cooks, R. G., Ambient mass spectrometry using desorption electrospray ionization (DESI): instrumentation, mechanisms and applications in forensics, chemistry, and biology. *J. Mass Spectrom.* **2005,** *40* (10), 1261-75.

156. Tabacova, S. A.; Kimmel, C. A., Atenolol: pharmacokinetic/dynamic aspects of comparative developmental toxicity. *Reprod. Toxicol.* **2002,** *16* (1), 1-7.

157. Reeves, P. R.; McAinsh, J.; McIntosh, D. A. D.; Winrow, M. J., Metabolism of Atenolol in Man. *Xenobiotica* **1978,** *8* (5), 313-20.

158. Williams, J. P.; Patel, V. J.; Holland, R.; Scrivens, J. H., The use of recently described ionisation techniques for the rapid analysis of some common drugs and samples of biological origin. *Rapid Commun. Mass Spectrom.* **2006,** *20* (9), 1447-56.

159. Williams, J. P.; Scrivens, J. H., Rapid accurate mass desorption electrospray ionisation tandem mass spectrometry of pharmaceutical samples. *Rapid Commun. Mass Spectrom.* **2005,** *19* (24), 3643-50.

160. Reinard, M. S.; Johnston, M. V., Ion Formation Mechanism in Laser Desorption Ionization of Individual Nanoparticles. *J. Am. Soc. Mass Spectrom.* **2008,** *19* (3), 389-99.

161. Venter, A.; Sojka, P. E.; Cooks, R. G., Droplet dynamics and ionization mechanisms in desorption electrospray ionization mass spectrometry. *Anal. Chem.* **2006,** *78* (24), 8549-55.

162. Knochenmuss, R.; Zhigilei Leonid, V., Molecular dynamics model of ultraviolet matrix-assisted laser desorption/ionization including ionization processes. *J. Phys. Chem. B* **2005,** *109* (48), 22947-57.

163. Nemes, P.; Barton, A. A.; Vertes, A., Three-Dimensional Imaging of Metabolites in Tissues under Ambient Conditions by Laser Ablation Electrospray Ionization Mass Spectrometry. *Anal. Chem.* **2009,** *81* (16), 6668-75.

164. Apitz, I.; Vogel, A., Material ejection in nanosecond Er:YAG laser ablation of water, liver, and skin. *Appl. Phys. A: Mater. Sci. Processes* **2005,** *81* (2), 329-38.

165. Berkenkamp, S.; Karas, M.; Hillenkamp, F., Ice as a matrix for IR-matrix-assisted laser desorption/ionization: Mass spectra from a protein single crystal. *Proc. Natl. Acad. Sci. USA* **1996,** *93* (14), 7003-7.

166. Laiko, V. V.; Taranenko, N. I.; Berkout, V. D.; Yakshin, M. A.; Prasad, C. R.; Lee, H. S.; Doroshenko, V. M., Desorption/ionization of biomolecules from aqueous solutions at atmospheric pressure using an infrared laser at 3 mu m. *J. Am. Soc. Mass Spectrom.* **2002,** *13* (4), 354-61.

167. Laiko, V. V.; Taranenko, N. I.; Doroshenko, V. M., On the mechanism of ion formation from the aqueous solutions irradiated with 3 mu m IR laser pulses under atmospheric pressure. *J. Mass Spectrom.* **2006,** *41* (10), 1315-21.

168. Konig, S.; Kollas, O.; Dreisewerd, K., *Anal. Chem.* **2007,** *79* (14), 5484-88.

169. Leisner, A.; Rohlfing, A.; Rohling, U.; Dreisewerd, K.; Hillenkamp, F., Time-resolved imaging of the plume dynamics in infrared matrix-assisted laser desorption/ionization with a glycerol matrix. *J. Phys. Chem. B* **2005,** *109* (23), 11661-6.

170. Jackson, S. N.; Kim, J. K.; Laboy, J. L.; Murray, K. K., Particle formation by infrared laser ablation of glycerol: implications for ion formation. *Rapid Commun. Mass Spectrom.* **2006,** *20* (8), 1299-304.

171. Sampson, J. S.; Murray, K. K.; Muddiman, D. C., Intact and top-down characterization of biomolecules and direct analysis using infrared matrix-assisted laser desorption electrospray ionization coupled to FT-ICR mass spectrometry. *J. Am. Soc. Mass Spectrom.* **2009,** *20* (4), 667-73.

172. Lee, J.; Soper, S. A.; Murray, K. K., Microfluidic chips for mass spectrometry-based proteomics. *J. Mass Spectrom.* **2009,** *44* (5), 579-93.

APPENDIX. LETTERS OF PERMISSION

From: Permission Requests - UK <permissionsuk@wiley.com>
Subject: **RE: permission request**
Date: June 12, 2009 9:43:32 AM CDT
To: Jianan Dong <jdong1@tigers.lsu.edu>

Dear Jianan Dong,

Thank you for your email request. Permission is granted for you to use the material below for your thesis/dissertation subject to the usual acknowledgements and on the understanding that you will reapply for permission if you wish to distribute or publish your thesis/dissertation commercially.

Best wishes,

Laura Mothersole

Permissions Assistant
Wiley-Blackwell
9600 Garsington Road
Oxford OX4 2DQ
UK
Tel: +44 (0) 1865 476160
Fax: +44 (0) 1865 471158
Email: laura.mothersole@wiley.com

From: Jianan Dong [mailto:jdong1@tigers.lsu.edu]
Sent: 25 May 2009 23:20
To: Permission Requests - UK
Subject: permission request

To whom it may concern:

I am writing this E-mail to you to formally request permission to use texts and figures from a publication under one of your journals in which I am the author/co-author. This information will be used in my dissertation for graduating with a Ph. D. in chemistry at Louisiana State University. I am trying to finish the dissertation by June 15th, so if possible I am requesting permission by this date. A reply to this email granting permission is all that is required by LSU for the dissertation. The following information identifies which article I am referring and contact information is listed at the end of this email.

Dong, J., Rezenom, Y, and Murray K. K. Desorption Electrospray Ionization of Aerosol Particles. Rapid Communication in Mass Spectrometry. 2007, 21, 3995-400

Louisiana State University uses the Electronic Thesis/Dissertation (ETD) system to display finished dissertation and displays the finished work to others outside the university through UMI/ProQuest publication services. More

information about his process can be found at the following url.
http://etd.lsu.edu/submit/letter.htm

If this email has reached the wrong person at your publishing company, please email me with the corrected instructions for copyright permission or forward the email on to the correct party. Thank you in advance for your help and I look forward to hearing from you soon.

Sincerely,
Jianan Dong
Graduate Student
Kermit Murray Research Group
Department of Chemistry
Louisiana State University
Baton Rouge, LA 70803
(w) 225-578-3385
(F) 225-578-3458

From: "CONTRACTS-COPYRIGHT (shared)" <Contracts-Copyright@rsc.org>
Subject: **RE: Website Email: permission request**
Date: May 29, 2009 7:39:53 AM CDT
To: 'jianan Dong' <jdong1@tigers.lsu.edu>

Dear Jianan Dong

The Royal Society of Chemistry (RSC) hereby grants permission for the use of your paper(s) specified below in the printed and microfilm version of your thesis. You may also make available the PDF version of your paper(s) that the RSC sent to the corresponding author(s) of your paper(s) upon publication of the paper(s) in the following ways: in your thesis via any website that your university may have for the deposition of theses, via your university's Intranet or via your own personal website. We are however unable to grant you permission to include the PDF version of the paper(s) on its own in your institutional repository. The Royal Society of Chemistry is a signatory to the STM Guidelines on Permissions (available on request).

Please note that if the material specified below or any part of it appears with credit or acknowledgement to a third party then you must also secure permission from that third party before reproducing that material.

Please ensure that the thesis states the following:

Reproduced by permission of The Royal Society of Chemistry

and include a link to the article on the Royal Society of Chemistry's website.

Please ensure that your co-authors are aware that you are including the paper in your thesis.

Best regards

Dr Sharon Bellard, Manager Contracts & Copyright
Royal Society of Chemistry, Thomas Graham House
Science Park, Milton Road, Cambridge CB4 0WF, UK
Tel +44 (0) 1223 432383, Fax +44 (0) 1223 423623
www.rsc.org

-----Original Message-----
From: jianan Dong [mailto:jdong1@tigers.lsu.edu]
Sent: 25 May 2009 23:17
To: CONTRACTS-COPYRIGHT (shared)
Subject: Website Email: permission request

To: Gill Cockhead
This Email was sent from the following RSC.ORG page:
/AboutUs/Copyright/Permissionrequests.asp

To whom it may concern:

I am writing this E-mail to you to formally request permission to use texts and figures from a publication under one of your journals in which I am the author/co-author. This information will be used in my dissertation for graduating with a Ph. D. in chemistry at Louisiana State University. I am trying to finish the dissertation by June 15th, so if possible I am requesting permission by this date. A reply to this email granting permission is all that is required by LSU for the dissertation. The following information identifies which article I am referring and contact information is listed at the end of this email.
Rezenom, Y., Dong, J., and Murray K.K. Infrared Laser-assisted Desorption Electrospray Ionization Mass Spectrometry Analyst. 2008, 133(2), 226-232

Louisiana State University uses the Electronic Thesis/Dissertation (ETD) system to display finished dissertation and displays the finished work to others outside the university through UMI/ProQuest publication services. More information about his process can be found at the following url.
http://etd.lsu.edu/submit/letter.htm

If this email has reached the wrong person at your publishing company, please email me with the corrected instructions for copyright permission or forward the email on to the correct party. Thank you in advance for your help and I look forward to hearing from you soon.

Sincerely,
Jianan Dong
Graduate Student
Kermit Murray Research Group
Department of Chemistry
Louisiana State University
Baton Rouge, LA 70803
(w) 225-578-3385
(F) 225-578-3458

Membership No. :

VITA

Jianan Dong is the daughter of Liming Dong and June Wang. She graduated in 1997 with a Bachelor of Science degree in biochemistry at Nanjing University of Technology, China. After graduation, she had been employed by Beijing Strong Biotech Company and worked on construction of granulocyte-macrophage colony stimulating factor express system for two years. She had also been employed by Beijing Proctor & Gamble Technology Company for two years as a research associate in 1999, and by Novozymes (China) Investment Company as a scientist in 2001. In 2003, Jianan enrolled in the doctoral program for chemistry at Louisiana State University. In 2005, she joined Dr. Kermit K. Murray research group. She has published one first author publication, and one co-author publication. She has presented at three science conventions under her degree professor. She is a member of the American Society for Mass Spectrometry. Jianan is currently a candidate for the degree of Doctor of Philosophy in chemistry, which will be awarded at the Fall 2009 Commencement.